Award Number: DAMD17-00-1-0500

TITLE: Novel Histone Deacetylase Inhibitors

PRINCIPAL INVESTIGATOR: Jeannie S. Strobl, Ph.D.

CONTRACTING ORGANIZATION: West Virginia Research Corporation
Morgantown, West Virginia 26506-6845

REPORT DATE: July 2003

TYPE OF REPORT: Annual

PREPARED FOR: U.S. Army Medical Research and Materiel Command
Fort Detrick, Maryland 21702-5012

REPORT DOCUMENTATION PAGE

Form Approved
OMB No. 074-0188

1. AGENCY USE ONLY (Leave blank)	2. REPORT DATE	3. REPORT TYPE AND DATES COVERED
	July 2003	Annual (15 Jun 02 - 14 Jun 03)

4. TITLE AND SUBTITLE
Novel Histone Deacetylase Inhibitors

5. FUNDING NUMBERS
DAMD17-00-1-0500

6. AUTHOR(S)
Jeannie S. Strobl, Ph.D.

7. PERFORMING ORGANIZATION NAME(S) AND ADDRESS(ES)
West Virginia Research Corporation
Morgantown, West Virginia 26506-6845

E-Mail: jstrobl@hsc.wvu.edu

8. PERFORMING ORGANIZATION REPORT NUMBER

9. SPONSORING / MONITORING AGENCY NAME(S) AND ADDRESS(ES)
U.S. Army Medical Research and Materiel Command
Fort Detrick, Maryland 21702-5012

10. SPONSORING / MONITORING AGENCY REPORT NUMBER

11. SUPPLEMENTARY NOTES

12a. DISTRIBUTION / AVAILABILITY STATEMENT
Approved for Public Release; Distribution Unlimited

12b. DISTRIBUTION CODE

13. ABSTRACT (Maximum 200 Words)

HDAC (histone deacetylase) is a novel target for anti-cancer drug discovery. A database of quinoline compounds was characterized for the ability to inhibit HDAC, promote differentiation and cell death in tissue culture lines of human breast cancer. Antimalarials, chloroquine and quinidine promote breast tumor cell differentiation and cell death. A novel mechanism, regulation of HDAC1 by stimulating ubiquitination and proteasomal degradation of HDAC1 is proposed to explain the actions of antimalarials in breast cancer. NSC 3852 and NSC 10010 are novel breast tumor differentiation agents. NSC 3852 inhibits HDAC enzyme activity in vitro. NSC 10010 causes differentiation by a unique mechanism, and does not inhibit HDAC activity or stimulate HDAC1 ubiquitination. We conclude that these novel compounds hold promise for breast cancer treatment and because of their independent mechanisms of action, may be even more active in combination than when used as single agents.

14. SUBJECT TERMS
Antimalarials, quinolines, differentiation

15. NUMBER OF PAGES
66

16. PRICE CODE

17. SECURITY CLASSIFICATION OF REPORT	18. SECURITY CLASSIFICATION OF THIS PAGE	19. SECURITY CLASSIFICATION OF ABSTRACT	20. LIMITATION OF ABSTRACT
Unclassified	Unclassified	Unclassified	Unlimited

Table of Contents

INTRODUCTION

Histone deacetylases (HDAC) are a family of enzymes that modify chromatin structure, transcription factor acetylation status, and regulate gene expression. Interest in HDAC as a target for anti-cancer drug development is based upon the antiproliferative and differentiating activity of HDAC inhibitors in tissue culture cell lines and their anti-tumor properties in transplanted tumors in animals. We are engaged in a drug screening process to identify antimalarial drugs, and drugs with analogous quinoline ring chemical structures, that promote the differentiation of human breast cancer cell lines, MCF-7 and MDA-MB-231. While we have identified only two new compounds that cause direct inhibition of HDAC enzyme, we have identified many quinoline ring compounds that cause growth arrest, differentiation and apoptosis in human breast cancer cells. The significance of this work is that it provides the basis for the development of novel breast cancer differentiation agents.

BODY

Tasks 1-3 – Complete

Task 4 – Histone deacetylase (HDAC) in vitro inhibition assays, apoptosis assays, growth inhibition assays, and cell differentiation assays- Complete.
Histone hyperacetylation assays with antimalarials – Complete.
Histone hyperacetylation assays with the NSC (National Service Center of the National Institutes of Health, Bethesda, MD) differentiation agents – Incomplete.
Data are included in the Appendix. Please refer to the Table below for the citations of interest.

TASK 4 SUMMARY TABLE

Assay	Manuscript	Figure/Table
HDAC	Martirosyan, et al. Identification of Novel Breast Cancer Cell Differentation Agents by Functional Screening, in revision.	Figure 7.
Apoptosis/Growth Inhibition	Martirosyan, et al.,*ibid* Zhou et al (2000) J. Biol. Chem. 275: 35256	Table 1 and Figure 8 Figure 6
Cell Differentiation Lipid Droplet accumulation assays and Ki67 Expression assays.	Martirosyan, et al., *ibid* Zhou et al. , *ibid*	Figures 1,2, 4 and 5 Text pages 10-11 Figures 7 and 8
Histone Hyperacetylation (antimalarials)	Martirosyan, et al., *ibid* Zhou et al., *ibid*	Figure 3 Figures 1 and 9
Histone Hyperacetylation (NSC compounds)	INCOMPLETE	

Task 5 – New objective, establish HDAC as a target for ubiquitination - Complete. Ubiquitinated HDAC proteins were demonstrated using Western blots. Total HDAC1 was immunoprecipitated from whole cell MCF-7 extracts and electrophoresed through SDS-polyacrylamide gels. After transfer and immobilization of the protein on membranes, ubiquitinated HDAC was detected with polyclonal antibodies directed against ubiquitin. MCF-7 human breast cancer cells treated with chloroquine or quinidine displayed increased levels of polyubiquitinated HDAC 1. Cells exposed to NSC 3852 (n=1) or NSC 10010 (n=1) exhibited a slight decrease in the level of polyubiquitinated HDAC1 compared with controls. This is Figure 1B (Appendix). We also showed rapid loss of HDAC1 protein from MCF-7 cells treated with either chloroquine or quinidine, but little or no loss of HDAC1 in response to NSC 3852 (Figure 1A ,Appendix).

Task 6- Screening for inhibition of cell growth using the MTS (a tetrazolium enzyme substrate) assay for mitochondrial dehydrogenase activity of living cells and for induction of apoptosis using the nucleosome ELISA has been completed in MCF-7 and MDA-MB-231 cell lines. Please refer to the Task 4 Summary Table above for the location of this information in the Appendix. To complete task 6, we will perform MTS, cell growth curves and apoptosis assays on the MCF-10A cell line, an immortalized,non-tumorigentic human mammary epithelial line.

Task 7 – Dropped

Task 8 – Two manuscripts appeared in print during 2002 as a result of the work supported by this grant. Two abstracts based upon the work outlined in this grant were published. One abstract was presented in September, 2002 at the DOD BCRP meeting; one abstract was accepted for presentation at the April, 2002 American Association for Cancer Research (AACR) meeting in Toronto that was rescheduled for Washington, DC in July, 2002. This abstract will be presented at the AACR meeting rescheduled for July 11-13, 2002. One manuscript was submitted, but not approved for publication. Experiments requested by this review are in progress and a re-submission is planned. One additional manuscript focused on the antitumor potential of one lead compound, NSC3852, is planned.

Approximately 2 entire months were devoted to the development of a SYBYL CoMFA (conformational molecular field analysis) based model for the prediction of novel breast tumor differentiation agents. The minimum recommended statistical parameters for the establishment of a CoMFA model are: 1) 5 compounds, 2) a compound response range of at least 2 orders of magnitude, and 3) an r^2 value >0.8. In our analyses, we analyzed our entire data set, as well as subsets of the compounds, using at least 5 compounds per condition. We used the Ki67 differentiation index as the end-point because this was the only parameter we measured that had a response range of 2 orders of magnitude as well as the MTS IC50 values as an end-point. A summary of the approaches used is presented in the CoMFA Summary Table below. The structures of all the compounds in our data base are presented in Figure 2 in the Appendix. None of the CoMFA approaches used yielded regression coefficients (r^2) that showed a statistically valid model of compound structure for predicting differentiation activity (Ki67 index) or growth inhibition (IC50). Our conclusion is that a CoMFA based model cannot be developed from the existing set of compounds.

CoMFA SUMMARY TABLE

Compound Set Used in the Analysis	Templates Used for the Chemical Alignment	R^2 Ki67	R^2 IC50
All compounds with a substituted position 4 pyrimidine ring	a) Quinoline ring b) Benzene ring c) Pyrimidine ring	a)-0.4 b)-0.9 c)-0.4	-0.2 -0.6 -0.2
All compounds with position 2 and 4 substituted pyrimidine ring	a) benzene ring b) quinoline ring	a)-0.4 b)-0.4	-0.2 -0.6
9 Compounds with Highest Ki67 Index	a) quinoline ring b) pyrimidine ring c) benzene ring	a)-0.3 b)-0.3 c)-0.2	-0.1 -0.1 -0.5
Compounds with a single quinidine ring	Quinoline ring	-0.2	-0.4
All compounds		-0.3	+0.1

KEY RESEARCH ACCOMPLISHMENTS

1. We demonstrated that HDAC1 protein in MCF-7 human breast tumor cells is a target for ubiquitination. The antimalarials chloroquine and quinidine stimulate levels of HDAC1 ubiquitination and lead to increased degradation of HDAC1.

REPORTABLE OUTCOMES

Manuscripts published (2)

1. Zhou Q, McCracken MA, Strobl JS (2002) Control of mammary tumor cell growth in vitro by novel cell differentiation and apoptosis agents. Breast Cancer Research and Treatment 75: 107-117.

2. Melkoumian, ZK, Martirosyan AR, Strobl JS (2002) Myc protein is differentially sensitive to quinidine in tumor versus immortalized breast epithelial cell lines International Journal of Cancer 102: 60-69.

Manuscripts submitted (1)

1. Martirosyan AR, Bata RR, Zhou Q, Freeman AB, Melkoumian ZK, Johnson DN, Howard RL, Fazarar J , Strobl JS (2002) Identification of novel breast cancer cell differentiation agents by functional screening of antimalarials and related antiproliferative quinolines. Molecular Cancer Therapeutics, in revision.

Abstracts (2)

1. Strobl JS, Zhou Q, Martirosyan AR (2002) Novel breast tumor differentiation agents. Era of Hope DOD Breast Cancer Research Program Meeting, Abst# 31-21. Poster presentation and Oral Symposium Presentation.
2. Martirosyan AR, Freeman AB, Strobl JS (2003) NSC3852, a new histone deacetylase inhibitor with breast tumor cell differentiation activity. Amer. Assoc. Cancer Res., Abst #R797. Poster presentation.

Seminar (1)

1. "Novel Differentiation Therapies for Breast Cancer" Basic Biomedical Science Department, Virgina College of Osteopathic Medicine, Blacksburg, VA, November, 2002.

Funding Record (5)

1. Strobl, JS (PI) Susan G. Komen Foundation BCTR0201140 "Breast Tumor Differentiation by Novel Agents Targeting Histone Deacetylase Ubiquitination and Heat Shock Proteins" Status: Superior rating, Alternate Grant Designation, Not-Funded.
2. Strobl, JS (PI) Susan G. Komen Foundation DISS0201686 "New Drug Candidates Target Rb/E2F/Myc Pathway" Status: Not-Funded.
3. Strobl, JS (PI) US Army BCRP-Concept Award "Breast Tumor Differentiation by HIF-1alpha Interference" Status: Not-Funded.
4. Strobl, JS (PI) WVU School of Medicine Internal Grant #1000161W "Breast Tumor Differentiation by Novel Agents Targeting Histone Deacetylase Ubiquitination and Heat Shock Protein Pathways" Status: Funded.
5. Strobl, JS (PI) US Army BCRP-Idea Award BC030501 "Restoration of Retinoblastoma Protein Function in Breast Cancer" Status: Pending.

Training Opportunities Supported (3)

1. Anna Martirosyan, M.D. is studying for the Ph.D. degree in Pharmacology and Toxicology; this grant provides stipend and supplies for her research.
2. Rayhana Rahim-Bata is studying for the Ph.D. degree in Pharmacology and Toxicology; this grant provides supplies for her research.
3. Charles Clarke, undergraduate Biology student (WVU) summer research experience and training in cancer cell biology and drug development; this grant provides supplies for his research.

CONCLUSIONS

HDAC1 continues to be viewed as important new target for new cancer drug discovery. By stimulating ubiquitination and proteasomal degradation of HDAC1 protein in MCF-7 cells, our experiments show that the antimalarials chloroquine and quinidine modulate the biological activity of this important new cancer drug target in breast tumor cells. Other differentiation agents we identified (NSC 3852, NSC 10010) act through different mechanisms in MCF-7 cells. NSC 3852 is a direct inhibitor of HDAC enzymatic activity that does not stimulate HDAC1 ubiquitination. NSC 10010 actively promotes breast

tumor differentiation agent, but does not stimulate HDAC1 ubiquitination or inhibit HDAC enzyme activity. The identification of novel breast tumor differentiation agents with different modes of action opens the possibility for new combinations of drugs to achieve even more effective control of tumor growth through the induction of cell differentiation. The CoMFA approach of the current compound data base failed to provide a predictive model for the refinement of quinolines as breast tumor differentiation agents. The structural diversity of compounds within this data base was such that compounds capable of stimulating differentiation through multiple mechanisms were included, thus explaining the failure to define a single critical pharmacophore.

In silico (computer simulated-analysis) of the absorption-distribution properties of NSC 3852 indicates that this compound has promise for further drug development. It is a low molecular weight compound (M.W. 174) with less than 5 hydrogen bond acceptors and only one hydrogen bond donor. It has two potential routes of absorption via paracellular (between cells) and passive diffusion, and is highly unlikely to be a substrate for the multi-drug resistance pump. Future work will focus on the further development of NSC 3852 as a therapeutic agent alone and in combination with chloroquine for breast cancer treatment.

REFERENCES

none

APPENDICES

Figure 1. (A) HDAC1 ubiquitination in MCF-7 cells; (B) HDAC1 protein levels in MCF-7 cells.

Figure 2. Quinoline Data base Structures for CoMFA.

Manuscript 1. Zhou, et al. (2002) Breast Cancer Research and Treatment 75: 107-117.

Manuscript 2. Melkoumian, et al. (2002) International Journal of Cancer 102: 60-69.

Manuscript 3. Martirosyan, et al. (2003) Identification of novel breast cancer cell differentiation agents by functional screening of anitmalarials and related antiproliferative quinolines. In revision.

Abstract 1. Strobl, et al. (2002) Novel breast tumor differentiation agents. Era of Hope #31-21.

Abstract 2. Martirosyan, et al. (2003) NSC3852, a new histone deacetylase inhibitor with breast tumor cell differentiation activity. AACR #R797.

APPENDIX MATERIALS

ANNUAL REPORT

DAMD17-00-1-500

JUNE 02- JUNE 03

JEANNINE S. STROBL
WEST VA.UNIV.
MORGANTOWN, WV

Figure 1

A

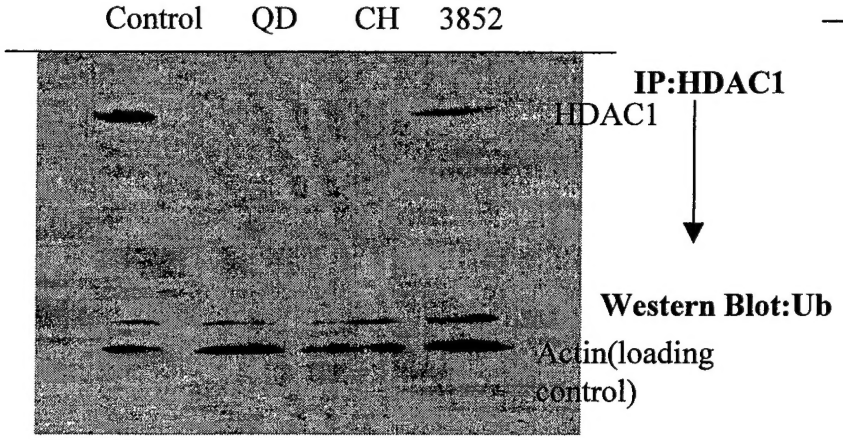

Effect of Antimalarials on the expression of HDAC1 protein in MCF-7 Cells. MCF-7 cells were untreated (control) or treated with antimalarials for 1 h. Total protein extracts(60ug) from each treatment indicated were subjected to 7.5% SDS-PAGE and blotted with anti-HDAC1.

B

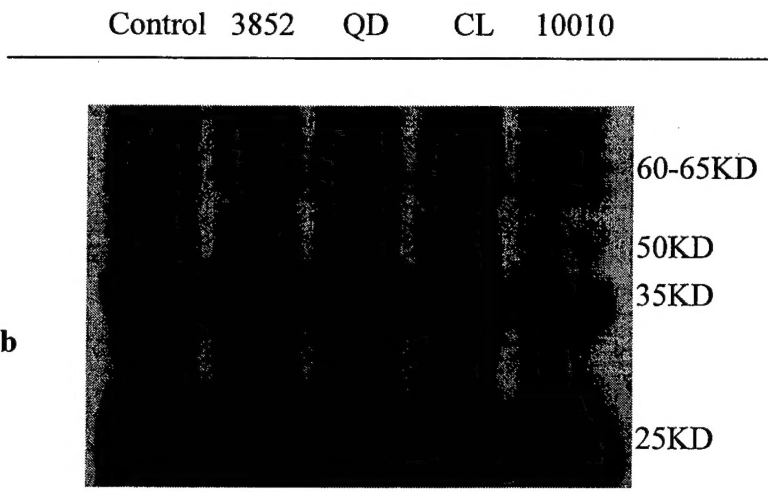

Effect of Antimalarials on HDAC1-Ub in MCF-7 Cells. Cells were untreated (control) or treated with antimalarials for 1 h. Cell lysates (200ug) were immunoprecipitated with anti-HDAC1, subjected to SDS-PAGE, and blotted with anti-Ub. QD = 90 uM Quinidine, CL = 33 uM Chloroquine.

Figure 2

10010 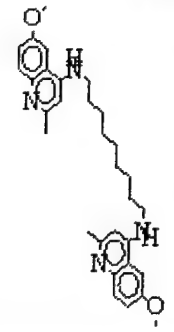	124637 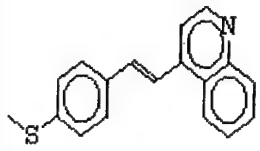	14050 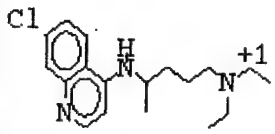	146397 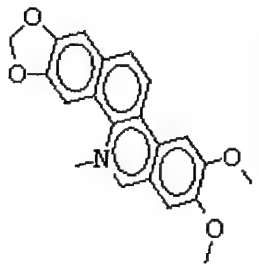	149765 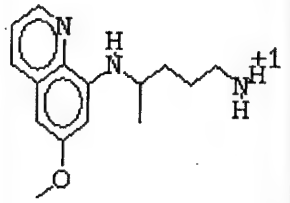	15783 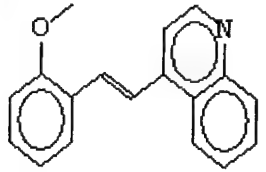
2039 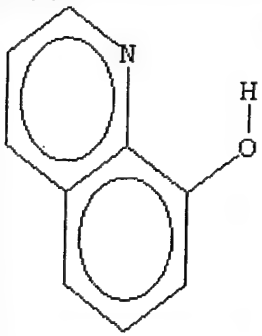	249913 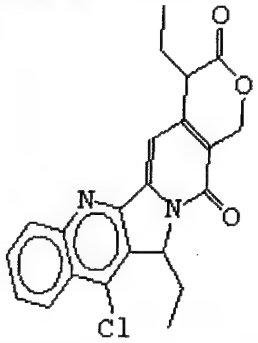	305819 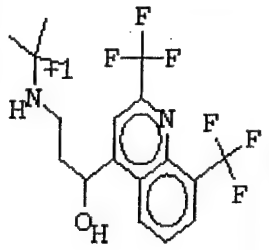	339004 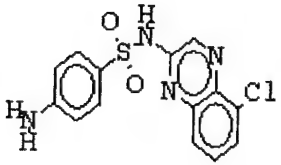	3852 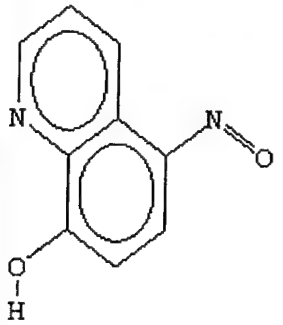	4238 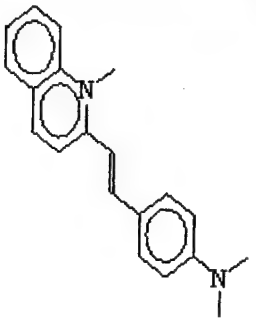
4239 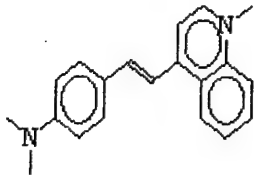	5362 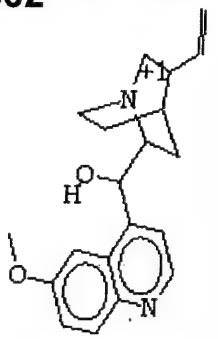	69603 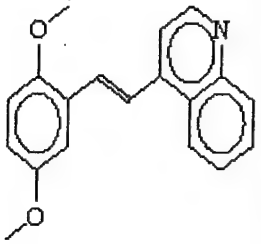	85700 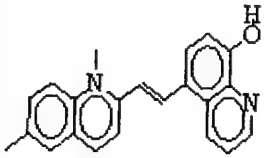	85701 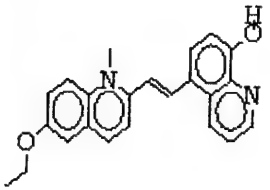	86371 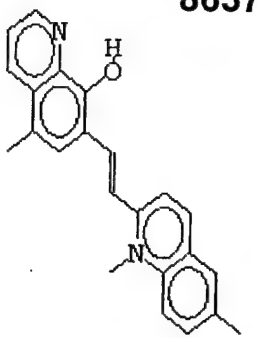

Figure 2 continued

86372 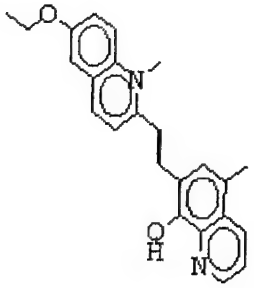	86373 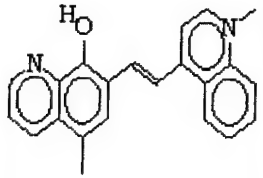	Amodiaquin 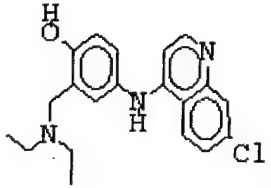	HCQ 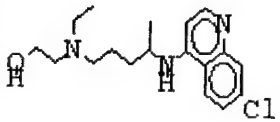	Methoquin 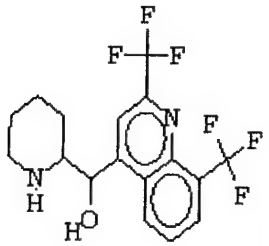	QD 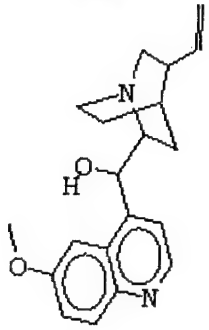
Quinoline 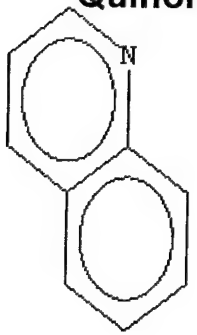					

Breast Cancer Research and Treatment **75:** 107–117, 2002.

Report

Control of mammary tumor cell growth *in vitro* by novel cell differentiation and apoptosis agents

Qun Zhou[1], Meredith A. McCracken[2], and Jeannine S. Strobl[1,2]
[1]*Department of Biochemistry and Molecular Pharmacology,* [2]*Genetics and Developmental Biology Program, West Virginia University, Morgantown, WV, USA*

Key words: apoptosis, breast cancer, cell differentiation agents, chloroquine, MCF-7, quinidine, quinine

Summary

The use of breast tumor differentiating agents to complement existing therapies has the potential to improve breast cancer treatment. Previously we showed quinidine caused MCF-7 cells to synchronously arrest in G1 phase of the cell cycle, transition into G0 and undergo progressive differentiation. After 72–96 h cells became visibly apoptotic. Using several analogs of quinidine we determined that MCF-7 cell cycle exit and differentiation are typical of quinoline antimalarial drugs bearing a tertiary amine side chain (chloroquine, quinine, quinidine). Differentiated cells accumulated lipid droplets and mammary fat globule membrane protein. Apoptosis was assayed by a nucleosome release ELISA. Quinidine and chloroquine triggered apoptosis, but not quinine, a quinidine stereoisomer that displayed weak DNA binding. The apoptotic response to quinidine and chloroquine was p53-dependent. A 4–15-fold induction of p21(WAF1) protein was observed in cells treated with quinidine or chloroquine prior to apoptosis, but p21(WAF1) was not increased in cells that differentiated in response to quinine. Chloroquine was most active in stimulating MCF-7 apoptosis, and quinine was most active in promoting MCF-7 cell differentiation. We conclude, distinct mechanisms are responsible for breast tumor cell differentiation and activation of apoptosis by quinoline antimalarials. Alkylamino-substituted quinoline ring compounds represented by quinidine, quinine, and chloroquine will be useful model compounds in the search for more active breast tumor differentiating agents.

Introduction

Our laboratory is investigating the use of quinoline antimalarials as inexpensive drugs with low toxicity for adjuvant breast cancer treatment. Quinidine is a natural alkaloid that is derived from the bark of the cinchona tree. Quinidine is used therapeutically to treat cardiac arrhythmia and malaria. Quinine is present in cinchona tree bark in even higher concentrations than quinidine. Quinine has antimalarial activity equivalent to that of quinidine but is not used as an antiarrhythmic agent [1]. Interestingly, quinidine and quinine are stereoisomers (Figure 1). In quinidine, the secondary alcohol of the side-chain in the 4-position of the quinoline ring is the dextrorotary conformation while in quinine the 4-hydroxyl group exists in the levorotatory conformation. The synthetic alkaloid, chloroquine is a more potent antimalarial than either quinidine or quinine. Chloroquine is a 4-alkylamino substituted quinoline that also possesses a chlorine substitution at the 7-position of the ring. Despite chloroquine's structural similarities with quinine and quinidine, chloroquine has a different mechanism of antimalarial activity, and chloroquine-resistant malaria responds to quinine treatment. The quinoline ring by itself lacks antimalarial or antiarrhythmic activity indicating that therapeutic properties are conferred by the side chain substituents. This group of pharmacologically active compounds might have anticancer properties.

We reported previously that quinidine causes moderate growth arrest and morphologic differentiation of human breast cancer cells *in vitro* [2–4]. In an experiment which compared MCF-7 cell numbers after 5

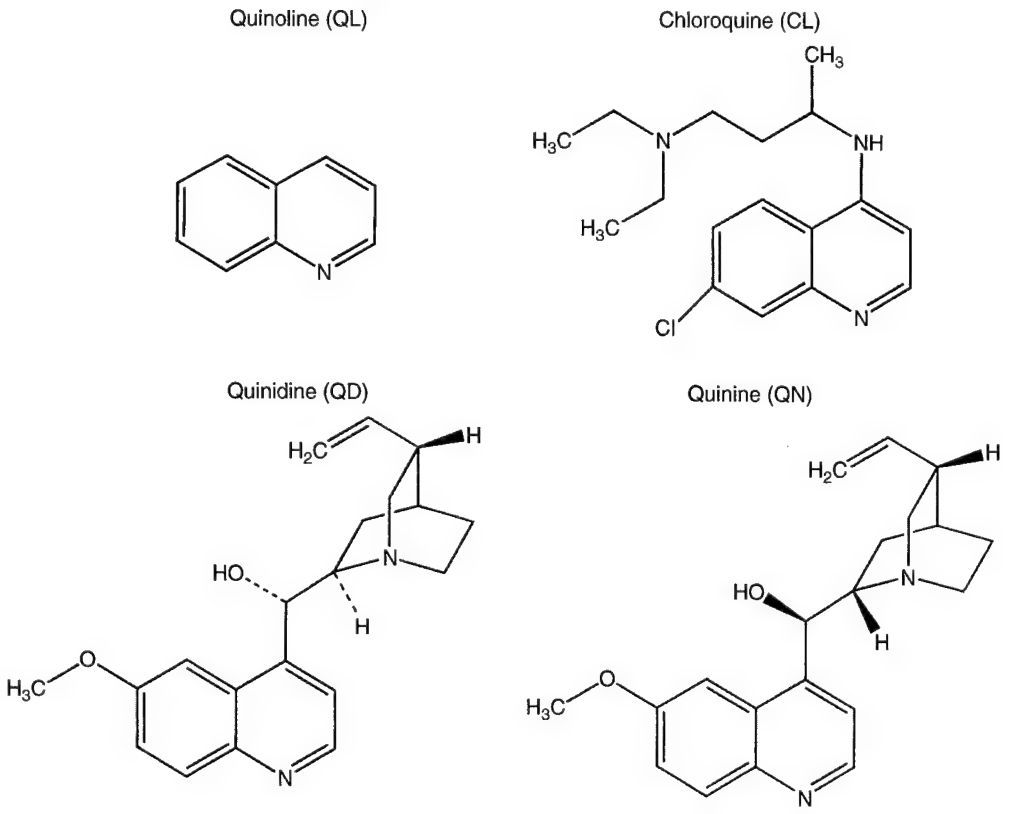

Figure 1. Structures of antimalarials.

days growth in the presence and absence of quinidine, 25 μM quinidine was found to reduce the increase in cell numbers by 50% [2]. Quinidine promoted cell cycle arrest in G1, exit into G0 marked by a loss of expression of Ki67 antigen, and lipid droplet accumulation and cytoplasmic enlargement, morphological evidence of cellular differentiation [3, 4]. Accumulation of MCF-7 cells in the G1/G0 phase of the cell cycle was maximal between 24 and 48 h with 90 μM quinidine. The potassium channel blocking activity of quinidine is implicated in the G1 arrest of MCF-7 cells, although the signaling pathway has not yet been elucidated [3]. The mechanism of quinidine action on growth in MCF-7 cells involves a number of changes in cell cycle proteins that regulate progression through G1 phase [4, 5]. Quinidine (90 μM) treatment caused increased p21(WAF1), p53, and p27 protein levels, and decreased cyclin D1, phosphorylated pRb, and Myc. Quinidine also raised levels of acetylated histone H4, a response that has been correlated with cellular differentiation in breast tumor cells [4, 6]. The differentiation response to quinidine in MCF-7 cells was well developed by 48–72 h. In cells continously exposed to quinidine for 72–96 h, apoptotic nuclei stained with Hoechst dye were apparent [3], suggesting that quinidine causes both growth arrest, via cell cycle arrest and differentiation, and cell death.

The present report describes the results of a comparative study of the effects of quinidine, quinoline and two additional quinoline antimalarials, quinine and chloroquine on MCF-7 cell apoptosis and differentiation. Our data show that quinoline antimalarials inhibit growth of human breast cancer cells *in vitro* and support the hypothesis that quinoline antimalarials cause cellular differentiation and apoptosis via distinct pathways.

Materials and methods

Chemicals

Chloroquine (CL), Oil Red O (ORO), quinidine (QD), quinine (QN), quinoline (QL) and trichostatin A (TSA) were purchased from Sigma Chemical Company (St. Louis, MO).

Tissue culture

Permanent cell lines derived from patients with breast carcinoma were used in these studies. MCF-7 cells between passage numbers 30–50, MCF-7*ras*, T47D and MDA-MB-231 cells were maintained in Dulbecco's Modified Eagle's medium (DMEM) (BioWhittaker, Walkersville, MD) supplemented with 10% heat-inactivated fetal bovine serum (FBS) (Hyclone Laboratories, Inc., Logan, Utah), and 40 ug/ml gentamicin. Experiments were performed in DMEM/5%FBS. The cells were cultured at 37°C in a humidified atmosphere of 93% air/7% CO_2.

MTS (3-(4,5-dimethylthiazol-2-yl)-5-(3-carboxymethoxyphenyl)-2-(4-sulfophenyl)-2H-tetrazolium) assay

MCF-7 cells were plated at 4.0×10^3 cells/well in 96-well plates in 225 µl of DMEM/5% FBS. Twelve hours after plating, the test agents were added and the cells were incubated for an additional 48 h. Cell growth was measured using a MTS assay kit (CellTiter 96 AQueous one solution assay, Promega, Madison, WI) according to the manufacturer's instructions. Assays were repeated at least three times. The concentration of each agent that inhibited cell growth by 50% (IC50) was determined using nonlinear regression analysis to fit the inhibition data (Prism 3.0, GraphPad Software, Inc., San Diego, CA).

Ki67 immunohistochemical assay

An immunohistochemical assay for Ki67 antigen was performed according to the protocol described by Wang et al. [3]. MCF-7 cells (2×10^5/dish) were plated on ethanol-washed glass coverslips in 35 mm^2 dishes. Twelve hours after plating, test compounds were added to the medium using the IC50 determined in the MTS assay. Forty-eight hours later, the cells were fixed in acetone:ethanol (50:50) on ice for 10 min, and washed with PBS-0.15% bovine serum albumin (BSA, fraction V, Sigma) (PBS-BSA). Cells were incubated for 10 min with 0.3% hydrogen peroxide in methanol, rinsed with PBS-BSA, and incubated for 30 min with 10% horse serum in PBS-BSA. Cells were incubated for 60 min with the primary antibody Ki67 (MIB-1, Dako Corporation, Glostrup, Denmark) diluted in PBS-BSA (1:77). After rinsing with PBS-BSA, the secondary antibody, biotinylated horse anti-mouse IgG (Vector Laboratories, Burlingame, CA) diluted in PBS-BSA (1:250) was added for 30 min. The cells were rinsed with PBS-BSA and incubated for 30 min with the avidin-biotin-peroxidase reagent (Vector Laboratories). After rinsing with PBS, the antigen-antibody complexes were visualized using diaminobenzidine (Stable DAB, Research Genetics, Huntsville, AL). The cells were counterstained with Mayer's hematoxylin (Fisher Scientific, Pittsburgh, PA), and the coverslips mounted using Permount (Fisher). Ki67 negative cells were visualized by light microscopy (400 × objective, Ortholux microscope, Ernst Leitz, Wetzlar, Germany). The percentage of Ki67 negative cells in a population of at least 500 cells per experimental condition was determined.

Oil red O assay

Lipid droplet accumulation in the cytoplasm was measured using Oil Red O (ORO) staining [7]. MCF-7 cells (1×10^5 per dish) were plated on ethanol-washed glass coverslips in 35 mm^2 dishes. Cells were treated with drug or vehicle for 48–72 h, fixed in 10% formaldehyde-0.2% calcium acetate in PBS for 3 min and stained for 10 min using the ORO stock solution (0.5% ORO in 98% isopropanol) diluted 6:4 in distilled water. The coverslips were rinsed in tap water, counterstained with Mayer's Hematoxylin solution, and mounted using 50:50 (v/v) glycerol/water. Lipid droplet accumulation was visualized by light microscopy (400 ×). Positive ORO cells had at least 10 lipid droplets per cell. The percentage of positive ORO cells was determined by counting at least 300 cells per experimental condition.

Western blotting

Cells were harvested from confluent T-75 flasks and subcultured (1×10^6) in 100 mm^2 dishes. Cell lysates were prepared by scraping cells into ice-cold harvesting buffer (1% SDS-10 mM Tris–HCl, pH 7.4). The lysates were boiled for 5 min, and protease inhibitors added (Protease Inhibitor Mixture, Roche Applied Sciences, Indianapolis, IN). The supernatants were collected after centrifugation in an Eppendorf microcentrifuge (14,000 rpm, 5 min) at 4°C. The protein concentration of the supernatant was determined using a BCA protein assay (Pierce, Rockford, IL) and BSA as a standard. Equal amounts of protein were loaded onto 12% SDS-polyacrylamide mini-gels. Colored

molecular weight protein markers (Amersham Pharmacia Biotech Inc., Piscataway, NJ) were used to estimate the molecular weight of the immunoreactive proteins. Proteins were transferred to polyvinylidene difluoride membranes (PVDF, Invitrogen, Carlsbad, CA) and blocked overnight at 4°C using 3% non-fat milk blocking buffer (3 g non-fat dry milk per 100 ml of TBS (20 mM Tris–HCl, pH 7.5, 0.5 M NaCl) and 0.05% (v/v) Tween 20. Membranes were incubated for 3 h at room temperature with the following primary antibodies: mouse monoclonal anti-p21 (WAF1) (Ap-1), mouse monoclonal anti-p53 (Ap-5) (Oncogene, Cambridge, MA) or mouse anti-human milk fat globule membrane (MFGM) protein (MAB-4043, Chemicon International, Temecula, CA). The primary antibodies were diluted 1 : 500 in Western washing solution (0.1% non-fat dry milk, 0.1% albumin (chicken egg), 1% (v/v) FBS, 10% (v/v) of 10 × PBS, pH 7.3, 0.2% (v/v) Tween-20). After washing three times with Western washing solution and one time with TBS, the antigen-antibody complexes were incubated 1 h at room temperature with HRP (horseradish peroxidase)-conjugated secondary antibody (anti-mouse IgG-HRP, Santa Cruz Biotechnology) diluted 1 : 3000 in Western washing solution. After washing three times with TBS, antibody binding was visualized using enhanced chemiluminescence (SuperSignal West Pico, Pierce) and autoradiography.

Densitometric analysis

Autoradiograms of the Western immunoblots were scanned using ChemiImager software (Alpha Innotech Corporation, San Leandro, CA). The blots were adjusted for brightness and contrast, and the mean density for each band was analyzed using ChemiImager analysis program. The background value was subtracted from each individual object.

Cell death ELISA (enzyme-linked immunosorbent assay)

Apoptotic cells were measured using the cell death ELISA kit (Roche Applied Science). Cells (4.0×10^3) were plated in each well of 96-well plates and treated in triplicate with either drug or vehicle (control cells) for 48 or 72 h. Cell cytoplasmic fractions were prepared and 20 µl aliquots were transferred into streptavidin-coated microtiter plates (MTP) for analysis as per the instructions of the supplier. Apoptosis, measured as nucleosome release into the cytoplasmic fraction, was quantified spectrophotometrically (A_{405} nm, EL340 Biokinetics Reader, Bio-Tek Instruments, Winooski, Vermont) using ABTS (2,2-Azino-di-3-ethylbenzthiazolin-sulfonat) as the substrate.

P21(WAF1) ELISA

Cells were plated (1×10^6 cells/100 mm^2 dish); 12 h later MTS IC50 of each test agent were added to the medium and incubated for 24 h. Fifty micrograms protein aliquots of the cell lysates were assayed for p21(WAF1) using a colorimetric ELISA (Oncogene, Boston, MA) according to the manufacturer's instructions.

DNA binding assay

Chloroquine, quinidine, and quinine emit an intense blue fluorescence when excited by ultraviolet light [8]. Intercalation into DNA quenches the chloroquine fluorescence [9], and this principle is the basis of the fluorescence assay we used to assess DNA binding by quinidine and quinine. Stock solutions of chloroquine, quinidine, and quinine in water were diluted 1 : 1 in 10 mM Tris, 1 mM EDTA, pH 8 (TE) or TE containing 1 µg of lambda DNA (Invitrogen, Carlsbad, CA) to a final concentration of 100 µg drug/ml. The final reaction volume was 20 µl. Drugs or drugs plus DNA were incubated for 15 min at room temperature in the dark in a 96-well plate (Nunc Immunoplate, Nunc Nalge International). Fluorescence was then measured using a CytoFluor4000 (PerSeptive Biosystems) instrument using an excitation wavelength of 360 nm and an emission wavelength of 460 nm. Background fluorescence from TE alone or TE plus DNA samples was subtracted from each measurement as appropriate. Data were expressed as the fluorescence quench ratio defined as the average fluorescence of drug alone (Em1) divided by that of drug in the presence of DNA (Em2).

Statistical analysis

Data are expressed as the mean ± SE for n number of replicates as indicated in the figure legends. One-way ANOVA (analysis of variance) followed by Bonferroni's t-tests were used to assess statistically significant differences between control- and drug-treated groups (GraphPad Instat, Intuitive Software for Science, San Diego, CA).

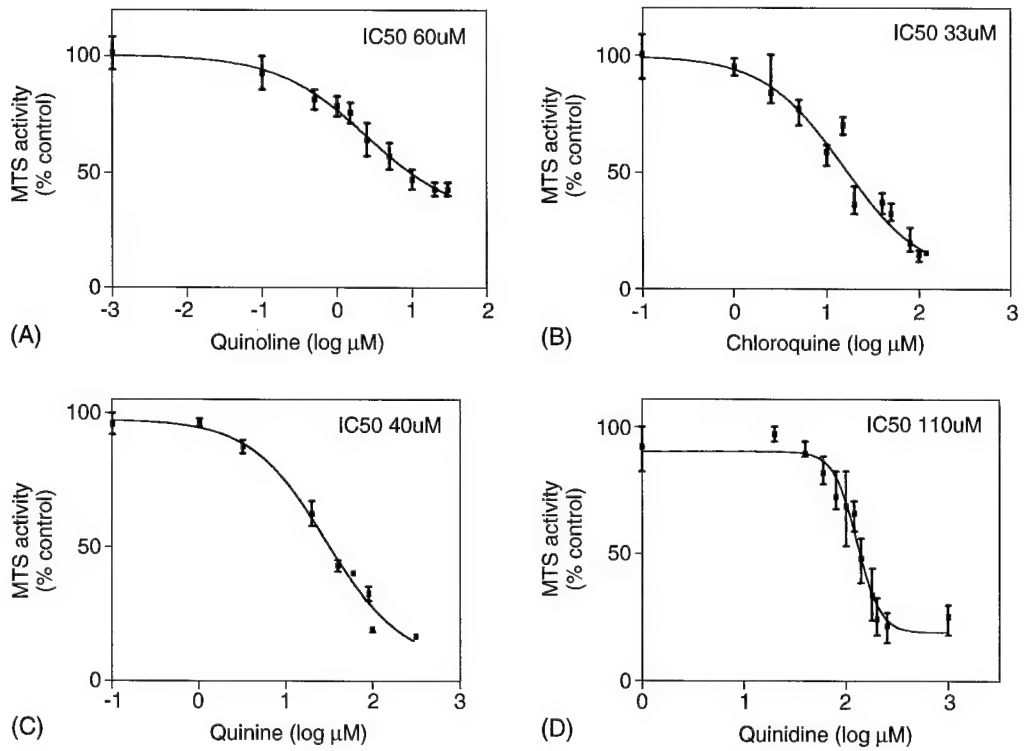

Figure 2. Antimalarials inhibited MTS metabolism in MCF-7 cells. MCF-7 cells (4000 cells/well) were grown in 96 well plates in the presence of increasing concentrations of each antimalarial for 48 h. Cell growth was estimated using the MTS assay. The IC50 value for each agent was determined using nonlinear regression analysis to fit inhibition data. Data are the mean ± SE of three independent experiments performed in quadruplicate. MTS activity of untreated cells was set 100%. The IC50 value for each antimalarial is shown in each panel.

Results

Antimalarials inhibit growth and promote MCF-7 cell differentiation

Quinidine inhibits MCF-7 cell proliferation, and to test whether this is a general response to structurally related chemicals, the effects of quinidine, quinine, chloroquine, and quinoline on MCF-7 cell growth were compared. The MTS assay directly measures mitochondrial metabolic activity; none of the test agents directly inhibited mitochondrial metabolism of MTS after a 2 h or a 6 h exposure (data not shown). Therefore, MTS activity measured after 48 h incubation with these compounds is a valid measure of the number of surviving cells (Figure 2). The IC50 was estimated for each drug in the MTS assay, and the order of potency of the compounds was chloroquine (IC50, 33 μM) > quinine (IC50, 40 μM) > quinoline (IC50, 62 μM) > quinidine (IC50, 110 μM). The effects of chloroquine, quinine, quinoline, and quinidine on cell numbers were investigated using the IC50 values determined in the MTS assay. Chloroquine (IC50, 33 μM) caused a ~60% decrease in cell numbers after a 60 h incubation as compared with control, growing MCF-7 cells suggesting that chloroquine caused cell death. In parallel cell cultures incubated with MTS IC50 of quinoline, quinidine, and quinine, the cell numbers after 60 h did not differ from the plating density. These compounds may primarily arrest cell growth, or alternatively permit a limited amount of proliferation balanced by cell loss (Figure 3).

Earlier studies showed quinidine caused G1 arrest and exit from the cell cycle [3]. Ki67 is a nuclear protein that is expressed throughout the cell cycle. The absence of Ki67 protein is a marker for non-proliferating cells that have entered G0 phase, and, therefore, provides a means of monitoring whether cell cycle exit might contribute to growth arrest [10]. By measuring Ki67 expression immunohistochemically, chloroquine (33 μM), quinidine (110 μM), and quinine (40 μM) were shown to promote exit from the cell cycle by 48 h. Under normal culture conditions, 95% of MCF-7 cells are engaged in the cell cycle, and express Ki67 antigen; 5% of the cells in the control population were negative for immunore-

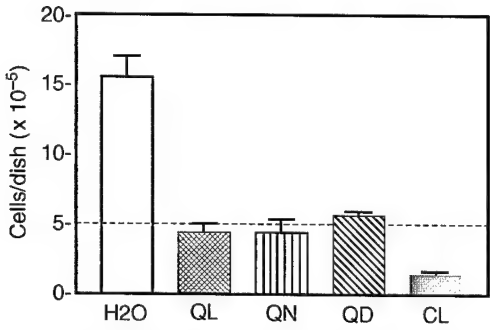

Figure 3. Effects of antimalarials on cell growth. MCF-7 cells (5×10^5) growing in 60 mm^2 dishes in DMEM/5%FBS were treated with concentrations of antimalarials corresponding to 50% inhibition of MTS activity as measured at 48 h. After 60 h incubation with antimalarials or solvent alone, viable cells that excluded trypan blue were counted using hemacytometer. Data are the mean of $n = 3 \pm$ SE independent experiments.

active Ki67 (Figure 4(A)). The percentage of Ki67 negative MCF-7 cells after 48 h growth in the presence of chloroquine, quinidine or quinine increased 6–7-fold to 30–40% compared to control cells ($p < 0.01$) (Figure 4(A)). Thus, growth inhibition by chloroquine, quinine, and quinidine can be explained in part by exit of cells from the cell cycle. Quinoline (62 μM), however, caused cell numbers to stabilize without shifting cells into G0.

Quinine, chloroquine, and quinidine also were similar in their ability to promote a more differentiated phenotype in MCF-7 cells, the accumulation of ORO positive lipid droplets in the cytoplasm [11] (Figure 4(B)). Quinoline was inactive in this assay as well. The data suggest that the stereoisomers, quinidine, and quinine act similarly, but with different potency, causing growth arrest, exit from the cell cycle and differentiation. Chloroquine was more potent and more toxic than quinidine and quinine. Chloroquine caused cell cycle exit; examination of the cells after ORO staining revealed morphologic evidence of differentiation (lipid droplets) as well as apoptotic cell death (condensed cells with heavy nuclear staining with hematoxylin). Quinoline caused arrest of cell growth without promoting cell cycle exit or any evidence of differentiation. Quinoline-treated cells showed no evidence of cytotoxicity, and the mechanism for the growth arrest is unclear.

In breast cells, the human milk fat protein is another cell differentiation marker [12]. The monoclonal antibody MFGM identifies antigens found on the milk fat globule membrane, which surrounds milk fat [13]. The expression of MFGM protein was measured by western blot analysis in MCF-7 cells exposed to antimalarials for 48 h. The densitometric signals in arbitrary units derived from scanning the immunoblots

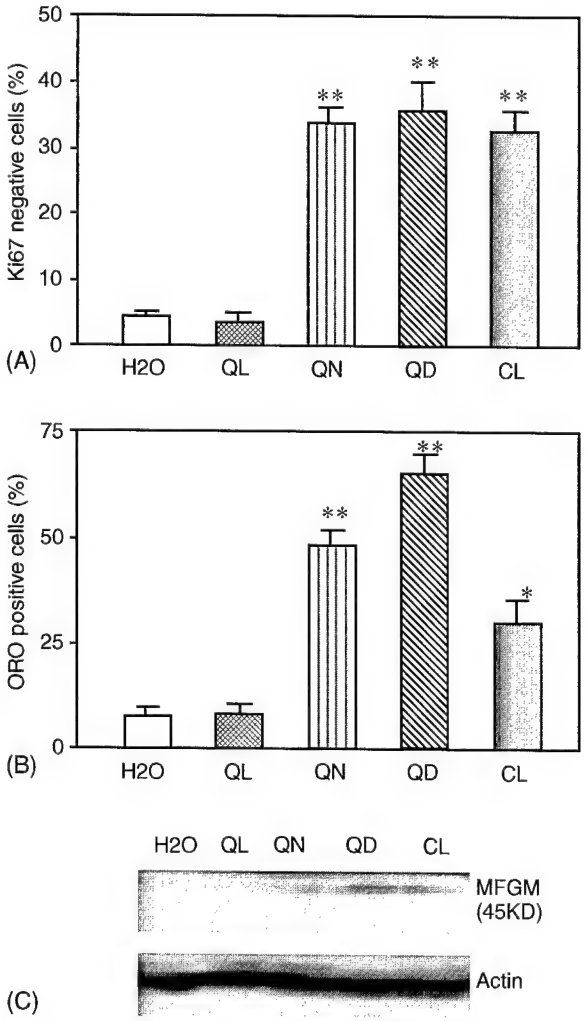

Figure 4. Cell differentiation by antimalarials. Ki67 expression, lipid droplet accumulation and human MFGM levels were measured in MCF-7 cells. MCF-7 cells were grown in 35 mm^2 dishes on sterile glass coverslips in DMEM/5%FBS. Cells were treated with solvent (distilled H_20) or the MTS IC50 of each antimalarial for 48 h (A) Ki67 immunoreactivity was performed as previously described by Wang et al. [3]. The data represent the mean percentage of Ki67 negative cells in each treatment group ($n = 3 \pm$ SE); 500 cells per experiment were counted. (B) Lipid droplet accumulation was measured using ORO staining in MCF-7 cells treated with antimalarials. The data represent the percentage ORO positive cells in each treatment group ($n = 3 \pm$ SE); 300 cells per treatment were counted. (C) Protein aliquots (25 ug) from the cell lysates were separated by 12% SDS-polyacrylamide gel electrophoresis and analyzed by western blotting using an antibody specific for MFGM. Actin protein was used as a loading control. Data are representive of two independent experiments. Statistically significant differences between control and treatment groups are indicated (*, $p < 0.05$; **, $p < 0.01$).

is provided in parantheses following each treatment. Quinidine (8872), quinine (7548), and chloroquine (8205) increased MFGM protein compared with control (5241) MCF-7 cells (Figure 4(C)). In contrast, MFGM protein levels were not changed by quinoline (5312) treatment. Changes of MFGM in MCF-7 cells by quinidine, quinine, and chloroquine are consistent with induction of lipid droplets. The coinduction of MFGM, and lipid droplets support our conclusion that quinidine, quinine, and chloroquine caused differentiation in MCF-7 cells.

Effect of antimalarials on apoptosis in MCF-7 cells

Morphological evidence that quinidine activated apoptosis in MCF-7 cells [3] prompted examination of apoptosis in cells exposed to antimalarials using the nucleosome release assay. Levels of apoptosis after 48 and 72 h were measured over a range of concentrations that spanned the respective MTS IC50 values for each compound. Etoposide (30 uM), a topoisomerase II inhibitor, elicits nucleosomal laddering in MCF-7 cells and was used as a positive control for this assay [14]. The enrichment of apoptotic response, defined as the ratio of the apotosis signal in the presence and absence of MTS IC50 concentrations of antimalarials, calculated after 48 and 72 h is summarized in Table 1. The concentration-response curve measured for each compound at 72 h is shown in Figure 5.

Quinidine and chloroquine stimulated nucleosome release in MCF-7 cells in a concentration-dependent fashion ($p < 0.05$). Chloroquine was more potent than quinidine and apoptosis was more extensive in cells exposed to chloroquine than quinidine. In contrast, quinoline, and quinine treatments did not change nucleosome release as compared with controls ($p > 0.05$). Quinoline displayed incomplete inhibition of MTS activity, no differentiating activity, and was not expected to activate apoptosis. However quinine inhibited MTS metabolism nearly as potently as chloroquine, and stimulated cellular differentiation. The experiments provide evidence that apoptosis, measured by nucleosome release, is differentially stimulated by the stereoisomers, quinidine, and quinine, while exit from the cell cycle, differentiation, and antimalarial activity are all stereo non-selective responses.

Table 1. The apoptosis enrichment factor was calculated using data obtained from ELISA, and is the ratio: units of absorbance drug treatment group/units of absorbance control group

Compounds	Apoptosis enrichment factor (mean ± SE, $N = 3$)	
	48 h	72 h
Quinoline (62 uM)	1.00 ± 0.06	1.09 ± 0.03
Quinine (40 uM)	1.13 ± 0.09	1.19 ± 0.07
Quinidine (110 uM)	1.50 ± 0.10*	1.73 ± 0.09*
Chloroquine (33 uM)	1.75 ± 0.14*	1.82 ± 0.07*
Etoposide (30 uM)	2.74 ± 0.13*	1.23 ± 0.20
Trichostatin A (35 nM)	0.96 ± 0.06	0.91 ± 0.05

Results of treatment times of 48 h and 72 h are compared.
Data shown are the mean ± SE of three experiments performed in triplicate.
*, $p < 0.05$ for drug treatment versus control.

To investigate the stereoselectivity of the apoptotic response further, levels of p53 and a downstream target of p53, p21(WAF1), were measured in MCF-7 cells exposed for 24 h to quinidine, quinine, chloroquine or quinoline. At their MTS IC50 levels, quinidine and chloroquine elevated p53 protein in MCF-7 cells, but in cells exposed to quinine and quinoline, p53 was undetectable (Figure 6(A)). Protein p21(WAF1) was increased in chloroquine and quinidine treated cells, but not in quinine or quinoline treated cells (Figure 6(B)). An ELISA was performed on MCF-7 whole cell extracts to quantify the changes in p21(WAF1) protein in response to the antimalarials (Figure 7(A)). Trichostatin acid (TSA) was used as a positive control for these experiments. Transcription of p21(WAF1) and p21(WAF1) protein levels have been shown to be increased by TSA [15, 16]. Chloroquine caused a 10–15-fold elevation in p21(WAF1) levels in MCF-7 cells at 24 h (Figure 7(B)). The p21(WAF1) response to chloroquine exceeded that of the potent histone deacetylase inhibitor, TSA. Quinidine elevated p21(WAF1) levels 4–5-fold, approximately the same as TSA, but neither quinine nor quinoline raised p21(WAF1) protein.

Moreover, p21(WAF1) protein expression in response to quinidine (90 uM) was different in wild type p53 and mutant p53 human breast cancer cells. Quinidine treatment increased p21(WAF1) protein in MCF-7 and MCF-7*ras* cells (wild type p53) (Figure 8), but p21(WAF1) protein was not detectable in malignant MDA-MB-231 and T47D cells (mutant p53) using western blot analysis. We previously reported that quinidine (90 uM) induced cellular differentiation in all of these lines of breast cancer cells [4].

DNA binding by antimalarials

Chloroquine intercalates into DNA [9, 17, 18], but DNA intercalation is not required for antimalarial

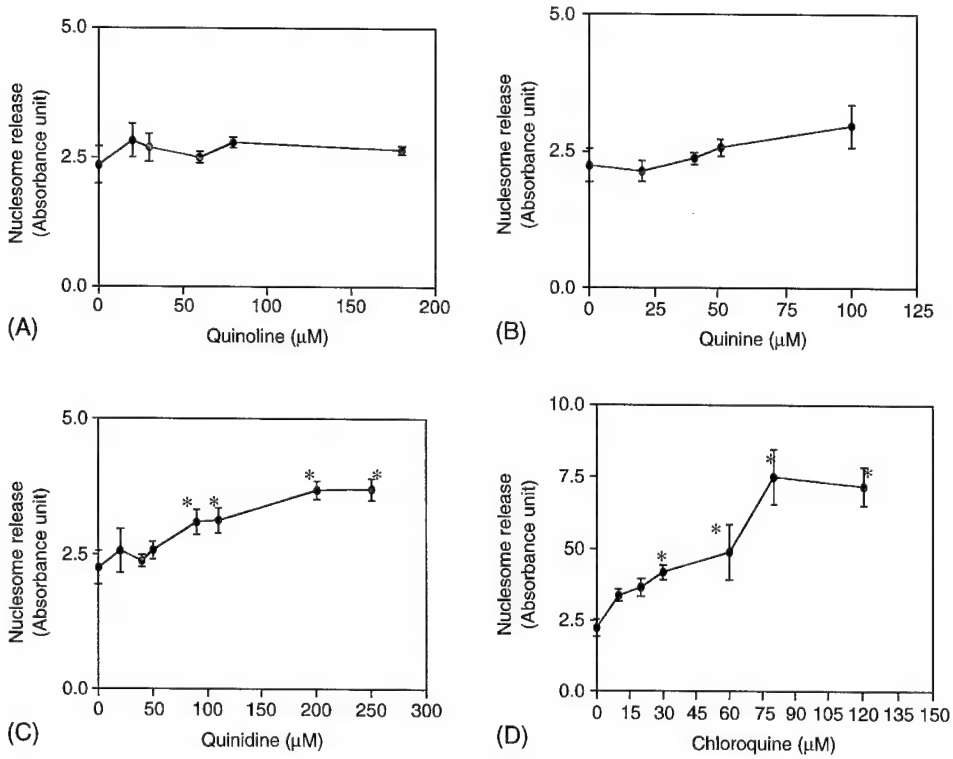

Figure 5. Nucleosome release apoptosis assay. MCF-7 cells (4000 cells/well) were grown in 96 well plates in the presence of increasing concentrations of antimalarials for 72 h. Nuclesome release was measured using the histone-DNA cell death detection kit as described in 'Materials and methods.' The level of nucleosomes released in each sample is indicated by the absorbance at 405 nm. Data are the mean ± SE of three independent experiments performed in triplicate. Statistically significant differences between control and drug treatment groups at specific drug concentrations are indicated (*, $p < 0.05$). Note the change in scale of the x-axis in Panel D.

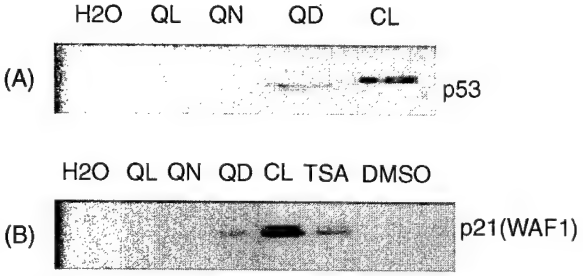

Figure 6. Western blot analysis of p21(WAF1) and p53 protein expression in human breast cancer cells. MCF-7 cells (1×10^6) were grown in 100 mm^2 dishes and treated with MTS IC50 of antimalarials for 24 h. Protein aliquots (50 μg) from the cell lysates were separated by 12% SDS-polyacrylamide gel electrophoresis and analyzed by western blotting using (A) mouse monoclonal antibody for p53. Data shown represent three independent experiments that showed the same results (B) mouse monoclonal antibody for p21(WAF1) (single experiment).

activity. We hypothesize that DNA intercalation is responsible for chloroquine-induced apoptosis, and that p53 induction by chloroquine is a consequence of DNA damage arising from intercalation. Our hypothesis predicts that chloroquine and quinidine but not quinoline and quinine intercalate into DNA. The binding of chloroquine, quinidine, and quinine to DNA was measured in an *in vitro* cell-free assay. The fluorescence signal from 2 μg of free chloroquine, quinidine, and quinine dissolved in 10 mM Tris-1 mM EDTA, pH 8 was equivalent. The addition of lambda DNA to solutions of chloroquine and quinidine, but not quinine, caused a statistically significant fluorescence quenching (Figure 9). The average fluorescence quench ratio for chloroquine in four independent experiments was 2.9 while that for quinidine was 1.8. Quinine exhibited a fluorescence quench ratio of 1.1 which was not statistically significant. The results imply stereo-selective DNA binding by quinidine, and are consistent with the pattern of quinidine activation of nucleosome release, p53 and elevations in p21(WAF1) protein levels. This is the first report of quinidine binding to DNA. Using an assay that measured changes in plasmid superhelical density, quinine was reported to intercalate into DNA, however this binding is relatively weak compared to chloroquine [18].

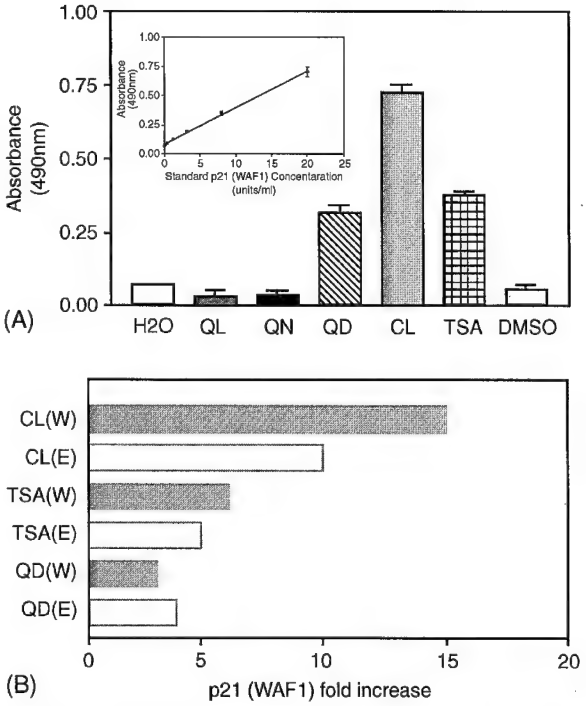

Figure 7. Effect of antimalarials on p21(WAF1) protein expression in MCF-7 human breast cancer cells. (A) p21(WAF1) ELISA. MCF-7 cells (1×10^6) were plated in 100 mm^2 dishes in DMEM/5% FBS, treated with solvent (distilled-H_2O or 0.01% DMSO) or MTS IC50 of each antimalarial for 24 h, and cell lysates prepared. TSA was dissolved in DMSO; antimalarials were dissolved in distilled H_2O. Proteins (50 μg) from the cell lysates were assayed using p21(WAF1) ELISA kit as detailed in 'Materials and methods' using a 20 min incubation time. Data are the mean ± SE of two independent experiments. (B) Comparison of p21(WAF1) protein changes detected in ELISA (E) and western blot analysis (W). W represents the fold increase in the signal density determined by densitometry; E represents the fold increase in absorbance in the ELISA. Fold increase is equal to drug treatment group divided by the control.

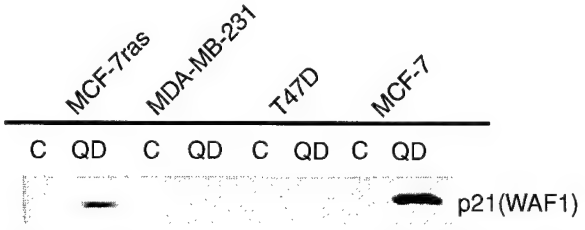

Figure 8. Effect of antimalarials on p21(WAF1) protein expression in human breast cancer cells. MCF-7, MDA-MB-231, T47D and MCF-7*ras* cells (1×10^6) were exposed to quinidine (90 μM) for 24 h. Protein aliquots (50 μg) from the cell lysates were separated by 12% SDS-polyacrylamide gel electrophoresis and analyzed by western blotting using mouse monoclonal antibody for p21(WAF1) (single experiment).

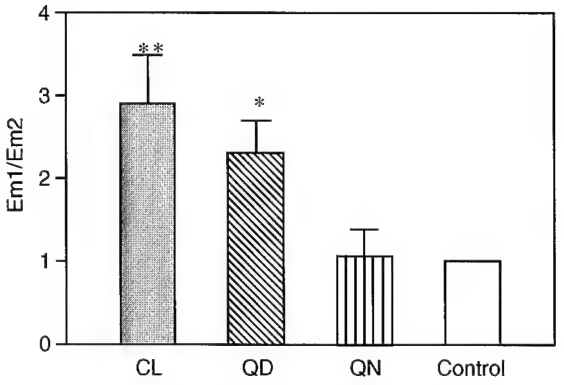

Figure 9. Fluorescence quench assay for DNA binding activity. Changes in antimalarial fluorescence upon DNA binding were measured using an excitation wavelength of 360 nm and an emission wavelength of 460 nm. Data were expressed as the fluorescence quench ratio defined as the average fluorescence of drug alone (Em1) divided by that of drug in the presence of DNA (Em2). Data represented the mean ± SE of three independent experiments. Statistically significant differences between control and treatment groups are indicated (*, $p < 0.01$; **, $p < 0.001$).

Discussion

In an effort to develop new anti-cancer therapeutic agents, we explored the anti-tumor potential of quinoline antimalarials using MCF-7 human breast cancer cells as our model system. The results of our experiments show antimalarial compounds inhibited cell growth *in vitro*, and two mechanisms for growth inhibition were identified: (1) promotion of cell cycle exit and cell differentiation and (2) activation of p53-dependent apoptosis.

Chloroquine was the most active apoptosis-inducing agent. DNA damage is a well-established apoptotic trigger that engages p53 protein as well as downstream targets of p53 including p21(WAF1) [19, 20]. Because chloroquine intercalates into DNA [21], and stimulates both p53 and p21 (WAF1) protein expression in MCF-7 cells we hypothesize that DNA damage is involved in the apoptotic response to chloroquine. The specific mechanism by which chloroquine might create DNA damage is unclear. Chloroquine is an unusual DNA intercalator because it has a two membered planar ring structure (Figure 1); in contrast, typical DNA intercalators have three or more fused planar rings [9, 21]. In addition, the tertiary aminoalkyl side-chain of chloroquine is modeled to occupy the minor groove of DNA, and this could have consequences for many DNA binding proteins and enzymes [21, 22]. Chloroquine has been reported to inhibit mammalian topoisomerase I and II [23, 24]. Inhibition of topoisomerase II activity is a clas-

sic response to DNA intercalating agents [25, 26] and topoisomerase inhibition is a potential mechanism of action of chloroquine in MCF-7 cells. Alternatively, the 10–15-fold increase in p21(WAF1) protein elicited in MCF-7 cells by chloroquine might be sufficient to activate apoptosis in the absence of DNA damage. Sheikh et al., showed that plasmid driven p21(WAF1) over expression in human breast tumor cell lines stimulated apoptosis [27]. In either this model or the DNA damage model, induction of p21(WAF1) protein emerges as a marker that can be used to screen compounds for apoptotic activity in human breast tumor cell lines.

Quinidine also increased p53 and p21 (WAF1) protein levels and stimulated apoptosis in MCF-7 cells, but was less active than chloroquine. An interesting feature of the apoptotic response of MCF-7 cells to quinidine, was the stereoselectivity. Quinine, a stereoisomer of quinidine, did not increase p53 or p21(WAF1) protein levels and did not trigger apoptotic cell death. Quinine was also less effective than either quinidine or chloroquine in binding DNA. The stereoisomers, quinine, and quinidine should prove very valuable in elucidating the mechanisms for apoptosis by quinoline drugs.

The MCF-7 response to quinine demonstrated that apoptotic cell death was not obligatory for cell growth arrest by antimalarial agents. Chloroquine, quinidine, and quinine all increased the percentage of G0 MCF-7 cells. Cell transition into the quiescent G0 phase is prerequisite for differentiation. Using lipid droplet accumulation measured by ORO staining and induction of the MFGM as markers of mammary cell differentiation, all three quinoline antimalarials were observed to induce differentiation in MCF-7 cells. Cell differentiation therapies such as FR901228, SAHA, and pyroxamide have recently entered into clinical trials and are an active area of cancer research [28, 29]. We propose on the basis of the data presented that quinoline antimalarial drugs be considered prototype compounds for the development of novel agents to stimulate breast tumor cell differentiation. Induction of differentiation by quinine was dissociated from both p21(WAF1) and apoptosis, and we conclude that differentiation is a distinct mechanism for inhibition of cell growth by antimalarials. Based on the differential response of MCF-7 cells to quinine and quinidine, we believe that a screening system based upon Ki67 expression is preferable to p21(WAF1) for identification of compounds that promote breast tumor cell differentiation.

Previous studies in our laboratory demonstrated that differentiation of MCF-7 cells by quinidine was associated with histone H4 hyperacetylation [4]. Elucidation of the regulation of histone acetylation state by antimalarials is expected to provide important insight into how quinoline antimalarials regulate breast tumor cell differentiation.

Acknowledgements

This work was supported by the Charleston Area Medical Center Foundation (8-2001), West Virginia University School of Medicine, and the US Army (DAMD 17-99-1-9449, DAMD 17-00-1-0500).

References

1. Webster Jr LT: Drugs used in the chemotherapy of protozoal infections: malaria. In: Goodman AG, Goodman LS, Rall TW, Murad F (eds) The Pharmacological Basis of Therapeutics. 7th edn MacMillan Publishing Company, NY, 1985, pp 1029–1048
2. Woodfork KA, Wonderlin WF, Peterson VA, Strobl JS: Inhibition of ATP-sensitive potassium channels causes reversible cell-cycle arrest of human breast cancer cells in tissue culture. J Cell Physiol 162: 163–171, 1995
3. Wang S, Melkoumian ZK, Woodfork KA, Cather C, Davidson AG, Wonderlin WF, Strobl JS: Evidence for an early G1 ionic event necessary for cell cycle progression and survival in the MCF-7 human breast carcinoma cell line. J Cell Physiol 176: 456–464, 1998
4. Zhou Q, Melkoumian ZK, Lucktong A, Moniwa M, Davie JR, Strobl JS: Rapid induction of histone hyperacetylation and cellular differentiation in human breast tumor cell lines following degradation of histone deacetylase-1. J Biol Chem 275: 35256–35263, 2000
5. Melkoumian ZK, Martirosyan AR, Strobl JS: Myc protein is differentially sensitive to quinidine in tumor versus immortalized breast epithelial cells. Int J Cancer (in revision)
6. Munster PN, Troso-Sandoval T, Rosen N, Rifkind R, Marks PA, Richon VM: The histone deacetylase inhibitor suberoylanilide hydroxamic acid induces differentiation of human breast cancer cells. Cancer Res 61: 8492–8497, 2001
7. Graham KA, Buick RN: Sodium butyrate induces differentiation in breast cancer cell lines expressing the estrogen receptor. J Cell Physiol 136(1): 63–71, 1988
8. Udenfriend S: Drugs and toxic agents. In: Fluorescence Assay in Biology and Medicine. Vol 1, Academic Press, NY, 1962, pp 400–443
9. Hahn FE: Chloroquine. In: Corcoran JW, Hahn FE, (eds) Antibiotics, Vol III, Mechanism of Action of Antimicrobial and Antitumor Agents. Springer-Verlag Press, NY, 1975, pp 58–78
10. Van Dierendonck JH, Keijzer R, Van De Velde CJ, Cornelisse CJ: Nuclear distribution of the Ki-67 antigen during the cell cycle: comparison with growth fraction in human breast cancer cells. Cancer Res 49(11): 2999–3006, 1989

11. Bancroft JD, Cook HC: Manual of Histological Techniques. Churchill Livingstone, Edinburgh 1984, pp 132–133
12. Munster PN, Srethapakdi M, Moasser MM, Rosen N: Inhibition of heat shock protein 90 function by ansamycins causes the morphological and functional differentiation of breast cancer cells. Cancer Res 61(7): 2945–2952, 2001
13. Turnbull JE, Baildam AD, Barnes DM, Howell A: Molecular expression of epitopes recognized by monoclonal antibodies HMFG and HMFG-2 in human breast cancers: diversity, variability and relationship to prognostic factors. Int J Cancer 38(1): 89–96, 1986
14. Giocanti N, Hennequin C, Balosso J, Mahler M, Favaudon V: DNA repair and cell cycle interactions in radiation sensitization by the topoisomerase II poison etoposide. Cancer Res 53(9): 2105–2111, 1993
15. Yoshida M, Horinouchi S: Trichostatin and leptomycin. Inhibtion of histone deacetylation and signal-dependent nuclear export. Ann NY Acad Sci 886: 23–36, 1999
16. Kim YB, Ki SW, Yoshida M, Horinouchi S: Mechanism of cell cycle arrest caused by histone deacetylase inhibitors in human carcinoma cells. J Antibiot (Tokyo) 53(10): 1191–1200, 2000
17. Davidson MW, Griggs BG, Boykin DW, Wilson WD: Molecular structural effects involved in the interaction of quinoline methanolamines with DNA. Implications for antimalarial action. J Med Chem 20: 1117–1122, 1977
18. Esposito F, Sinden RR: Supercoiling in prokaryotic and eukaryotic DNA: changes in response to topological perturbation of plasmids in *E. coli* and SV40 *in vitro*, in nuclei and in CV-1 cells. Nucl Acids Res 15: 5105–5124, 1987
19. Vogelstein B, Kinzler KW: Has the breast cancer gene been found? Cell 79(1): 1–3, 1994
20. El-Deiry WS, Tokino T, Waldman T, Oliner JD, Velculescu VE, Burrell M, Hill DE, Healy E, Rees JL, Hamilton SR: Topological control of p21WAF1/CIP1 expression in normal and neoplastic tissues. Cancer Res 55(13): 2910–2919, 1995
21. O' Brien RL, Allision JL, Hahn FE: Evidence for intercalation of chloroquine into DNA. Biochim Biophys Acta 129(3): 622–624, 1966
22. Michael RO, Williams GM: Chloroquine inhibition of repair of DNA damage induced in mammalian cells by methyl methanesulfonate. Mutat Res 25(3): 391–396, 1974
23. Sorensen M, Sehested M, Jensen PB: pH-dependent regulation of camptothecin-induced cytotoxicity and cleavable complex formation by the antimalarial agent chloroquine. Biochem Pharmacol 54(3): 373–380, 1997
24. Snyder RD: Use of catalytic topoisomerase II inhibitors to probe mechanisms of chemical-induced clastogenicity in Chinese hamster V79 cells. Environ Mol Mutagen 35(1): 13–21, 2000
25. Chen AY, Liu LF: DNA topoisomerases: essential enzymes and lethal targets. Annu Rev Pharmacol Toxicol 34: 191–218, 1994
26. Solary E, Bertrand R, Pommier Y: Apoptosis induced by DNA topoisomerase I and II inhibitors in human leukemic HL-60 cells. Leuk Lymphoma 15(1–2): 21–32, 1994
27. Sheikh MS, Rochefort H, Garcia M: Overexpression of p21WAF1/CIP1 induces growth arrest, giant cell formation and apoptosis in human breast carcinoma cell lines. Oncogene 11(9): 1899–1905, 1995
28. Yoshida M, Furumai R, Nishiyama M, Komatsu Y, Nishino N, Horinouchi S: Histone deacetylase as a new target for cancer chemotherapy. Cancer Chemother Pharmacol (suppl 1): S20–26, 2001
29. Marks PA, Richon VM, Rifkind RA. Histone deacetylase inhibitors: inducers of differentiation or apoptosis of transformed cells. J Natl Cancer Inst 92(15): 1210–1216, 2000

Address for offprints and correspondence: JS Strobl, Department of Biochemistry and Molecular Pharmacology, Robert C Byrd Health Sciences Center, West Virginia University, Morgantown, WV, 26506, USA; *Tel.*: 304-293-7151; *Fax*: 304-293-6854; *E-mail*: jstrobl@hsc.wvu.edu

Int. J. Cancer: **102,** 60–69 (2002)

Publication of the International Union Against Cancer

MYC PROTEIN IS DIFFERENTIALLY SENSITIVE TO QUINIDINE IN TUMOR *VERSUS* IMMORTALIZED BREAST EPITHELIAL CELL LINES

Zaroui K. MELKOUMIAN, Anna R. MARTIROSYAN, and Jeannine S. STROBL*

Department of Biochemistry and Molecular Pharmacology, West Virginia University, Morgantown, WV, USA

Quinidine regulates growth and differentiation in human breast tumor cells, but the immortalized mammary epithelial MCF-10A cell line is insensitive to quinidine. We found that a morphologically similar differentiation response was evoked by quinidine and c-*myc* antisense oligonucleotides in MCF-7 cells and this prompted us to investigate the actions of quinidine on c-*myc* gene expression. Myc protein levels were suppressed in human breast tumor cell lines, but not in MCF-10A cells, an observation that supports the hypothesis that suppression of c-*myc* gene expression is involved in the preferential growth and differentiation response of breast tumor cells to quinidine. Quinidine reduced c-*myc* mRNA levels in MCF-7 cells. Acute induction of c-*myc* mRNA by estradiol, as well as the c-*myc* response to sub-cultivation in fresh serum and H-*ras* driven elevations in c-*myc* mRNA were depressed by 50–60% in the presence of quinidine. Quinidine decreased c-*myc* promoter activity in MCF-7 cells in a transient reporter gene assay and a 168 bp region of human c-*myc* promoter (−100 to +68 with respect to the P1 promoter) was sufficient to confer responsiveness to quinidine. Quinidine is a potential lead compound for developing pharmacological agents to regulate Myc. In addition, the study of quinidine-regulated events is a promising approach to unravel differentiation control pathways that become disrupted in breast cancer.

Key words: *breast cancer; c-myc; differentiation; E2F; MCF-10A; MCF-7; Rb; quinidine*

Our study investigates the actions of quinidine on Myc expression in breast epithelial cells. Quinidine, a natural alkaloid, was first used therapeutically as an anti-malarial and only later, its effectiveness in the suppression of cardiac arrhythmia was discovered. The response of cardiac muscle to quinidine is caused by the blockade of sodium and potassium ion channels however, the basis for quinidine action on the malarial parasite is unknown.[1] The anti-proliferative activity of quinidine in human breast cancer cells *in vitro* was first established in our laboratory. MCF-7, MCF-7*ras*, MDA-MB-231, MDA-MB-435 and T47D human breast cancer cell lines were growth arrested and exhibited a differentiation response to quinidine.[2] A number of approaches have been taken to elucidate the mechanism of action of quinidine in human breast epithelium.[2–4] Disruption of potassium ion permeability as a result of blockade of the plasma membrane ATP-sensitive potassium channels (K_{ATP}) is hypothesized to control cell cycle progression in MCF-7 cells by preventing cell transit from G1 into S-phase.[4,5] Within 12–24 hr, the profile of G1 regulatory proteins in MCF-7 cells was typical of a G1-arrested condition. The protein, p21/WAF1, an inhibitor of cyclin-dependent kinases 4 and 6 was increased. Total retinoblastoma protein, Rb was suppressed and the hypophosphorylated Rb form was prominent. After several days in quinidine, cells exhibited evidence of cellular differentiation. The current studies address the changes in c-*myc* gene expression that accompany the anti-proliferative actions of quinidine in human breast epithelial cells. Downregulation of c-*myc* occurred in MCF-7 tumor cells but not in the immortalized breast epithelial cell line, MCF-10A. We used quinidine as a chemical probe to explore the pathways involved in the differential regulation of Myc in these 2 cell lines.

C-myc is a protooncogene whose gene product has a regulatory role in cell cycle progression, cell differentiation and apoptosis.[6,7] Aberrant expression of *c-myc* is very common in breast cancers,[8] suggesting its importance in the genesis or progression of breast cancer. It has been demonstrated that *c-myc* expression is critical for the growth of both ER-positive and ER-negative breast cancer cells *in vitro* as well as for tumor growth *in vivo*.[9] *C-myc* mRNA induction occurs within 20 min after addition of estradiol to quiescent MCF-7 human breast cancer cells.[10] In the complex with its dimerization partner, Max, Myc then act as a transcription factor to activate/suppress the expression of its target genes involved in the regulation of cell cycle progression and proliferation. Some of the *c-myc* target genes include *cdc25A*, *p15Ink4b*, *p19ARF*, *gadd 45*, *odc*, *cad*, *p53*, *cyclin D1* and *E2F*.[11,12] Reversible control of mammary epithelial cell proliferation is possible by the turn-on and turn-off of Myc protein production using a tetracycline-inducible Myc expression system.[13] Studies in different cell lines have shown that downregulation of *c-myc* by antisense oligonucleotides or expression of dominant negative *c-myc* gene accompanies terminal differentiation and permanent withdrawal from the cell cycle.[14–18] Collectively, these studies suggest that Myc is an appropriate pharmacologic target for breast cancer intervention.

MATERIAL AND METHODS

Tissue culture

MCF-7 cells passage 40–50, MCF-7*ras*,[19] MDA-MB-231 and MDA-MB-435 cells were maintained in DMEM (BioWhittaker, Walkersville, MD) supplemented with 10% heat-inactivated FBS (HyClone, Logan, UT), 2 mM glutamine and 40 μg/ml gentamicin. MDA-MB-468 (ATCC) cells were grown in 50:50 DMEM/F-12 medium (Invitrogen, Carlsbad, CA). Phenol-red free (PRF) DMEM was obtained from BioWhittaker (Walkersville, MD). Most experiments were carried out in DMEM supplemented with 5% FBS. To study the effects of quinidine on estradiol induction of c-*myc*, cells were subcultivated into PRF-DMEM containing 2% charcoal-stripped FBS and subjected to several exchanges of the media to strip cells of endogenous estrogens.[20,21] Normal human mammary epithelial cells, HMEC, (Clonetics, San Diego, CA) and MCF-10A (ATCC) were grown in MEGM according to the directions from suppliers. HMEC were grown from frozen stocks and

Abbreviations: ER, estrogen receptor; HBSS, Hank's Balanced Salt Solution; HMEC, human mammary epithelial cells; K_{ATP}, ATP-sensitive potassium channel; MAPK, mitogen activated protein kinase; MEGM, mammary epithelium growth medium; PRF, phenol red-free; Q, quinidine; Rb, retinoblastoma protein; TBS, Tris-buffered saline; TGFβ1, transforming growth factor beta-1.

Grant sponsor: US Department of Defense Breast Cancer Research Program; Grant number: DAMD 17-99-1-9447, DAMD 17-00-1-500.

*Correspondence to: Department of Biochemistry and Molecular Pharmacology, West Virginia University, Morgantown, WV 26506-9142. Fax: +304-293-6854. E-mail: jstrobl@hsc.wvu.edu

Received 10 January 2002; Revised 3 June 2002; Accepted 13 July 2002

DOI 10.1002/ijc.10648

Published online 29 August 2002 in Wiley InterScience (www.interscience.wiley.com).

used for 1–3 passages only. The cells were maintained at 37°C in a humidified atmosphere of 94% air, 6% CO_2. Cells were passaged every 5–6 days (about 70–80% confluent) at ratios of 1:5 (MCF-7, MDA-MB-468) or 1:10 (MCF-7*ras*, MDA-MB-231, MDA-MB-435 and MCF-10A). All cell counts were carried out using a hemocytometer and 0.02% Trypan blue to assess cell viability.

Chemicals

Quinidine-HCl (Q) was purchased from Sigma Chemical Co. (St. Louis, MO). Concentrated stock solutions (10 mM) were prepared fresh for use by dissolving in sterile water. Estradiol-17β (Steraloids, Wilton, NH) was dissolved in 95% ethanol at a concentration of 2 mM and diluted $1:10^6$ in the medium to a final concentration of 2 nM. Transforming growth factor-beta (TGFβ1, T) (R&D Systems, Minneapolis, MN) stock solution (2.5 μg/ml) was prepared in 4 mM HCl, 1 mg/ml BSA and stored at −20°C.

Plasmids

The human *c-myc* probe used for Northern blots was a 9 kb *EcoR*1-*Hind* III genomic fragment spanning exons I and II and intron I isolated from the plasmid pHSR-1 obtained from the American Type Culture Collection.[22] The reporter plasmids containing different regions of the human *c-myc* promoter (Del-1, Del-2, Del-4, Frag-E) linked to the firefly luciferase gene were kindly provided by Dr. Bert Vogelstein (Johns Hopkins University).[23] The promoterless luciferase plasmid was constructed by deleting the *c-myc* promoter region from the Del-4 plasmid using *Pvu* II restriction enzyme. The human *cyclin D1*-luciferase plasmid (1745CD1-Luc) was kindly provided by Dr. Richard Pestell (The Albert Einstein College of Medicine, Bronx, NY).[24] The E2F-TA-Luc plasmid and control plasmid, TA-Luc, were purchased from Clontech Laboratories, Inc. (Palo Alto, CA).

Oligonucleotide transfections

C-Myc antisense (5′-AACGTTGAGGGGCAT-3′) and sense oligonucleotides (5′-ATGCCCCTCAACGTT-3′) were purchased from Sigma-Genosys (Woodlands, TX) and diluted in sterile water to yield concentrated stock solutions of 175 μM. The stock solutions were stored at −20°C for 2 months. Cells were plated at the density of 2.2×10^5/35 mm^2 dish on glass cover slips in DMEM/5% FBS. Cells were allowed to attach to the cover slips and then the medium was exchanged to DMEM/2% FBS ± 9 μM *c-myc* antisense oligonucleotides or 9 μM of *c-myc* sense oligonucleotides as the negative control.

Antibodies

Myc (9E10, sc-40), β-catenin (E-5, sc-7963), Sp1 (PEP2), Sp3 (D-20) and E2F-1 (KH 95), antibodies (Santa Cruz Biotechnology, Santa Cruz, CA) were used at a dilution as recommended by the supplier. Another E2F-1 antibody (KH 20 + KH 95) directed against 2 regions of the Rb binding pocket was purchased from Upstate Biotechnology (Lake Placid, NY). Rb (clone G3-245) antibody that recognizes phosphorylated and non-phosphorylated forms was purchased from Pharmingen (San Diego, CA) and a phospho Rb-specific antibody ($Ser_{807/811}$) was purchased from Cell Signaling Technology (Beverly, MA). Peroxidase-conjugated secondary antibodies were used and signals were visualized using Super Signal (Pierce, Rockford, IL) or LumiGlo (Cell Signaling Technology).

Oil-red O assay

Cells were plated in 35 mm^2 tissue culture dishes on sterile glass cover slips in DMEM/5% FBS ± quinidine. After treatment, the cells were fixed (10% formaldehyde and 0.2% calcium acetate in PBS) for 3 min and stained with fresh Oil-Red O working solution (Oil-Red O stock solution [0.5% Oil-Red O in 98% isopropanol] diluted in distilled water in a 3:2 ratio) for 10 min. Cells were rinsed in water and counterstained with Mayer's hematoxylin to visualize the cell nuclei. The images were obtained using an Ortholux microscope (Ernst Leitz Wetzlar, Germany) (40× objective) and the data quantified using Image-Pro Plus software (Media Cybernetics, Silver Spring, MD).

Cell cycle analysis

Cell cycle analysis was carried out after propidium iodide staining[25] using a FACScan (Becton Dickinson, San Jose, CA) and CellFIT software.

Western blots

Cells were rinsed with 1× PBS (phosphate buffered saline: 137 mM NaCl, 2.7 mM KCl, 4.3 mM $Na_2HPO_4 \times 7H_2O$, 1.4 mM KH_2PO_4, pH 7.3) and harvested by scraping in boiling lysis buffer (1% SDS, 10 mM Tris, pH 7.4). After boiling for 5 min, the cell extract was the supernatant obtained after centrifugation in an Eppendorf microfuge (14,000*g*, 5 min, 4°C). Twenty microliter aliquots were removed for determination of protein concentrations (BCA assay, Pierce Company). To the remaining extracts, 1 mM DTT and protease inhibitors were added to the final concentrations indicated: PMSF (phenylmethylsulfonyl fluoride, 0.1 mM), aprotinin (1 μg/ml) and leupeptin (1 μg/ml). Cell extract proteins were diluted in sample buffer and denatured by heating at 100°C for 3 min immediately before loading onto 10% polyacrylamide gels. Proteins were separated and transferred to PVDF (polyvinylidene difluoride) membranes (Invitrogen, Bethesda, MD). Autoradiographic signals were quantified by densitometry (Personal Densitometer SI, Molecular Dynamics, Sunnyvale, CA) and Image QuaNT software, version 4.1. Myc signals were normalized to the 97 kDa β-catenin protein signals.

Northern blots

Total cellular RNA was purified by the method of Chomczynski and Sacchi.[26] Fifteen μg of RNA for each sample were separated on 1.2% agarose-1.9 % formaldehyde gels in MOPS running buffer (20 mM MOPS, 5 mM sodium acetate, 0.5 mM EDTA, pH 8.0) and transferred to 0.2 μm nitrocellulose paper (Schleicher and Schuell, Keene, NH) by capillary action. Pre-hybridization (15–20 hr) and hybridization reactions (40–42 hr) were carried out in the micro-hybridization oven (Bellco Glass Inc., Vineland, NJ) at 42°C for 15–20 hr. Hybridization solution included $1.5–2 \times 10^6$ cpm/ml of denatured *c-myc* DNA fragment labeled with [αP^{32}]dCTP by random priming (Rediprime DNA labeling kit, Amersham Corp., Arlington Heights, IL). The blots were washed in 2× SSC (standard saline citrate)-0.1% SDS twice for 20 min each at 37°C. A high stringency wash of the *c-myc* probe was carried out for 15 min at 42°C in 0.1× SSC-0.1% SDS buffer. The hybridization signals were quantified using PSI-PC (Molecular Dynamics) and ImageQuant software, version 4.1. Hybridization signals were normalized to levels of 18S or 28S RNA in the ethidium bromide stained gels.

Reporter gene assay

Confluent MCF-7 cells were re-seeded at a density of 8×10^5/60 mm^2 dish in 5 ml DMEM/5% FBS. After 20–24 hr, when cells were 40–50% confluent, the cell monolayers were rinsed with 1× HBSS buffer (5.4 mM KCl, 108 mM NaCl, 0.34 mM $Na_2HPO_4 \times 7H_2O$, 4.2 mM $NaHCO_3$, 0.44 mM KH_2PO_4, pH 7.2) and 5 ml of DMEM/2% FBS were added. One hour later, transfection mixes containing 5 μg of plasmid DNA in DOTAP transfection reagent (Roche Molecular Biochemicals) were added to the cells. Transfections were terminated 6–7 hr later by exchanging the medium with fresh medium ± quinidine. Cells were harvested 24 hr later by scraping into ice-cold lysis buffer (25 mM Tris-phosphate, pH 7.8, 1% Triton X-100, 2 mM EDTA, 10% glycerol). Supernatants from the cell lysates were obtained by centrifugation in an Eppendorf microfuge (14,000*g*, 5 min, 4°C). Aliquots (20 μl) were removed for protein determinations using the BCA assay. To measure luciferase activity, 50 μl of cell extracts were added to 250 μl of ice-cold luciferase sample buffer (25 mM glycylglycyl, pH 7.8, 15 mM $MgSO_4$) in polypropylene tubes. The samples were warmed to 25°C. Luciferase activity was measured using an Auto Luminat (LB 953, EG and G-Bertholdt) equipped with a dual

injection system for the addition of ATP and luciferin. The relative luciferase units obtained from 50 μl of cell extracts were normalized to 200 μg of cellular proteins. Light generation from purified luciferase (Sigma) was used as the standard in each experiment to ensure that all determinations were carried out under linear assay conditions.

Statistics

SigmaPlot software (SPSS Inc., Chicago, IL), version 5.0 and JMP software (SAS Institute, Inc., Cary, NC) were used for statistical analysis. One-way ANOVA followed by the Dunnett's test for comparison of multiple groups with control or the Tukey-Kramer test for comparison between the different groups was used. A significance level of 0.05 was used.

RESULTS

*Cellular differentiation of MCF-7 cells in response to C-*myc *antisense oligonucleotides and quinidine*

Lipid droplets are found in the cytoplasm of normal mammary epithelium and induction of differentiation in human breast cancer cell lines by retinoic acid,[27,28] vitamin D analog, 1-α-hydroxy-vitamin D5[29] and oncostatin M [30] is marked by the accumulation of cytoplasmic lipid droplets. Quinidine (90 μM) promoted the appearance of a more differentiated phenotype in MCF-7 cells characterized by an enlarged cytoplasm, rearrangement of the cytokeratin 18 cytoskeleton and the accumulation of cytoplasmic lipid droplets.[2] Figure 1 summarizes a series of experiments in which differentiation in human mammary cells *in vitro* in response to either quinidine (90 μM) or c-*myc* antisense or sense oligonucleotides was evaluated by Oil Red O staining of cytoplasmic lipid droplets. Only normal human mammary epithelial cells (HMEC) showed cytoplasmic lipid droplets in control, untreated cultures. HMEC exposed to quinidine (90 μM) for 72 hr showed no increase in lipid droplet accumulation and no signs of cytotoxicity. The latter observation was consistent with an earlier report that indicated quinidine did not inhibit HMEC proliferation.[2] HMEC, however, barely proliferate. In a 10-day growth experiment, the HMEC doubled over a period of ~120 hr and then remained at a stable cell number for another 5 days (in the presence or absence of 90 μM quinidine). MCF-10A cells are immortalized human mammary epithelial cells that do not form tumors in animals.[31] MCF-10A cells, however, proliferate more rapidly in culture (doubling time 37 hr) than the early passage MCF-7 cells used in these experiments (doubling time 57 hr). MCF-10A cells provide 1 test for discriminating whether quinidine acts upon all cells with a rapid proliferation rate, or whether quinidine differentially affects tumorigenic mammary epithelial cells. Control MCF-10A cells did not accumulate cytoplasmic lipid droplets and neither quinidine treatment or c-*myc* antisense oligonucleotides elicited this response (data not shown). In contrast, lipid droplet accumulation

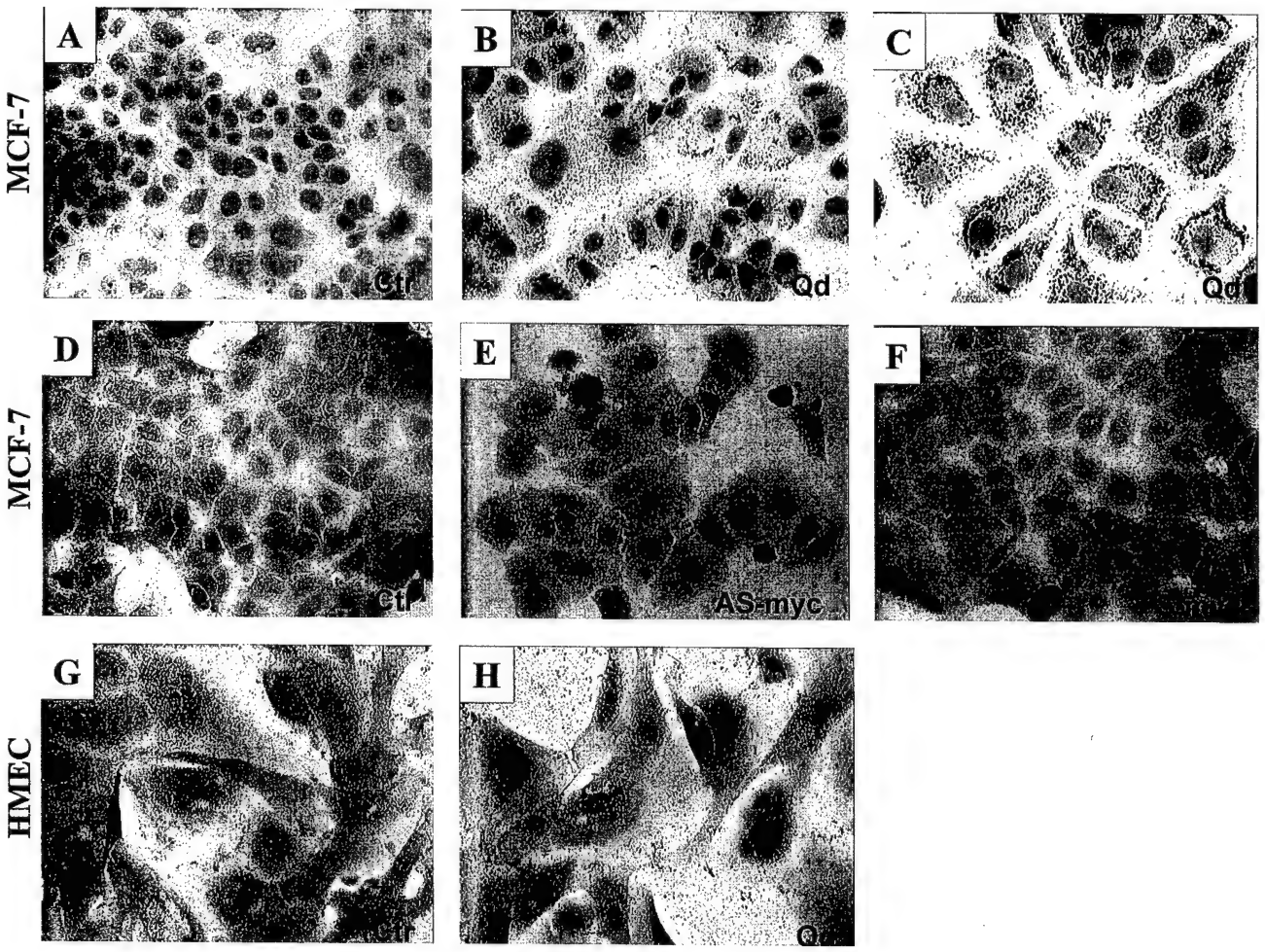

FIGURE 1 – Cellular differentiation of MCF-7 cells in response to c-myc antisense oligonucleotides and quinidine. Oil Red O staining of MCF-7 cells treated with nothing (*a,d*), 90 uM quinidine for 72 (*b*) or 120 (*c*) hr, *c-myc* antisense (*e*) or sense (*f*) oligonucleotides for 96 hr. Oil Red O staining of normal human mammary epithelial cells, HMEC, control (*g*) or treated with 90 uM quinidine (*h*) for 72 hr. Cells were counterstained with hematoxylin to visualize the cell nuclei (blue color).

and cytoplasmic enlargement was evident in MCF-7 cells treated with 90 μM quinidine for 72 hr and with c-*myc* antisense for 96 hr. Control (untreated) MCF-7 cells and MCF-7 cells exposed to c-*myc* sense oligonucleotides for 96 hr did not accumulate lipid droplets. We conclude that quinidine and c-*myc* antisense oligonucleotides promote a more differentiated phenotype in MCF-7 cells. Quinidine promoted lipid droplet accumulation in MDA-MB-231, MDA-MB-435, MCF-7*ras* and T47D cells[2] suggesting that this differentiation response is common among human mammary tumor cell lines.

Quinidine suppresses myc induction and cell growth in human breast cancer cells in vitro, *but not that of non-tumorigenic mammary epithelial cells*

Transient induction of *c-myc* mRNA and protein occurs 20–30 min after mitogenic stimulation of quiescent MCF-7 human breast cancer cells.[10] We tested whether quinidine affected Myc protein induction after release of MCF-7 cells from confluency into medium containing fresh serum. MCF-7 cells were grown in tissue culture flasks until 90–95% confluent to obtain cell populations that were 85% G0/G1 phase.[4] These confluent cells were then subcultivated into the medium containing fresh serum (5%) plus 90 μM quinidine or H_2O (vehicle). Myc protein levels were measured at the times indicated (Fig. 2). A maximal 15-fold induction of Myc protein occurred 90 min after sub-cultivation. The response is transient and Myc protein levels returned to baseline by 3 hr. Quinidine suppressed the rise in Myc protein, with a maximal 60% inhibition observed at 60 min.

Myc is a target for ubiquitination and degradation through the proteasome pathway.[32] The proteasome inhibitor, MG-132 did not preserve Myc protein levels in quinidine-treated cells (data not shown) suggesting that quinidine does not inhibit Myc levels by stimulating Myc degradation.

Quinidine also suppressed Myc expression that was stimulated in response to sub-cultivation in other breast tumor cell lines (Fig. 3, hatched bars): MCF-7*ras* (by 82%), MDA-MB-231 (by 66%), MDA-MB-435 (by 59%). The degree of suppression of Myc protein levels by quinidine correlated well with the extent of inhibition of proliferation in each of these cell lines (Fig. 3, solid bars). MCF-10A is a rapidly proliferating but non-tumorigenic mammary epithelial cell line that expresses high Myc protein levels. In contrast to the tumor cell lines, quinidine had no effect on Myc protein expression or proliferation of MCF-10A cells (Fig. 3). These results demonstrate the ability of quinidine to selectively inhibit growth and Myc protein in tumorigenic breast cells but not in an immortalized, non-tumorigenic breast epithelial line.

Suppression of myc protein and growth arrest by quinidine is not mediated through TGF-β1 response pathways

Transforming growth factor β-1 (TGF-β1) regulates epithelial cell growth, differentiation, adhesion, movement and death, but most mammary tumor cell lines are resistant to the growth inhibitory effects of TGF-β1, due to defects or deficiencies in TGF-β1 receptors or the TGF-β1 signaling pathway. C-*myc* is an important target of TGF-β1.[33,34] In MCF-10A cells, TGF-β1 stimulates the formation of an inhibitory complex on the c-*myc* promoter and rapid downregulation of *c-myc* mRNA, but this response is lost from MCF-10A cells after transformation with c-Ha-*ras* and c-*erb*B2 oncogenes.[35] TGF-β1 resistant MDA-MB-468 breast tumor cells lack Smad4, a transcription factor and an essential TGFβ1 signaling molecule.[35] In MDA-MB-231 cells, resistance to TGFβ is not fully understood, however, ectopic expression of TGF-β type III receptor suppressed tumorigenicity of MDA-MB-231 cells.[36] In contrast, MCF-7 cells have a partial response to TGFβ

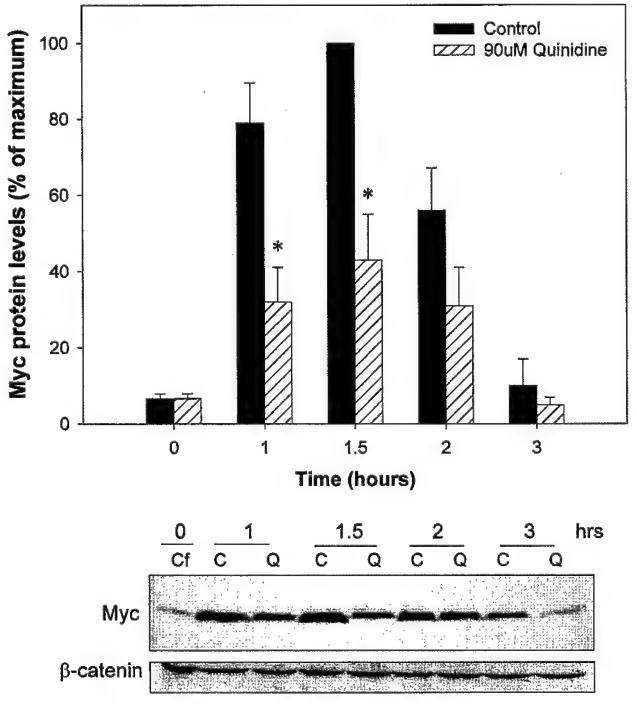

FIGURE 2 – Quinidine suppresses Myc protein induction in MCF-7 cells. Confluent (Cf) MCF-7 cells were subcultivated at 0 time in DMEM/5% FBS (solid bars) or in DMEM/5% FBS containing 90 μM quinidine (hatched bars). Cells were harvested for Western blot analysis at the times indicated. Myc protein signals were quantified by densitometry and normalized to the β-catenin signals. Data shown in the bar graph are the mean Myc protein signals ± SD of $n = 3$ experiments expressed as a percent of maximal stimulation (at 1.5 hr). The gel scans below the bar graph are a single representative experiment carried out with 80 μg of cell extract protein/lane. *Significantly different from control ($p < 0.05$).

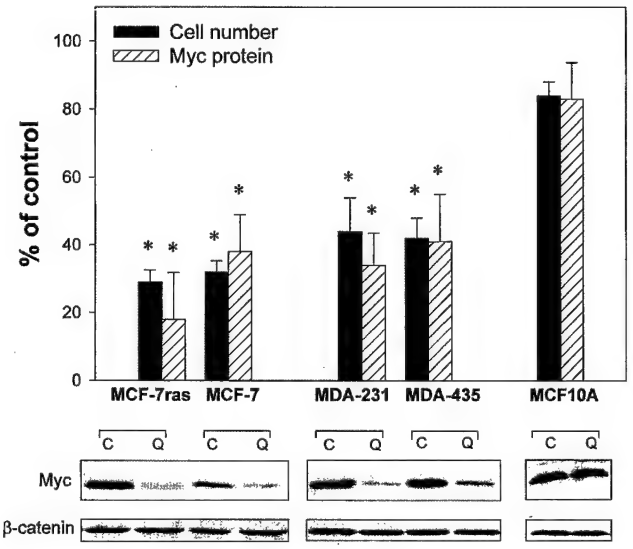

FIGURE 3 – Quinidine suppresses Myc induction and cell growth in human breast cancer cells *in vitro*, but not that of non-tumorigenic mammary epithelial cells. For the cell count assay (solid bars) confluent cells were subcultivated at the density of 1×10^5/35 mm^2 dish in DMEM/5% FBS ± 90 μM quinidine or MEGM (for MCF-10A) ± 90 μM quinidine and counted 96 hr later using a hemocytometer. For the Western blot assay (hatched bars) total cellular proteins from control or 90 μM quinidine treated cells were extracted 1 (MCF-7*ras*, MCF-7, MCF10A) or 2 (MDA-MB-231, MDA-MB-435) hr after sub-cultivation of confluent cells into DMEM/5% FBS. Myc protein signals were quantified by densitometry and normalized to the β-catenin signals. Data are the mean ± SD of $n = 3$ experiments. *Significantly different from control values ($p < 0.05$).

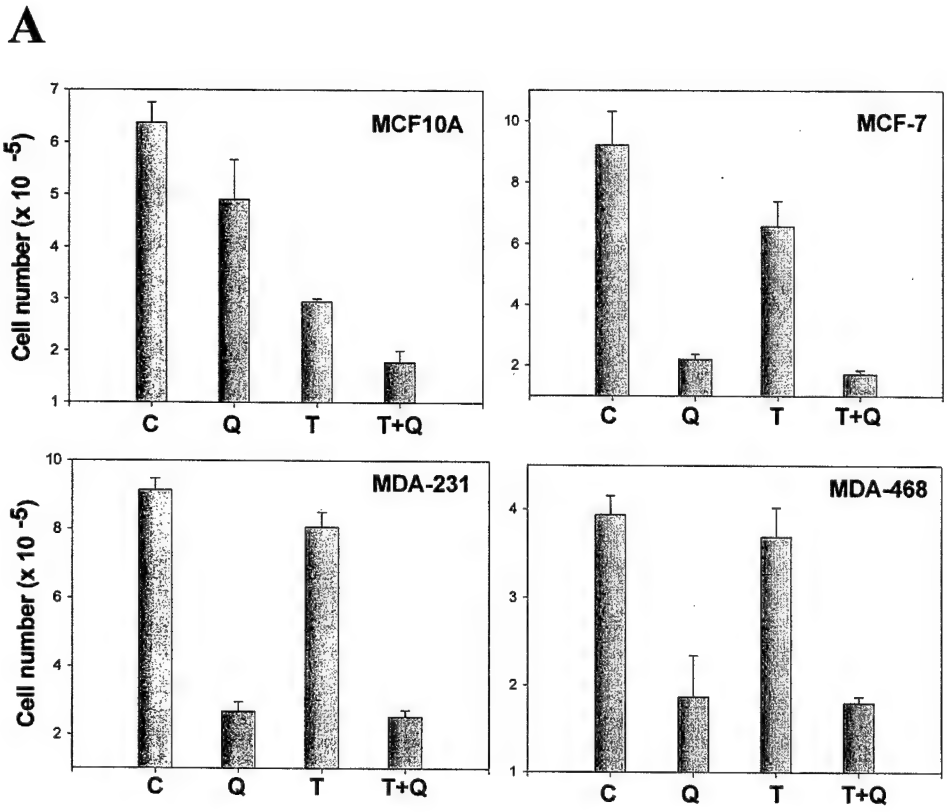

FIGURE 4 – Suppression of Myc protein and growth arrest by quinidine is not mediated by TGFβ1 response pathway. (*a*) Confluent cells were subcultivated in DMEM/5% FBS at the density of 1×10^5 (MDA-MB-231, MDA-MB-468, MCF-10A) or 2×10^5 (MCF-7) per 35 mm^2 tissue culture dish in the presence of: C-vehicle (4 mM HCl, 1 mg/ml BSA −0.5 μl/ml of medium), Q-90 μM quinidine, T-5 ng/ml TGFβ1, T+Q-90 μM quinidine + 5 ng/ml TGFβ1. Cells were harvested 72 or 96 (for MCF-7) hours later and counted using a hemocytometer. The bar graphs show cell numbers as mean ± SE of $n = 2$ experiments (MCF-7, MDA-MB-231, MDA-1B-468).The MCF-10A data are the mean ± SD of triplicates in a single experiment. (*b*) Confluent MCF-10A cells were subcultivated in MEGM containing C, Q, T or T+Q as described in (*a*). Total cellular proteins were extracted 24 hr later and analyzed for Myc and β-catenin by Western blot.

growth inhibition and ectopic TGFβRIII restores autocrine TGF-β1 activity in MCF-7 cells.[37] Despite these distinct defects in TGFβ1 signaling, quinidine inhibited proliferation in all breast tumor cell lines tested, implying that quinidine acts independently of TGF-β1 pathways (Fig. 4*a*). Furthermore, quinidine had no effect on the growth of MCF-10A cells (Fig. 3) in which the TGF-β1 pathway is intact. This result is important because it argues against the possibilities that quinidine acts either to restore a TGF-β1 response network, or to compensate for TGF-β1 defects. In Figure 4, the effects of quinidine and TGF-β1 on proliferation and Myc protein levels in a single experiment is summarized. We found (Fig. 4*a*) in this experiment that after 72 hr in quinidine MCF-10A cell numbers decreased slightly (24%), TGF-β1 alone caused a 54% reduction in cell numbers and that the combination quinidine plus TGFβ1 appeared to have an additive effect, reducing overall cell numbers by 71%. Similar reductions in the level of Myc protein in MCF-10A cells by quinidine (17%), TGF-β1 (54%) and the combination (Q+T, 71%) were observed (Fig. 4*b*). The data support the hypothesis that quinidine and TGF-β1 act through independent mechanisms to reduce c-*myc* expression and cell proliferation.

*Quinidine suppresses acute induction of C-*myc *MRNA and S-phase progression by estradiol*

Acute induction of *c-myc* mRNA transcription in MCF-7 cells exposed to estradiol is critical to progression through G1 phase of the cell cycle and the proliferative response to estradiol.[10,38] At 1 hr, quinidine suppressed estradiol-induced *c-myc* mRNA levels in MCF-7 cells in a concentration dependent fashion. Maximum inhibition (60%) of c-*myc* mRNA was achieved with 90 μM quinidine (Fig. 5*a*). These results are in good agreement with 60% suppression of Myc protein at 1 hr by 90 uM quinidine after cell sub-cultivation into fresh serum (Fig. 2). We conclude that inducible *myc* gene expression is suppressed but not completely inhibited by quinidine. Despite incomplete suppression of Myc, the actions of 90 μM quinidine were sufficient to inhibit estradiol stimulated MCF-7 cell cycle progression into S-phase (Fig. 5*b*). Confluent cells (80–85% G0/G1) were subcultivated into PRF-DMEM + 2% stripped FBS; 30 hr after plating, only 11% of the control cells progressed into the S-phase. Estradiol (2 nM) stimulated 34% of the cells to enter into S-phase by 30 hr and this response was nearly completely blocked in the presence of quinidine (14% S-phase cells).

*Quinidine suppresses basal and H-*ras*-driven C-*myc *MRNA and protein expression*

In MCF-7 cells, Myc is transiently induced during the G0-G1 phase transition and then remains at a constant low level throughout the cell cycle.[7] To ascertain whether quinidine affected basal *c-myc* expression, MCF-7 cells were incubated for 24 hr with 30 or 90 μM quinidine. A 24-hr treatment with 30 μM quinidine re-

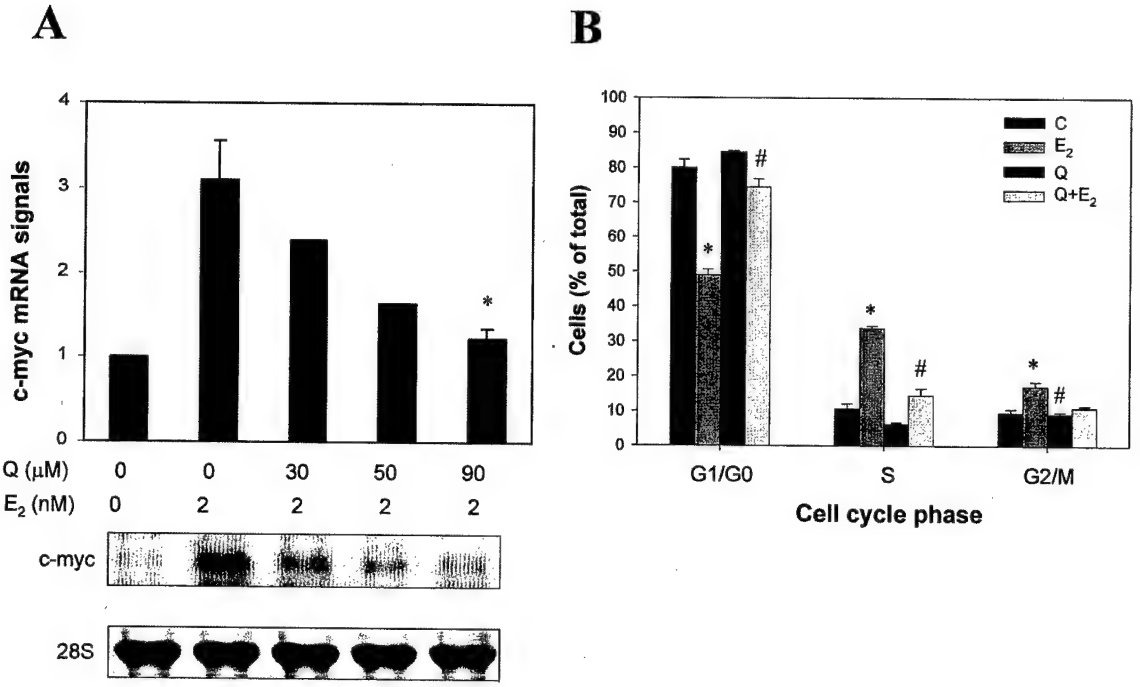

FIGURE 5 – Quinidine suppresses acute induction of c-myc mRNA and S-phase progression by estradiol. (*a*) Confluent MCF-7 cells were subcultivated in PRF-DMEM/2% stripped serum, and estrogen-depleted for 40 hr. Induction of c-myc mRNA by 2 nM estradiol ± indicated concentrations of quinidine was measured after 1 hr by isolating total cellular RNA and Northern blotting. C-*myc* mRNA signals were normalized to the 28S ribosomal signal in the ethidium bromide stained gel. Data shown on the bar graph are the mean ± SD of $n = 3$, except for 30 and 50 μM quinidine that are from a single experiment. Values for E_2 and $Q+E_2$ treated groups are reported relative to control group (control = 1). (*b*) MCF-7 cells were treated with C-0.01% ethanol (vehicle), Q-90 μM quinidine, E_2-2 nM estradiol, $Q+E_2$-90 μM quinidine + 2 nM E_2. Cell cycle phase distribution was analyzed by flow cytometry 30 hr later. Data are the mean ± SD of $n = 4$ experiments. *Significantly different from control cells ($p < 0.05$). #Significantly different from E_2 cells ($p < 0.05$).

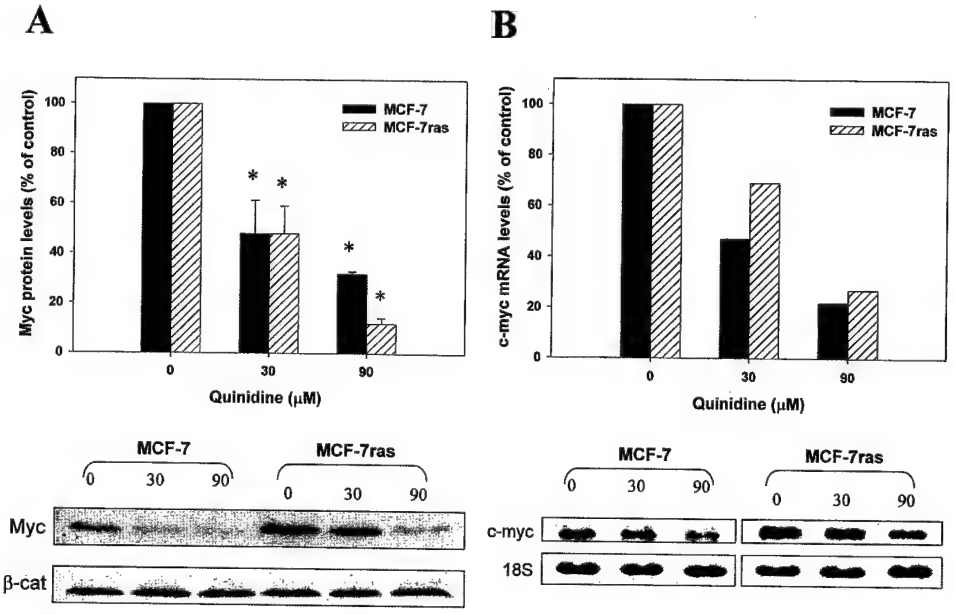

FIGURE 6 – Quinidine suppresses basal and H-*ras*-driven *c-myc* mRNA and protein expression. Confluent MCF-7 (solid bars) and MCF-7*ras* (hatched bars) cells were subcultivated into DMEM/5% FBS ± indicated concentrations of quinidine. Cells were harvested 24 hr later and Myc protein (*a*) or mRNA (*b*) levels were analyzed by Western or Northern blots, respectively. Myc protein and mRNA signals were normalized to the β-catenin and 18S ribosomal RNA signals, respectively. Data shown on the bar graphs are the mean ± SD of $n = 4$ (MCF-7) and $n = 3$ (MCF-7*ras*) experiments for (*a*) or $n = 1$ for (*b*). *Significantly different from control values ($p < 0.05$).

duced Myc protein (Fig. 6*a*) and mRNA (Fig. 6*b*) levels by approximately 50% and 90 μM quinidine had a more pronounced effect upon basal Myc protein and mRNA levels. MCF-7 cells stably transfected with H-*ras* (MCF-7*ras*) have an activated *ras* signaling pathway and express higher levels of Myc protein and mRNA than wild-type MCF-7 cells. Quinidine reduced Myc protein and mRNA expression in MCF-7*ras* cells to that seen in wild-type MCF-7 cells exposed to quinidine, suggesting that quinidine interferes with H-*ras* activated pathways that stimulate Myc. Collectively, our data demonstrate quinidine inhibits basal c-*myc* expression, estradiol-inducible c-*myc* expression, c-*myc* expression stimulated by sub-cultivation and H-*ras*-driven c-*myc* expression in MCF-7 human breast tumor cells.

*Quinidine inhibits C-*myc *promoter activity*

The ability of quinidine to inhibit c-*myc* promoter activity was tested using myc-luciferase reporter plasmids transiently transfected into MCF-7 cells. Cells were incubated in the presence of quinidine for 24 hr after transfection and luciferase activity was measured in the cell extracts. Luciferase activity in mock-transfected cells was <0.1% of the activity in control cells transfected with Del-1 (Fig. 7*a*). Quinidine treatment caused a concentration-dependent decrease in the activity of the Del-1 *c-myc* promoter. Ninety μM quinidine decreased *c-myc* promoter activity by 60%, similar to the observed levels of inhibition of Myc protein and mRNA.

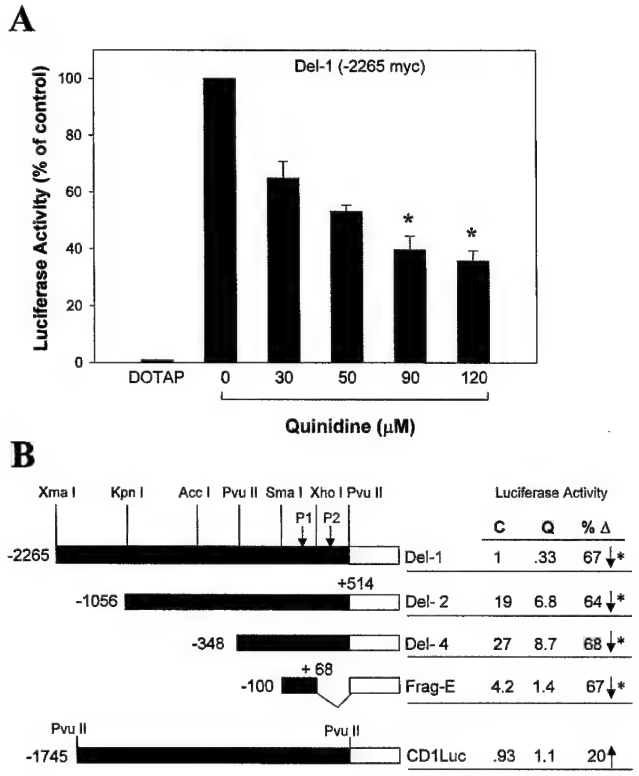

FIGURE 7 – Suppression of *c-myc* promoter activity by quinidine. (*a*) MCF-7 cells were transfected with 5 μg/dish of Del-1 (-2265 myc) *C-myc*-luciferase reporter plasmid or with the transfection mix alone (DOTAP). At the end of transfection cells were incubated for 24 hr in DMEM/5% FBS + the indicated concentrations of quinidine before preparing cell extracts for luciferase assay. Data shown are the mean luciferase activity ± SD of $n = 3$ experiments (90 and 120 μM quinidine) and $n = 2$ experiments (30 and 50 μM quinidine). The data are expressed as a percent of luciferase activity in control cells (100%). Luciferase activity in mock-transfected cells (DOTAP) was <0.01% that of control cells. Luciferase cpm in MCF-7 cell extracts in these experiments were: background (≤30), del-1 (200–500) and del-4 (2,800–6,000). *Significantly different from control (0 quinidine) cells ($p < 0.05$). (*b*) Structures of the reporter plasmids. *C-myc* and *cyclin D1* promoter regions are solid and the luciferase coding region is indicated in white. P1 and P2 are the sites of the transcription initiation from the respective *c-myc* promoters. The nucleotide locations of 5′ and 3′-ends of the myc-Luc constructs are given with respect to the P1. The effect of quinidine on *c-myc* promoter activity in 5′-deletion mutants is shown to the right of each promoter structure. Cells were transfected with 5 μg/dish of *c-myc*-Luc (Del-1, Del-2, Del-4, Frag-E) or *cyclin D1*-Luc (CD1) reporter plasmids. At the end of transfection cells were incubated for 24 hr in DMEM/5% FBS ± 90 uM quinidine before preparing cell extracts for luciferase assay. Luciferase activity driven by Del-1 in the absence of quinidine was set equal to one, and the activity of all the other promoters ± 90 μM quinidine was compared to 1. The percent change in luciferase activity by quinidine for each promoter is indicated. *Significantly different from control values ($p < 0.05$). Luciferase activity in cells transfected with promoterless construct was <2% of the activity in control cells transfected with Del-1. Data are the mean ± SD of at least $n = 3$ experiments.

To better define the region of the *c-myc* promoter responsive to quinidine, a series of 5′-deletion mutants of Del-1 was tested (Fig. 7*b*). The *cyclin D1*-luciferase (CD1) and promoterless luciferase (Luc) plasmids were used as controls. Relative luciferase activity driven by the various plasmids was compared to Del-1. Quinidine suppressed the activity of all the *myc* 5′-deletion mutants by 60–70%, but had a minimal effect on luciferase expression driven by the *cyclin D1* promoter, suggesting that the effect of quinidine is promoter specific and not related to more general effects associated with cell cycle arrest in G1. Quinidine did not inhibit the enzymatic activity of the purified luciferase protein (data not shown). We conclude that quinidine suppresses the activity of the *c-myc* promoter and that a 168 bp region of human c-myc promoter from −100 to +68 with respect to the P1 promoter is sufficient to confer responsiveness to quinidine.

Although quinidine does not appear to act by restoring TGFβ1 pathways that suppress Myc production, the TCE, a TGF-β1 control element, −86 bp to −63 bp with respect to P1, that was first identified in keratinocytes, is present in the quinidine responsive region of the c-*myc* promoter.[39] This element controls repression of the c-*myc* promoter by Rb and this might be important to the quinidine response.

The actions of quinidine on the c-*myc* Del-4 promoter and the cyclin D1 (CD1) promoter were compared in MCF-10A and MCF-7 cells. The cyclin D1 promoter was active in MCF-10A cells (877 cpm ± 23, mean ± range of duplicates in $n = 2$ experiments) and was not regulated by quinidine (90 μM, 24 hr) (894 cpm ± 23, $n = 2$). The c-*myc* Del-4 promoter, the most active of the c-*myc* promoter constructs in MCF-7 cells, was completely inactive in MCF-10A cells in 3 of 4 experiments. This was not an experimental artifact, because 2 of these experiments showed excellent activity of the cyclin D1 promoter in the MCF-10A cells and this same Del-4 construct was active in MCF-7 cells transfected in parallel with the MCF-10A cells. This result suggested that the cis-acting elements required for transcription of the *myc* gene differ in MCF-10A and MCF-7 cells.

Quinidine differentially regulates Rb/E2F1 in MCF-7 and MCF-10A cells

E2F transcription factors drive G1-S progression by activating the expression of genes required for entry into S-phase.[40,41] Two E2F consensus DNA binding sites are located between P1and P2 of the c-*myc* promoter and participate in the activation of c-*myc* transcription by E2F family members. These sites are present in Del-4 (−348 *myc)* and might contribute to its strong promoter activity in MCF-7 cells. E2F1 protein levels were reduced by 54% in MCF-7 cells exposed to 90 μM quinidine for 24 hr (Figs. 8,9) and total E2F transcriptional activity measured using an E2F-driven luciferase reporter gene decreased by 82 ± 2% (mean ± SE, $n = 3$). Quinidine did not affect protein levels of 2 other c-*myc* transcriptional activators, Sp1 and Sp3,[42] either at 4 hr or 24 hr (Fig. 8). The results suggest that decreased E2F activity contributed to the suppression of c-*myc* promoter activity as well as Myc protein levels observed in MCF-7 cells exposed to quinidine for 24 hr. There was, however, no decrease in E2F1 protein in MCF-7 cells after a 4 hr incubation with 90 μM quinidine (data not shown), implying that quinidine inhibition of early myc mRNA and protein induction (Figs. 2,5) occurred by a different mechanism. Nevertheless, Myc acts a positive regulator of E2F protein levels.[43] Therefore, suppression of early Myc expression by quinidine might contribute to the fall in E2F1 levels that occurred by 24 hr.

Hypophosphorylated Rb protein regulates E2F transcriptional activity by sequestering E2F in an inactive state in the Rb binding pocket. Using antibodies that recognize total Rb or only the phos-

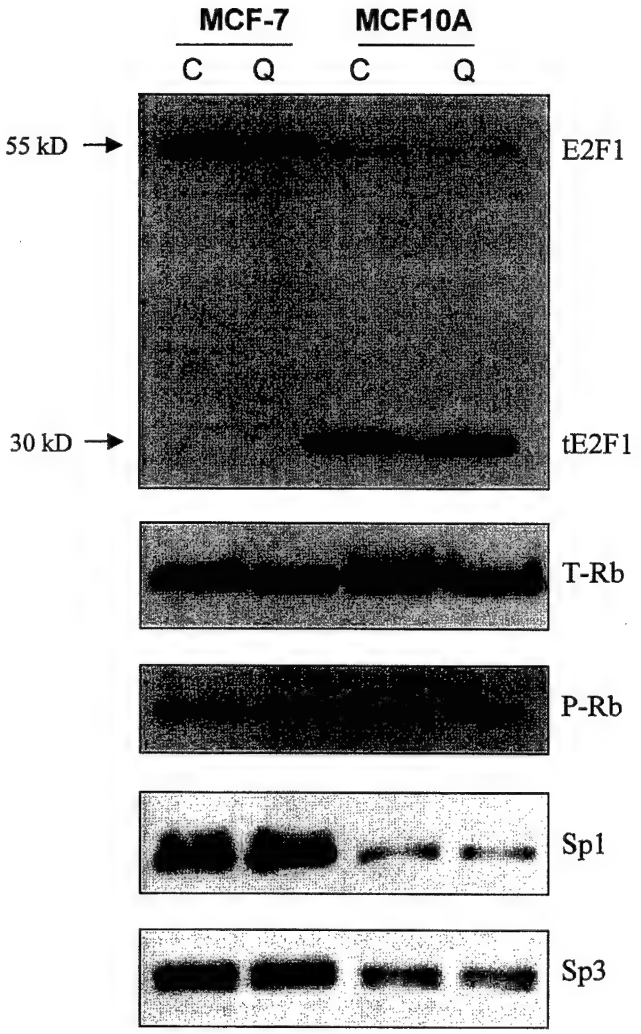

FIGURE 8 – Differential actions of quinidine on Rb and E2F1 in MCF-7 and MCF-10A cells. Cells from confluent flasks were subcultured in DMEM + 5% FBS ± 90 μM quinidine. Control (C) and quinidine-treated (Q) cells were harvested after 24 hr and levels of immunoreactive E2F1, total Rb (T-Rb), phospho ($Ser^{807/811}$)Rb (P-Rb), Sp1 and Sp3 were measured by Western blot. Total protein per lane was identical in MCF-7 and MCF-10A cells: E2F1 (60 μg/lane), T-Rb (80 μg/lane), P-Rb (60 μg/lane), Sp1 (10 μg/lane) and Sp3 (40 μg/lane). Data shown are representative of 2–4 independent experiments.

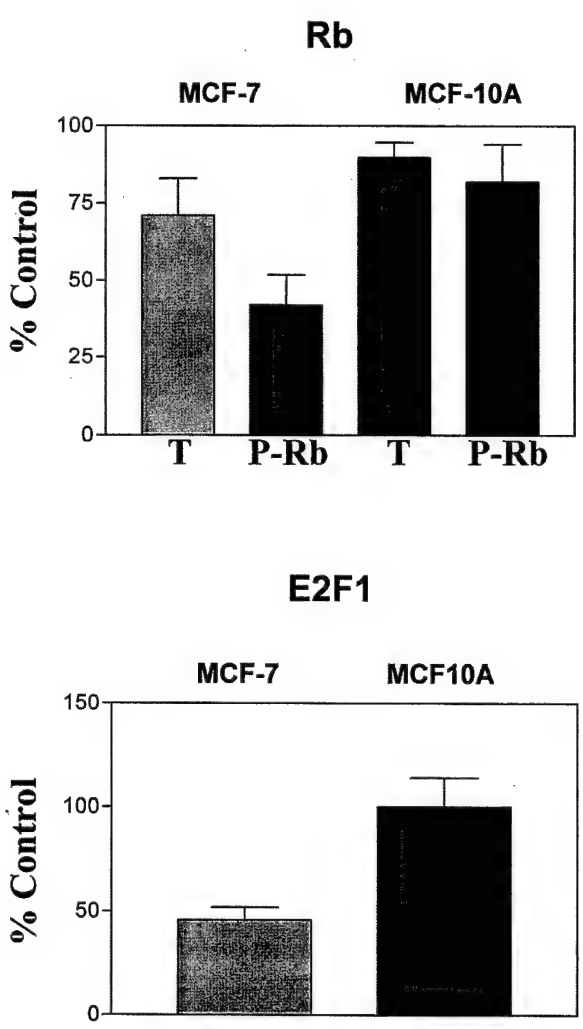

FIGURE 9 – Phospho($Ser^{807/811}$)Rb and E2F1 are decreased in quinidine-treated MCF-7 cells. Western blot immunoreactive signals corresponding to Total Rb, phosphoRb (p-Rb), and 55 kDa E2F1 protein levels obtained from extracts of cells exposed to 90 μM quinidine for 24 hr were quantified by densitometry. The value of the control signal for each protein was set to 100% in each experiment. Data shown are the signal in quinidine-treated cells expressed as a fraction of the control. Data shown are the mean ± SE of $n = 4$ experiments for MCF-7 cells and the mean and range of $n = 2$ experiments for E2F1 and Total Rb in MCF-10A cells, and the mean ± SE of $n = 3$ experiments for p-Rb in MCF-10A cells.

phorylated form of Rb ($Ser^{807/811}$) we showed that quinidine-treated MCF-7 cells were relatively depleted of phosphorylated Rb (Figs. 8,9). Immunoprecipitation of total Rb confirmed the presence of increased E2F1 bound to Rb after quinidine treatment compared to control MCF-7 cells (data not shown). Thus, quinidine acts via at least 2 mechanisms to reduce levels of free E2F1 protein resulting in suppression of E2F-mediated gene activation.

E2F1, Sp1 and Sp3 protein levels were lower in MCF-10A cells than in MCF-7 cells and did not change with quinidine (90 μM, 24 hr) treatment (Figs. 8,9). Rb protein phosphorylation levels were nearly identical in control and in quinidine treated MCF-10A cells. These observations support the hypothesis that quinidine regulation of E2F1 in MCF-7 cells is critical to its actions on growth and Myc expression. In addition, MCF-10A cells expressed a unique E2F1 immunoreactive protein, which we refer to as truncated, or tE2F1 (Fig. 8). This 30 kDa protein bound E2F1 antibodies from 2 commercial sources highly specifically. The monoclonal antibodies that were used recognize 2 regions within the E2F1 Rb binding domain and we conclude that MCF-10A cells express a truncated, E2F1-like protein that retains the Rb binding domain. This protein appears to be transcriptionally inactive. We could not detect luciferase activity in MCF-10A cells transfected with the E2F driven-luciferase reporter gene (data not shown) using as a positive control for the transfection assays, the cyclin D1-driven luciferase reporter gene. Collectively, our results suggest that the 55 kDa E2F-1 plays a minor role in driving proliferation in MCF-10A cells. This idea merits more rigorous examination, however the observed quinidine resistance of MCF-10A cells fits well the model that quinidine inhibition of E2F-1 transcriptional activity is important for its antiproliferative action and suppression of Myc expression.

DISCUSSION

In the present study, we demonstrated that pharmacological inhibition of mammary epithelial tumor cell proliferation by quin-

idine was closely associated with reduced Myc protein expression. Quinidine reduced Myc expression by 50–70% at all levels of investigation including protein, mRNA and c-*myc* promoter activity in MCF-7 cells. Given the importance of Myc to cell survival and growth and the redundancy built into signaling pathways that control these processes, quinidine is a remarkably effective Myc expression inhibitor. Quinidine interfered with estrogen-inducible *myc* expression, *ras*-MAPK pathways stimulating *myc* and mechanisms invoked by the release of cells from confluency into fresh serum leading to myc activation all of which are likely to engage components of growth factor signaling pathways.

The cdk/Rb/E2F pathway plays a critical role in G1 cell cycle progression and cellular differentiation.[40,41] Rb regulates levels of free E2F transcription factors. Unphosphorylated Rb acts as a tumor suppressor protein and sequesters E2F proteins in a transcriptionally inactive state by binding them in the Rb binding pocket. Phosphorylation of Rb or the binding of certain oncogenic viral proteins to this binding pocket, causes the release of E2F1, 2 and 3 and triggers G1-S cell cycle progression. Our results showed that after 24 hr in quinidine MCF-7 cells exhibit an overall suppression in the activity of the cdk/Rb/E2F pathway. Eighty percent of MCF-7 cells were arrested in G1/G0 phase of the cell cycle.[3,4] Protein levels of cdk4 and cyclin D1 were reduced and levels of the cyclin-dependent kinase inhibitor, p21/WAF1, were increased favoring the retention of retinoblastoma protein in its hypophosphorylated, tumor suppressor state.[2] Myc expression and that of a Myc target protein, E2F1, were suppressed, but levels of the transcription factors, Sp1 and Sp3, were unaffected by quinidine treatment. E2F activated transcription was decreased by 82% in MCF-7 cells incubated with quinidine for 24 hr. We conclude that suppression of E2F transcriptional activity is an important mechanism of quinidine action.

We also propose the idea that hypophosphorylated retinoblastoma is an important mediator of the response to quinidine. Hypophosphorylated Rb is a transcriptional repressor of myc. The activity of the human c-myc promoter was inhibited by quinidine in transiently transfected MCF-7 cells and the quinidine responsive region, −100 bp to +68 bp, contains the Rb responsive region. Quinidine did not promote the differentiation of MDA-MB-468 human breast tumor cells that lack Rb protein (Strobl, unpublished) and the reintroduction of Rb into Rb −/− SAOS cells, elicited a large cytoplasm phenotype remarkably similar to that seen in quinidine-treated MCF-7 cells.[44]

The acute rise in Myc that occurred 90 min after exposure to estradiol or subculturing in fresh serum, was suppressed by quinidine independently of its actions upon E2F1 or Rb. E2F1, Sp1 and Sp3 proteins levels did not change during a 4 hr incubation of MCF-7 cells with quinidine and the appearance of hypophosphorylated Rb in quinidine-treated MCF-7 cells occurred between 12 and 24 hr.[2] Ionic changes elicited by quinidine might attenuate the rapid induction of c-*myc* in MCF-7 cells.

In lymphocytes, a rapid induction of c-*myc* gene expression was initiated in response to stimuli that raised intracellular Ca^{+2} and pharmacological inhibition of potassium channels prevented the rise in intracellular Ca^{+2} in many cell systems.[45,46] Quinidine blocked potassium channels in MCF-7 cells at concentrations that antagonize c-*myc* induction in MCF-7 cells, causing membrane depolarization within 3 min.[3,4] Membrane depolarization can alter intracellular Ca^{+2} by reducing the driving force for calcium entry through non-selective cation channels.[46] In addition, quinidine has been reported to inhibit inositol 1,4,5-trisphosphate binding to its receptor thereby blocking Ca^{+2} release from intracellular stores.[47]

MCF-10A cells continued to proliferate in the presence of quinidine and Myc protein levels were not significantly reduced. In comparison with MCF-7 cells, MCF-10A cells maintained high levels of phosphorylated Rb expression in the presence of quinidine. MCF-10A cells also failed to differentiate in response to treatment with either quinidine or c-*myc* antisense oligonucleotides and these results are consistent with the hypothesis that both hypophosphorylated Rb and reduced Myc expression are required for the Oil Red O differentiation response in mammary epithelial cells.

MCF-10A cells exhibited evidence of a highly expressed 30 kDa immunoreactive E2F1-like protein. MCF-10A cells expressed extremely low levels of 55 kDa E2F1 protein. We could not demonstrate transcriptional activation of an E2F-driven luciferase reporter gene in MCF-10A cells and in gel mobility shift assays using extracts of MCF-10A cells, Botos *et al.*,[48] could find no evidence for the presence of E2F1 binding to the DNA consensus sequence for E2F. We conclude that MCF-10A cells over express a 30 kDa protein that retains a Rb binding domain, but lacks E2F DNA binding and transcriptional activity. The binding of a truncated E2F1-like protein to hypophosphorylated Rb could competitively inhibit the binding of other Rb pocket protein binding partners or interfere with the ability of hypophosphorylated Rb to promote differentiation. The altered E2F-1/Rb pathway in MCF-10A cells is a likely explanation for their resistance to quinidine actions on Myc and cell differentiation.

ACKNOWLEDGEMENTS

The authors are grateful to Dr. B. Vogelstein, Johns Hopkins University and Dr. R. Pestell, Albert Einstein College of Medicine for providing myc-luciferase and cyclin D1-luciferase constructs, respectively.

REFERENCES

1. Hondeghem LM, Roden DM. Agents used in cardiac arrhythmias. In: Katzung BG, ed. Basic and clinical pharmacology, 8th ed. New York: Lange Medical Publications, 2001, 219–244.
2. Zhou Q, Melkoumian ZK, Lucktong A, Moniwa M, Davie JR, Strobl JS. Rapid induction of histone hyperacetylation and cellular differentiation in human breast tumor cell lines following degradation of histone deacetylase-1. J Biol Chem 2000;275:35256–3.
3. Woodfork K, Wonderlin W, Peterson V, Strobl J. Inhibition of ATP-sensitive potassium channels causes reversible cell-cycle arrest of human breast cancer cells in tissue culture. J Cell Physiol 1995;162: 163–71.
4. Wang S, Melkoumian Z, Woodfork K, Cather C, Davidson A, Wonderlin W, Strobl J. Evidence for an early G1 ionic event necessary for cell cycle progression and survival in the MCF-7 human breast carcinoma cell line. J Cell Physiol 1998;176:456–64.
5. Wonderlin WF, Woodfork K, Strobl J. Changes in membrane potential during the progression of MCF-7 human mammary tumor cells through the cell cycle. J Cell Physiol 1995;165:177–85.
6. Amati B, Land H. Myc-Max-Mad: a transcription factor network controlling cell cycle progression, differentiation and death. Curr Opin Genet Dev 1994;4:102–8.
7. Henriksson M, Luscher B. Proteins of the Myc network: essential regulators of cell growth and differentiation. Adv Cancer Res 1996; 68:109–82.
8. Deming SL, Nass SJ, Dickson RB, Trock BJ. C-myc amplification in breast cancer: a meta-analysis of its occurrence and prognostic relevance. Br J Cancer 2000;83:1688–95.
9. Nass SJ, Dickson RB. Defining a role for c-Myc in breast tumorigenesis. Breast Cancer Res Treat 1997;44:1–22.
10. Dubik D, Shiu RP. Transcriptional regulation of c-myc oncogene expression by estrogen in hormone-responsive human breast cancer cells. J Biol Chem 1988;263:12705–8.
11. Dang CV. C-Myc target genes involved in cell growth, apoptosis and metabolism. Mol Cell Biol 1999;18:1–11.
12. Staller P, Peukert K, Kiermaier A, Seoane J, Lukas J, Karsunky H, Moroy T, Bartek J, Massague J, Hanel F, Eiler, M. Repression of p15INK4b expression by Myc through association with Miz-1. Nat Cell Biol 2001;3:392–9.
13. D'Cruz CM, Gunther EJ, Boxer RB, Hartman JL, Sintasath L, Moody SE, Cox JD, Ha SI, Belka GK, Golant A, Cardiff RD, Chodosh LA. c-MYC induces mammary tumorigenesis by means of a preferred pathway involving spontaneous Kras2 mutations. Nat. Med 2001;7: 235–9.
14. Ebinuma H, Saito H, Saito Y, Wakabayashi K, Nakamura M, Kurose

I, Ishii H. Antisense oligodeoxynucleotide against c-myc mRNA induces differentiation of human hepatocellular carcinoma cells. Int J Oncol 1999;15:991–9.
15. Canelles M, Delgado MD, Hyland KM, Lerga A, Richard C, Dang CV, Leon J. Max and inhibitory c-Myc mutants induce erythroid differentiation and resistance to apoptosis in human myeloid leukemia cells. Oncogene 1997;14:1315–27.
16. Griep AE, Wesphal H. Antisense Myc sequences induce differentiation of F9 cells. Proc Natl Acad Sci USA 1988;85:6806–10.
17. Holt JT, Redner RL, Neinhuis AW. An oligomer complimentary to c-myc mRNA inhibits proliferation of HL-60 promyelocytic cells and induces differentiation. Mol Cell Biol 1988;8:963–73.
18. Prochownik EV, Kukowska J, Rodgers C. c-Myc antisense transcripts accelerate differentiation and inhibit G1 progression in murine erythroleukemia cells. Mol Cell Biol 1988;8:3683–95.
19. Kasid A, Lippman M, Papageorge A, Lowy D, Gelmann E. Transfection of v-ras^{H} DNA into MCF-7 human breast cancer cells bypasses dependence on estrogen for tumorigenesis. Science 1985;228: 745–28.
20. Strobl JS, Kirkwood KL, Lantz TK, Lewine MA, Peterson VA, Worley JF. Inhibition of human breast cancer cell proliferation in tissue culture by the neuroleptic agents pimozide and thioridazine. Cancer Res 1990;50:5399–405.
21. Strobl JS, Lippman ME. Prolonged retention of estradiol by human breast cancer cells in tissue culture. Cancer Res 1979;39:3319–27.
22. Alitalo K, Schwab M, Lin C, Varmus H E, Bishop JM. Homogeneously staining chromosomal regions contain amplified copies of an abundantly expressed cellular oncogene (c-myc) in malignant neuroendocrine cells from a human colon carcinoma. PNAS 1983;89: 1707–11.
23. He TC, Sparks AB, Rago C, Hermeking H, Zawel L, da Costa LT, Morin PJ, Vogelstein B, Kinzler KW. Identification of c-MYC as a target of the APC pathway. Science 1998;281:1509–12.
24. Albanese C, Johnson J, Watanabe G, Eklund N, Vu D, Arnold A, Pestell RG. Transforming p21ras mutants and c-Ets-2 activate the cyclin D1 promoter through distinguishable regions. J Biol Chem 1995;270:23589–97.
25. Vindelov L, Christensen I. Detergent and proteolytic enzyme-based techniques for nuclear isolation and DNA content analysis. Methods Cell Biol 1994;41:219–29.
26. Chomczynski P, Sacchi N. Single-step method of RNA isolation by acid guanidium thiocyanate-phenol-chloroform extraction. Anal Biochem 1987;162:156–9.
27. Jing Y, Zhang J, Waxman S, Mira-y-Lopez R. Upregulation of cytokeratins 8 and 18 in human breast cancer T47D cells is retinoid-specific and retinoic acid receptor-dependent. Differentiation 1996; 60:109–17.
28. Bacus SS, Kiguchi K, Chin D, King CR, Huberman E. Differentiation of cultured human breast cancer cells (AU-565 and MCF-7) associated with loss of cell surface HER-2/neu antigen. Mol Carcinogen 1990;3:350–62.
29. Mehta RR, Bratescu L, Graves JM, Green A, Mehta RG. Differentiation of human breast carcinoma cells by a novel vitamin D analog: 1α-hydroxyvitamin D5. Int J Oncol 2000;16:65–73.
30. Douglas AM, Grant SL, Goss GA, Clouston DR, Sutherland RL, Begley CG. Oncostatin M induces the differentiation of breast cancer cells. Int J Cancer 1998;75:64–73.
31. Giunciuglio D, Culty M, Fassina G, Masiello L, Melchiori A, Paglialunga G, Arand G, Ciardiello F, Basolo F, Thompson EW, Albini A. Invasive phenotype of MCF10A cells overexpressing c-Ha-ras and c-erbB-2 oncogenes. Int J Cancer 1995;63:815–22.
32. Gross-Mesilaty S, Reinstein E, Bercovich B, Tobias KE, Schwartz AL, Kahana C, Ciechanover A. Basal and human papillomavirus E6 oncoprotein-induced degradation of Myc proteins by the ubiquitin pathway. Proc Natl Acad Sci USA 1998;95:8058–63.
33. Alexandrow M, Kawabata M, Aakre M, Moses H. Overexpression of the c-Myc oncoprotein blocks the growth-inhibitory response but is required for the mitogenic effects of transforming growth factor beta 1. Proc Natl Acad Sci USA 1995;92:3239–43.
34. Derynck R, Feng X. TGF-β receptor signaling. Biochem Biophys Acta 1997;1333:F105–50.
35. Chen C, Knag Y, Massague J. Defective repression of c-myc in breast cancer cells: a loss at the core of the transforming growth factor β growth program. Proc Natl Acad Sci USA 2001;98:992-999.
36. Sun L, Chen C. Expression of transforming growth factor β type III receptor suppresses tumorigenicity of human breast cancer MDA-MB-231 cells. J Biol Chem 1997;272:25367–72.
37. Chen C, Wang X, Sun L. Expression of transforming growth factor β (TGFβ) type III receptor restores autocrine TGFβ1 activity in human breast cancer MCF-7 cells. J Biol Chem 1997;272:12862–7.
38. Prall OW, Rogan EM, Musgrove EA, Watts CK, Sutherland RL. c-Myc or cyclin D1 mimics estrogen effects of cyclinE-cdk2 activation and cell cycle reentry. Mol Cell Biol 1998;18:4499–508.
39. Pietenpol J, Munger K, Howley P, Stein R, Moses HL. Factor-binding element in the human c-myc promoter involved in transcriptional regulation by transforming growth factor β1 and by the retinoblastoma gene product. Proc Natl Acad Sci USA 1991;88:10227–31.
40. Sears RC, Nevins JR. Signaling networks that link cell proliferation and cell fate. J Biol Chem 2002;277:11617–20.
41. Trimarchi JM, Lees JA. Sibling rivalry in the E2F family. Nat Rev Mol Cell Biol 2002;3:11–20.
42. Majello B, De Luca P, Suske G, Lania L. Differential transcriptional regulation of c-myc promoter through the same DNA binding sites targeted by Sp1-like proteins. Oncogene1995;10:1841–8.
43. Oster SK, Ho CSW, Soucie EL, Penn LZ. The *myc* oncogene: marvelously complex. Adv Cancer Res 2002;84:82–154.
44. Huang H-J, Yee J-K, Shew J-Y, Chen P-L, Bookstein R, Friedmann T. Suppression of the neoplastic phenotype by replacement of the RB gene in human cancer cells. Science 1988;242:1563–6.
45. Liburdy RP, Callahan DE, Harland J, Dunham E, Sloma TR, Yaswen P. Experimental evidence for 60 Hz magnetic fields operating through the signal transduction cascade. Effects on calcium influx and c-MYC mRNA induction. FEBS Lett 1993;334:301–8.
46. Wonderlin WF, Strobl JS. Potassium channels, proliferation and G1 progression. J Membr Biol 1996; 154: 91-107.
47. Mesra UK, Gawdi G, Pizzo SV. Chloroquine, quinine and quinidine inhibit calcium release from macrophage intracellular stores by blocking inositol 1,4,5-triphosphate binding to its receptor. J Cell Biochem 1997;64:225–32.
48. Botos J, Smith R III, Kochevar DT. Retinoblastoma function is a better indicator of cellular phenotype in cultured breast adenocarcinoma cells than retinoblastoma expression. Exp Biol Med 2002;227: 354–62.

Manuscript Under Revision

Identification of Novel Breast Cancer Cell Differentiation Agents by Functional Screening

Anna R. Martirosyan, Rayhana R. Bata, David N. Johnson, Andrew B. Freeman, Qun Zhou, Zaroui K. Melkoumian, Rachael L. Howard, Jeannine S. Strobl

Department of Biochemistry & Molecular Pharmacology, West Virginia University, Morgantown, WV 26506

Corresponding Author:

Jeannine S. Strobl, Ph.D.
Department of Biochemistry & Molecular Pharmacology
Robert C. Byrd Health Sciences Center
1 Medical Center Drive
West Virginia University
Morgantown, WV 26506-9142
Phone 304-293-7151
FAX 304-293-6846
Email jstrobl@hsc.wvu.edu

Running Title: Breast Cancer Differentiation Agents

Key words: breast cancer, differentiation therapy, histone deacetylase, MCF-7, MDA-MB-231, quinidine

Abbreviation: HDAC, histone deacetylase

ABSTRACT

Quinidine, a natural product therapeutic agent used to treat cardiac arrhythmia and malarial parasite infections, has a remarkable ability to cause human breast cancer cells to differentiate in vitro. Cell differentiation is characterized by growth arrest and exit from the cell cycle, rearrangement of the cytokeratin 18 cytoskeleton, accumulation of cytoplasmic lipid droplets and MFMG protein, and after 5-7 days, apoptotic cell death. We conducted a screen for breast tumor cell differentiation agents among drugs commonly used as antimalarials and in a series of structurally related antiproliferative compounds available from the National Cancer Institute. In general, antimalarials bearing an aminoalkyl side-chain substitution in the quinoline ring raised levels of acetylated histone H4, a marker of cell differentiation. Among the antimalarials, chloroquine was the most potent inducer of breast tumor cell differentiation measured by the loss of Ki67 antigen expression that indicated an exit of cells from the cell cycle into G_0. None of the antimalarials inhibited histone deacetylase activity in HeLa cell extracts supporting the hypothesis that these antimalarials promote cell differentiation by a novel mechanism. Of 14 quinoline-based NSC antiproliferative compounds, five were identified (NSC3852, NSC10010, NSC69603, NSC86371, and NSC305819) as breast tumor differentiation agents with activity $\geq$ quinidine. NSC3852 and NSC86371 inhibited histone deacetylase activity. Five of the six NSC identified stimulated apoptosis in breast tumor cell lines more effectively than the antimalarials. We conclude that these quinolines constitute a novel class of breast tumor cell differentiation agents.

INTRODUCTION

The family of proteins known as histone deacetylases (HDACs) has emerged as an important source of new targets for cancer drug development (reviewed in 1,2). There are 15 known HDAC proteins subgrouped into class I, II and III HDAC enzymes. The biology of the class I nuclear HDACs, hdac1 and hdac 2, in mammalian tumor cells is best understood. Class I HDACs are ubiquitous in human tumor cell lines. They catalyze the deacetylation of histones as well as transcription factors such as p53, GATA, E2F, and the estrogen receptor (ERα). In addition, the ability of hdac1 and 2 to recruit repressor protein complexes containing retinoblastoma protein (pRb), Rbp46/48, NCoR, SMRT, and Mi2 to specific chromatin regions is thought to contribute importantly to their effects on cell proliferation and differentiation in tumor cells (reviewed in 3). The binding of DNA methyltransferase (Dmt1) and methyl-CpG-binding proteins to histone deacetylase integrates control of gene expression by DNA methylation and protein acetylation (reviewed in 4).

The study of histone deacetylase regulation of gene expression has been facilitated by the availability of pharmacologic inhibitors (reviewed in 5,6). Trichostatin A (TSA) is among the first highly potent HDAC inhibitors identified. TSA is a benzamide derivative possessing an alkyl side chain terminating in hydroxamic acid. The side chain projects into the catalytic cleft of HDAC, reversibly inhibiting enzyme activity by chelating Zn^{+2} at the active site and physically blocking substrate access the active site. The hydroxamic acid series of HDAC inhibitors also includes superoylanilide hydroxamic acid (SAHA) and oxamflatin and act by a similar or identical mechanism.

A growing number of natural compounds, primarily mycotoxins but also bacterially derived products, have been found to inhibit HDAC. These compounds exhibit antifungal (TSA)

and broad spectrum antiprotozoal activity (e.g. apicidin, depudecin) as well as antiproliferative activity in mammalian cells, highlighting the broad biological significance of HDAC. Many of the HDAC inhibitors derived from fungi are cyclic tetrapeptides. These include apicidin, trapoxin, HC-toxin, chlamydocin and WF-3161 (7). The (2-amino-9,10-epoxy-8-oxodecanoic acid) (Aoe) moiety extending from the peptide ring of trapoxin, HC-toxin, WF-3161 and chlamydocin is thought to mediate irreversible inhibition of HDAC by occupying the substrate binding pocket and covalently modifiying critical amino acid(s) in the active site through the epoxide. Similarly, depudicin, a fungal metabolite with a linear, non-peptide structure contains 2 epoxide groups that may account for its irreversible inhibition of HDAC. The other fungal products, apicidin and depsipeptide, lack the epoxide moiety and reversibly inhibit HDAC. Apicidin contains a 2-amino-8-oxodecanoyl side chain and this could cause apicidin to act as a substrate mimetic, and inhibit HDAC by a mechanism similar to that of TSA (5,6). Depsipeptide (FK-228) is a bicyclic tetrapeptide devoid of an alkyl side chain, and may act by a novel mechanism (8).

In addition to the compounds already discussed, there are the low potency butyrates (sodium butyrate, phenylbutyrate and phenylacetate) (9), potent synthetic HDAC inhibitors (MS-275 and other hydroxamates) (6,10,11), and novel agents such as scriptaid (12) and valproic acid (13). All of these compounds share the ability to either reverse the transformed phenotype of tumor cells or inhibit tumor cell proliferation, and therefore are of considerable interest as potential cancer therapeutic agents.

Quinidine is a natural alkaloid produced by cinchona tree bark. In human breast tumor cells quinidine caused histone hyperacetylation, growth arrest, differentiation, and apoptosis by a novel mechanism involving degradation of hdac1 by the proteasome pathway (14). Quinidine

and TSA elicited similar phenotypic responses in MCF-7 cells. In the present study we report other natural and synthetic quinolines mimic quinidine in stimulating histone hyperacetylation, and identify quinolines as a new chemical class of breast tumor cell differentiation agents.

MATERIALS AND METHODS

Chemicals. Quinidine, chloroquine, primaquine, amodiaquin, quinine, quinoline, quinolinic acid and trichostatin A were purchased from Sigma Chemical Company (St. Louis, MO). Hydroxychloroquine sulfate was the kind gift of Mylan Pharmaceuticals, Inc. (Morgantown, WV). Dr. Robert Schultz (Drug Synthesis & Chemistry Branch, Developmental Therapeutics Program, Division of Cancer Treatment and Diagnosis, National Cancer Institute, Bethesda, MD) generously provided us with all the investigational new drugs (NSC), including the antimalarials, mefloquine (NSC157387) and halofantrine methylsulfate (NSC305789). All other reagents were purchased from Sigma or Fisher Scientific (Pittsburgh, PA).

Antibodies. The Ki67 antibody was purchased from Dako Corporation (Glostrup, Denmark) and polyclonal anti-acetylated histone H4 was purchased from Upstate (Waltham, MA). The beta-actin antibody was purchased from Sigma. Peroxidase-conjugated secondary antibodies were used at dilutions recommended by the suppliers and reactions were visualized using Super Signal (Pierce, Rockford, IL).

Cell culture. The human breast cancer cell lines, MCF-7 (passages 43-60) and MDA-MB-231 were grown in DMEM supplemented with 10% heat-inactivated fetal bovine serum, 2 mM glutamine, and 40 μg/ml gentamicin at 37° C in a humidified atmosphere of 6% CO_2/94% air.

Cells were passaged weekly. Experiments were conducted with cell populations sub-cultured from confluent flasks into medium containing 5% serum.

MTS Assay. 3-(4,5-dimethylthiazol-2-yl)-5-(3-carboxymethoxyphenyl)-2-(4-sulfophenyl)-2H-tetrazolium (MTS) (Promega, Madison, WI) is metabolized by the mitochondria of living cells to produce a colored formazan product quantifiable spectrophotometrically by the increase in absorption at 490 nm. MCF-7 or MDA-MB-231 cells were replica plated into 96-well plates and incubated for 24 h without drugs. Serial dilutions of each compound were added to the wells and cells were incubated in their presence (or solvent alone) for 48 h before addition of the MTS substrate. The absorbance (490 nm) in each well was determined after a 2 h incubation at 37 °C with the MTS. Concentration-response data obtained in this manner were analyzed using PrismGraphPad software, with data fitting to a non-linear regression. MTS $_{IC50}$ values obtained in this manner were used to estimate the antiproliferative effects of all the compounds.

Cell Differentiation End-Points. Cells were plated onto sterile glass coverslips placed into 35 mm^2 tissue culture dishes. Test compounds were used at the MTS_{IC50} values and incubations conducted for 48-72h. Differentiated mammary epithelial cells accumulate cytoplasmic lipid droplets. To visualize the appearance of cytoplasmic lipid droplets in MCF-7 and MDA-MB-231 cells in response to drug treatment, the fixed cells were stained with Oil Red O and counterstained with Mayer's hematoxylin (15). A cell containing at least 1 lipid droplet was considered positive for Oil Red O staining, and the fraction of positive cells in a population of at least 500 cells/drug condition was used as an index of cell differentiation. Differentiated cells exit the cell cycle, and are marked by the loss of immunoreactive nuclear Ki67 antigen. Immunocytochemical detection of Ki67 was performed on MCF-7 cells grown for 48 h in

MTS_{IC50} levels of test compounds or solvent alone using the methods described previously (16,17), and a Ki67 index calculated using the formula:

% Ki67 negative cells in drug-treated / % Ki67 negative cells in control cells.

Immunoblotting. To monitor histone H4 acetylation, histones were prepared from crude nuclear pellets. Equal amounts of histone protein were loaded onto 12 % SDS-polyacrylamide gels. Proteins were transferred to polyvinylidene difluoride membranes and membranes subjected to blocking and washing conditions as detailed previously (14). Signals were visualized using autoradiography.

Fluorometric Hdac Activity Assay. HeLa cell extracts contain predominantly hdac1 and hdac2 and were used as the HDAC source to screen compounds for direct HDAC inhibitory activity (HDAC Fluorescence Activity Assay, BIOMOL Research Laboratories, Inc., Plymouth Meeting, PA). MTS_{IC50} levels of each compound were added to HeLa cell extracts diluted in reaction buffer. Reactions were initiated by the addition of substrate (40μM final concentration), and were conducted for 10 minutes at 37° C in triplicate wells of a 96-well plate. Reactions were stopped by the addition of developer, and the release of fluorescently tagged product was quantified using 360nm excitation and 460nm emission.

Apoptosis Determinations. The release of nucleosomal fragments into the cytoplasm of apoptotic cells was quantified using the Cell Death Detection ELISA^{PLUS} kit (Roche Applied Science). As a measure of the ability of each compound to induce apoptosis in MCF-7 and MDA-MB-231 cells, the nucleosome-enrichment fraction was calculated as the ratio of the absorbance (405 nm) of drug-treated cultures / solvent exposed cultures. MCF-7 and MDA-MB-231 cells replica plated in triplicate into 96-well plates were exposed to MTS_{IC50} levels of

compounds for 72 h or 24 h, respectively. Cell cytoplasmic fractions from each well were assayed in duplicate for the presence of nucleosomes as directed by the supplier.

Statistical Analysis. Data were analyzed for statistical significance using a one-way ANOVA followed by Dunnett's t-test to compare drug-treated groups to the appropriate solvent control group. The level of statistical significance used was $P < 0.05$.

RESULTS

The Cell Differentiation Response to Antimalarials. Figures 1 and 2 compare the lipid droplet differentiation response in MCF-7 cells treated for 40-72h with quinoline antimalarials (quinidine, quinine, primaquine, chloroquine, amodiaquine, mefloquine), halofantrine or the HDAC inhibitor, trichostatin A (TSA). Quinoline and quinolinic acid were used as controls. Each antimalarial was screened using a range of concentrations; the data shown are the results obtained using the highest concentration of each antimalarial that did not cause overt cytotoxicity. For comparison, MCF-7 cells treated with 40 nM TSA is shown. The strongest lipid droplet accumulation responses are depicted in Figure 1 and the weaker lipid droplet responses are in Figure 2. Lipid droplets were quantified by counting the number of droplets/cell and by counting the fraction of cells containing 1 or more lipid droplets/cell. Both methods gave equivalent results. The rank order of efficacy for induction of lipid droplet accumulation in MCF-7 cells was: quinine (90 μM) ≥quinidine (90 μM) ≥ primaquine (10 μM) ≥ TSA (40 nM) > amodiaquin (10 μM) >chloroquine (10 μM)>quinoline (50 μM)>quinolinic acid (50 μM)>halofantrine (1 μM) ≥ mefloquine (1 μM). Eighty to ninety percent of cells exposed to quinine, quinidine or primaquine accumulated lipid droplets. In contrast, less than 10% of cells

incubated with quinolinic acid, mefloquine or halofantrine showed lipid droplets. A similar pattern of responses was observed when MCF-7 cells were treated for 48 h with concentrations of these drugs that inhibited MTS metabolism by 50% (MTS_{IC50} levels) (Table 1). TSA (40 nM) caused approximately 75% of MCF-7 cells to accumulate lipid droplets by 40 h. For comparison, the TSA MTS IC_{50} in MCF-7 cells was 35nM, and 8.5 nM was the TSA IC_{50} measured for HDAC activity in HeLa cell extracts. TSA was the most potent inducer of differentiation in this experiment, however the data show that strong differentiation responses were elicited by many of the quinoline antimalarials.

Histone H4 Hyperacetylation and Cell Differentiation by Antimalarials. The ability of quinidine to stimulate MCF-7 histone acetylation and differentiation was shared by other antimalarial drugs. Histone H4 hyperacetylation in response to MTS_{IC50} levels of the antimalarial drugs chloroquine, primaquine and quinine was comparable to that of quinidine and TSA (Figure 3). The antimalarials halofantrine and amodiaquin also increased histone H4 acetylation (data not shown). However, the antimalarial, mefloquine, and structural analogs lacking antimalarial activity (quinoline and quinolinic acid) did not raise histone H4 acetylation levels (data not shown). All of the antimalarials that stimulated histone H4 acetylation and differentiation as measured by lipid droplet accumulation possessed an aminoalkyl substitution of the quinoline ring, suggesting that this is an important chemical determinant of these responses. Halofantrine, has an aminoalkyl side chain and stimulated histone H4 hyperacetylation (24 h,11 μM halofantrine), but few cells accumulated lipid droplets in response to either 48h (11 μM halofantrine) or 72 h treatment with 1 μM halofantrine. Halofantrine is unique among the antimalarials tested because it is a phenanthrene ring compound rather than a quinoline. These

data suggested that the quinoline ring was important to the differentiation response, and a more extensive screen for breast tumor cell differentiation agents among quinoline compounds was performed.

Investigational Drugs Promote Cell Differentiation. Quinoline derivatives with demonstrated antiproliferative activity in human tumor cell lines were chosen from the compound (NSC) library maintained by the Developmental Therapeutics Program of the National Cancer Institute. Full chemical names and structures, and results of growth inhibition assays in the 60 tumor cell line screen, are posted on the NCI website (http://dtp.nci.nih.gov/). Table 1 compares the antiproliferative activity of 17 NSC agents, 7 antimalarial drugs, hydroxychloroquine (a structural analog of chloroquine used as an immunosuppressant (18), quinoline, and quinolinic acid in MCF-7 and MDA-MB-231 human breast tumor cells. Reductions in sulforhodamine blue (SRB) staining (GI_{50}) a measure of growth arrest reported by the NCI is compared with antiproliferative data obtained using the inhibition of MTS metabolism (IC_{50}) independently determined under our experimental conditions. In most instances, the IC_{50} values in the MTS assays performed in our laboratory and the NCI SRB inhibition assays were in agreement. The compounds in Table 1 are listed in order of decreasing potency for inhibition of MTS metabolism in the MCF-7 cell line. Our functional screening assays were performed using the MTS IC_{50} values determined in the MCF-7 cells and MDA-MB-231 cells. Most of the compounds listed in Table 1, with the exception of (quinoline, halofantrine, mefloquine, and NSC86372), caused lipid droplet accumulation in the breast cancer cell lines, our primary screen for potential cell differentiation agents. Compounds differed in their time course and magnitude

of lipid droplet accumulation. The concentrations needed to elicit lipid droplet accumulation among the compounds ranged from 0.1X the MTS_{IC50} to 2X-10X the MTS_{IC50}.

To facilitate discrimination of the most active cell differentiation agents, the differentiation potential of each was assessed by measuring MCF-7 cell exit from the cell cycle into G_0 as marked by the loss of Ki67 antigen immunoreactivity after a 48h incubation. The Ki67 index for 24 compounds is summarized in Figure 4, and shows 5 NSC agents and chloroquine have higher differentiating activity than quinidine by this measure. It is noteworthy that all of the compounds exhibiting a high Ki67 index (hydroxychloroquine and to the right, Figure 4)) stimulated lipid droplet accumulation $\leq MTS_{IC50}$. The compounds with low Ki67 indices (mefloquine, quinoline, NSC86372, and halofantrine) were those compounds that were negative for lipid droplet accumulation. Thus using two criteria, lipid droplet accumulation and Ki67 index, it was possible to identify compounds with the greatest cell differentiation activity. Representative photographs of Oil Red O lipid droplet accumulation and Ki67 responses in MCF-7 cells exposed to NSC10010 are shown in Figure 5.

A comparison of the chemical structures (Figure 6) indicated that the quinoline antimalarials (chloroquine and quinidine) and the novel acting NSC differentiation compounds share a common structural motif, a substitution in the 4-position of the quinoline ring. In 4 compounds (quinidine, chloroquine, NSC305819, NSC10010), this substituent is an aminoalkyl side chain.

HDAC Inhibition by Cell Differentiation Compounds. To test whether the quinoline differentiation compounds shared the same mechanism of action as TSA, HDAC inhibition in cell-free HeLa extracts was measured. Two of the differentiation compounds, NSC86371 and NSC3852, inhibited HDAC activity at their MTS_{IC50} levels (Figure 7). The chemical structures

of both compounds (Figure 6) differed from the reference quinoline antimalarials and the other most active differentiation compounds. The HDAC inhibitory quinoline differentiation compounds lacked an aminoalkyl side-chain in the 4-position of the quinoline ring. None of the antimalarial agents was a direct HDAC inhibitor, nor did the quinoline ring alone inhibit HDAC. The quinoline differentiation compounds, including highly active NSC305819, NSC10010 and NSC69603, had no statistically significant effect on HDAC activity, and we conclude that this series of compounds contains novel cell differentiation agents.

Cell Differentiation and Apoptosis. Among therapeutic anticancer agents, the ability to induce apoptosis is a desirable feature. The apoptotic activity of the antimalarial compounds and the quinoline differentiation compounds was screened using the MCF-7 and MDA-MB-231 cells in a nucleosome-release ELISA (Figure 8). MCF-7 and MDA-MB-231 cells are representative of tumor cells with disparate apoptotic sensitivities. The MCF-7 cell line has wild-type p53, wild-type bcl-2 and mutant caspase-3; in contrast, MDA-MB-231 cells express mutant p53, inactive bcl-2 and wild-type caspase-3. Not surprisingly, in MCF-7 cells, the antimalarial compounds and their inactive control compounds, quinoline and quinolinic acid, were inactive in the nucleosome release assay. In general, the NSC agents caused apoptosis activity under the same conditions. In MCF-7 cells, the direct HDAC inhibitor, NSC86371, elicited a strong apoptotic response, and as a differentiation agent with one known mechanism of action, NSC86371 might be a good candidate for drug development. Three other quinoline differentiation compounds had apoptotic activity in MCF-7 cells: NSC305819, NSC10010, and NSC3852. NSC69603 is among the most active differentiation compounds, and its inability to cause apoptosis in MCF-7 cells is an indication of its unique properties as a cell differentiation agent.

There were similarities and striking differences in the apoptotic response of MDA-MB-231 and MCF-7 cells by the quinoline differentiation compounds. The antimalarials, with the exception of chloroquine, were not apoptotic in MDA-MB-231 cells. Similarly, the active quinoline differentiation compound, NSC69603 was not apoptotic in either cell line. Two other highly active differentiation agents, NSC10010 and NSC3852 induced apoptosis in MDA-MB-231 as well as MCF-7 cells. However, in contrast to our observations with the MCF-7 cells, NSC305819 and NSC86371 did not stimulate apoptosis in MDA-MB-231 cells; NSC146397, a compound that produced a very modest cell differentiation response, stimulated the strongest apoptotic response in MDA-MB-231 cells. We conclude that NSC69603 is a quinoline differentiation compound lacking in apoptotic activity. NSC10010 and NSC3852 are quinoline differentation compounds that elicit modest apoptotic responses in MCF-7 and MDA-MB-231 cells. NSC305819 and NSC86371 are quinoline differentiation compounds with very good potential for apoptosis induction, yet because of the cell line specific nature of the apoptotic response, a better understanding of the mechanistic basis for the sensitivity to apoptosis is required in order to better predict tumor cells susceptibility.

DISCUSSION

A recent hypothesis asserts that the origins of human cancers can be traced to mutational events in three critical pathways amidst a spectrum of genes controlling cell growth, death, and differentiation (19). Evidence in support of this hypothesis can be gleaned from mutational analyses of human breast tumors. In human breast cancer, gene amplification in c-*myc*, c-*neu* (*erb*B2/HER2), and the 11q13 locus occur most frequently (20-22). Overexpression of c-*myc* activates TERT gene expression and telomerase activity (23). Telomere elongation and

prevention of cell senescence is one critical event in cancer formation. The tumor suppressor proteins retinoblastoma (pRb) and p53 are engaged in a second critical pathway controlling cell cycle progression and gene expression, and inactivating mutations in these proteins are common in breast cancer (24). The third critical pathway identified involves the serine/threonine phosphatase, PP2A, but the essential role of PP2A in human tumors has not yet been defined. In addition to the evidence that breast tumors harbor critical cancer mutations, subsets of human breast tumors exhibit other mutations that confer additional abnormal properties to the tumors. The *erb*B2 amplification, which predominates in estrogen receptor negative breast cancers, activates growth factor signaling pathways including *ras*, an oncogene of broad importance to tumorigenesis (25). The 11q13 chromosomal locus is frequently amplified in estrogen receptor positive breast tumors. The 11q13 locus harbors a number of potentially important genes including CCND1, the gene encoding the cell cycle regulator, cyclin D1, EMS1, a SH3-protein capable of engaging the *src* oncogene signaling pathways, and *int-2*, the gene encoding fibroblast growth factor 3 (22). Patients with hereditary breast cancer exhibit mutations in Brca1/2, loci encoding a large, multifunctional proteins that participate in DNA replication, genome integrity as well as breast epithelial differentiation (26,27).

The genetic basis of breast cancer is being defined with the hope that this effort will establish a rational basis for effective control of this disease. In principle, suppression of the transformed phenotype in tumor cells will occur when normal expression of critical oncogenes is re-established, and this principle is tested pharmacologically by the use of cancer cell differentiation agents to control cancer. The actions of quinidine in human breast tumor cell lines exemplify this idea, targeting several critical oncogenes in breast tumors (14,15). Quinidine suppressed c-*myc* expression, restored pRb to its hypophosphorylated, active tumor suppressor-state, and

induced p53 expression. Quinidine also decreased cyclin D1 protein levels, and suppressed growth of *ras*-transformed breast tumor cells. These effects were accompanied by phenotypic differentiation of the cells, confirming that reversal of the transformed phenotype occurs when expression of critical oncogenes is normalized.

Histone deacetylase has been recognized for several years as an important new cancer drug target because of its ability to regulate gene transcription in tumor cells. Our functional screen for breast tumor cell differentiation agents identified two new small molecule inhibitors of histone deacetylase, NSC3852 and NSC86371. Although these are relatively low potency inhibitors, NSC3852 (5-nitroso-8-quinolinol) and NSC86371 (2-[2-(8-hydroxy-5-methyl-7-quinolyl)vinyl]-1,6-dimethyl iodide) are structurally distinct from the cyclic peptide natural products and the hydroxamic histone deacetylase inhibitors, and therefore might possess unique pharmacologic properties. Preliminary work with NSC3852 indicated that the nitroso substitution in NSC3852 was essential to histone deacetylase inhibition because 8-quinolinol (NSC2039) had no effect on histone deacetylase activity.

Functional screening for breast tumor cell differentiation also identified several active antimalarial compounds. Phenotypic differentiation and growth arrest in G_0 phase of the cell cycle was most prominent with chloroquine, but also occurred in cells exposed to quinidine, quinine, hydroxychloroquine, and amodiaquin. Only a subset of the therapeutically useful antimalarial agents that we screened were capable of tumor cell differentiation, and all of these were quinoline rings substituted in the 4-position with an alkylamino side chain. The two most active antimalarial compounds, chloroquine (data not shown) and quinidine, caused rapid elimination of histone deacetylase1 protein. The novelty of this response suggests that these

compounds might be used to complement existing differentiation therapies, particularly since their human pharmacology and toxicology is well established.

NSC10010 (N,N-Bis(2-methyl-6-methoxy-4-quinaldyl)-1,9-diamine-nonane dihdrochloride hydrate) and NSC305819 are novel breast tumor differentiation agents bearing striking chemical similarities to drugs possessing antimalarial activity; both contain quinoline rings with alkylamine substitutions in the 4-position. NSC69603 (4-(2,5-dimethoxystryl)-quinoline), was also an active differentiation agent, but atypically, contained a dimethoxystryl substituent in the 4- position of the quinoline ring. The structure of NSC69603 predicts that its cell differentiating activity might be distinct from that of the antimalarial compounds.

The chemical parallels between antimalarials and the new quinoline class of breast tumor cell differentiation agents identified by functional screening suggest the malarial literature as a rich new source for tumor cell differentiation agents. The fortuitous identification of NSC10010 as a breast tumor cell differentiating agent, a bisquinoline nearly identical to an antimalarial (N, N-Bis(7-chloroquinolin-4-yl)nonane-1,9-diamine)) supports this hypothesis. In fact, an extensive series of 4-substituted bisquinolines have been synthesized because they show good activity against chloroquine-sensitive and chloroquine-resistant malaria (28). The sensitivity of chlorquine-resistant malaria to bisquinolines has been attributed to the poor drug export by *pfmdr* (Plasmodium falciparum multi-drug resistant pump), one important malarial resistant factor. Drug resistance pumps in human tumor cells and Plasmodia are both senstive to verapamil, raising speculation that bisquinolines would provide a novel source of breast tumor cell differentiation agents and/or chemosensitizers in multi-drug resistant tumor cells. We conclude that antimalarial bisquinolines provide an exciting category of compounds for future evaluation as breast tumor differentiating agents.

Figure Legends

Figure 1. MCF-7 Cell Differentiation by TSA and Antimalarials. MCF-7 cells were incubated with quinidine (QD,90 μM), quinine (QN, 90 μM), or primaquine (PQ, 10 μM) for 72 h or TSA (40 nM) for 40 h; cells were fixed and stained with Oil Red O. Typical microscopic fields are shown. In addition, the differentiation response was quantified by counting the number of lipid droplets in each cell and the fraction of cells in each category was computed.

Figure 2. MCF-7 Cell Differentiation Elicited by Selective Antimalarials. MCF-7 cells were incubated with ethanol (CTRL, 0.1%), chloroquine (CQ, 10 μM), halofantrine (HF, 1 μM), or mefloquine (MQ, 1μ M) for 72 h. Cells were fixed and stained with Oil Red O. Typical microscopic fields are shown. Lipid droplets were quantified as described in Figure 1.

Figure 3. Antimalarials Increase Histone H4 Acetylation in MCF-7 Cells. MCF-7 cells (1 x 10^7 cells/T150 flask) were incubated in the presence of MTS IC_{50} levels of chloroquine (CQ), quinidine (QD), TSA, quinine (QN) or primaquine (PQ) for 24 h. Histone proteins (50 μg) were electrophoresed through 12% SDS polyacrylamide gels; immunoblotting was performed using antibody against acetylated histone H4.

Figure 4. Ki67 Index of Differentiation in MCF-7 Cells. Compounds (MTS IC_{50} levels) were added to the cells; 48h later, immunohistochemistry was performed to detect Ki67 antigen. The Ki67 index is the ratio of the % of Ki67 negative cells in (drug-treated/control cells). Control cells were treated with water, 0.1% DMSO, or 0.1% ethanol as appropriate in each experiment. Data represent the mean ±S.E. of n= 3 independent experiments except NSC86372 (n=2), primaquine (n=6), NSC2039 (n=1), NSC124637 (n=2), hydroxychloroquine (n=5), NSC86373 (n=4), NSC305819 (n=4), chloroquine (n=7). * $p<0.05$

Figure 5. Differentiation of MCF-7 Cells by NSC10010. MCF-7 cells were incubated with 4 μ M NSC10010 or solvent control (0.003% DMSO) for 48 hours. Cells were fixed and stained with Oil Red O to detect lipid droplet accumulation or immunohistochemistry was performed to detect Ki67 antigen. Results shown are typical of n = 3 experiments.

Figure 6. Chemical Structures of Quinoline Differentiation Compounds.

Figure 7. Effect of Quinoline Differentiation Compounds on HDAC Activity. MTS IC_{50} levels of compounds were added to HeLa cell extracts containing HDAC diluted into reaction buffer. Reactions were initiated by the addition of substrate. Fluorescent product was measured after 10 minutes at 37^0C. Data shown are the fluorescent product released as % of control (mean ± SE) of n=3 experiments performed in triplicate. * $p<0.05$

Figure 8. Apoptosis in MCF-7 and MDA-MB-231 Cells. Cells were subcultured into 96-well plates, and MTS IC_{50} levels of compounds were added; 72 h (MCF-7) or 24 h (MDA-MB-231) later, apoptosis was assayed using a nucleosome release ELISA. Nucleosome release in control cells is 1.0, and the ratio of nucleosomes released in drug-treated/control cells is plotted. Data represent the mean ±SD of triplicate determinations in a single experiment.

ACKNOWLEDGEMENTS This work was supported by grants from the US Army Breast Cancer Research Program (DAMD 17-00-1-500, DAMD 17-99-1-9447, and DAMD 17 –02-1-0622), The West Virginia University School of Medicine, and the Spurlock Cancer Research Fund.

REFERENCES

1. Marks, P.A., Rifkind, R.A., Richon, V.M. and Breslow, R. Inhibitors of histone deacetylase are potentially effective anticancer agents. Clin.Cancer Res. 7: 759-760, 2001.

2. Vigushin, D.M. and Coombes, R.C. Histone deacetylase inhibitors in cancer treatment. Anti-cancer Drugs 13: 1-13, 2002.

3. Johnson, C.A. Chromatin modification and disease. J. Med. Genet. 37: 905-915, 2000.

4. Wolffe, A.P., Urnov, F.D. and Guschin, D. Co-repressor complexes and remodelling chromatin for repression. Biochem. Soc. Trans. 28: 379-386, 2000.

5. Weidle, U.H. and Grossmann, A. Inhibtion of histone deacetylases: a new strategy to target epigenetic modifications for anticancer treatment. Anticancer Res. 20: 1471-1486, 2000.

6. Marks, P.A., Richon, V.M. and Rifkind, R.A. Histone deacetylase inhibitors: inducers of differentiation or apoptosis of transformed cells. J. N.C.I. 92: 1210-1216, 2000.

7. Darkin-Rattray, S.J., Gurnett, A.M., Myers, R.M., Dulski, P.M., Crumley, T.M., Allocco, J.J., Cannova, C., Meinke, P.T., Colletti, S.L., Bednarek, M.A., Singh, S.B., Goetz, M.A., Dombrowski, A.W., Polishook, J.D. and Schmatz, D.M. Apicidin: A novel antiprotozoal agent that inhibits parasite histone deacetylase. Proc. Natl. Acad. Sci. (USA) 93: 13143-13147, 1996.

8. Furumai, R., Matsuyama, A., Kobashi, N., Lee, K.-H., Nishiyama, M., Nakajima, H., Tanaka, A., Komatsu, ., Nishino, N., Yoshida, M., and Horinouchi, S. FK228

(Depsipeptide) as a natural prodrug that inhibits class I histone deacetylases. Cancer Res. 62: 4916-4921, 2002.

9. Samid, D., Hudgins, W.R., Shack,S., Liu, L, Prasanna, P., and Myers, C.E. Phenylacetate and phenylbutyrate as novel, nontoxic differentiation inducers. Adv. Exp. Med. Biol. 400A:501-505, 1997.

10. Komatsu, Y., Tomizaki, K.-y., Tsukamoto, M., Kato, T., Nishino, N., Sato, S., Yamori, T., Tsuruo, T., Furumai, R., Yoshida, M., Horinouchi, S., and Hayashi, H. Cyclic hydroxamic-acid-containing peptide 31, a potent synthetic histone deacetylase inhibitor with antitumor activity. Cancer Res. 61: 4459-4466, 2001

11. Remiszewski, S.W., Sambucetti, L.C., Atadjia, P., Bair, K.W., Cornell, W.D., Green, M.A., Howell, K.L., Jung, M., Kwon, P., Trogani, N. and Walker, H. Inhibitors of human histone deacetylases: synthesis and enzyme and cellular activity of straight chain hydroxamates. J. Med. Chem. 45: 753-756.

12. Su, G.H., Sohn, T.A., Ryu, B., and Kern, S.E. A novel histone deacetylase inhibitor identified by high-throughput transcriptional screening of a compound library. Cancer Res. 60: 3137-3142, 2000.

13. Gottlicher, M., Minucci, S., Zhu, P., Kramer, O.H., Schimpf, A., Giavara, S., Sleeman, J.P., Lo Coco, F., Nervi, C., Pelicci, P.G., and Heinzel, T. Valproic acid defines a novel class of HDAC inhibitors inducing differentiation of transformed cells. EMBO J. 20: 6969-6978, 2001.

14. Zhou, Q., Melkoumian, Z.K., Lucktong, A., Moniwa, M., Davie, J.R., and Strobl, J.S. Rapid induction of histone hyperacetylation and cellular differentiation in

human breast tumor cell lines following degradation of histone deacetylase-1. J. Biol. Chem. 275: 35256-35263.

15. Melkoumian, Z.K., Martirosyan, A.R., and Strobl, J.S. Myc protein is differentially sensitive to quinidine in tumor versus immortalized breast epithelial cell lines. Int. J. Cancer 102: 60-69, 2002.

16. Wang, S., Melkoumian, Z.K., Woodfork, K.A., Cather, C., Davidson, A.G., Wonderlin, W.F. , and Strobl, J.S. Evidence for an early G1 ionic event necessary for cell cycle progression and survival in the MCF-7 human breast carcinoma cell line. J. Cell. Physiol. 176: 456-464, 1998.

17. Zhou, Q., McCracken, M.A., and Strobl, J.S. Control of mammary tumor cell growth in vitro by novel cell differentiation and apoptosis agents. Breast Cancer Res. Treat. 75: 107-117, 2001.

18. Kremer, J.M. Rationale use of new and existing disease-modifying agents in rheumatoid arthritis. Ann. Int. Med. 134: 695-706, 2001.

19. Hahn W.C. and Weinberg, R.A. Modelling the molecular circuitry of cancer. Nature Rev. Cancer 2: 331-341, 2002.

20. Deming, S.L., Nass, S.J., Dickson, R.B., and Trock, B.J. C-myc amplification in breast cancer: a meta-analysis of its occurrence and prognostic relevance. Br.J. Cancer 83: 1688-1695, 2000.

21. Jardines, L., Weiss, M., Fowble, B. and Greene, M. neu(cerbB-2/HER2) and the epidermal growth factor receptor (EGFR) in breast cancer. Pathobiol. 61: 268-282, 1993.

22. Fantl, V., Smith, R., Brookes, S., Dickson, C. and Peters, G. Chromosome 11q13 abnormalities in human breast cancer. Cancer Surv. 18: 77-94, 1993.

23. Park, N.H., Guo, W., Kim, H.R., Kang, M.K., and Park, N.H. c-myc and Sp1/3 are required for transactivation of hamster telomerase catalytic subunit gene promoter. Int. J. Oncol. 19: 755-761, 2001.

24. Geradts, J. and Ingram, C.D. Abnormal expression of cell cycle regulatory proteins in ductal and lobular carcinomas of the breast. Mod. Pathol. 13: 945-953, 2000.

25. Timms, J.F., White, S.L., O'Hare, M.J., Waterfield, M.D. Effects of ErbB-2 overexpression on mitogenic signalling and cell cycle progression in human breast epithelial cells. Oncogene 21: 6573-6586, 2002.

26. Scully, R. and Livingston, D.M. In search of the tumour-suppressor functions of BRCA1 and BRCA2.Nature 408: 429-432, 2000.

27. Lane, T.F., Deng, C., Elson, A., Lyu, M.S., Kozak, C.A. and Leder, P. Expression of Brca1 is associated with terminal differentiation of ectodermally and mesodermally derived tissues in mice. Genes Dev. 9: 2712-2722, 1995.

28. Vennerstrom, J.L., Ellis, W.Y., Ager, A.L. Jr., Andersen, S.L., Gerena, L., and Milhous, W.K. Bisquinolines.1. N, N-bis(7-chloroquinolin-4-yl)alkanediamines with potential against chloroquine-resistant malarial. J. Med. Chem. 35: 2139-2134, 1992.

29. Bray, P.G., Hawley, S.R., Mungthin, M. and Ward, S.A. Physiocochemical properties correlated with drug resistance and the reversal of drug resistance in Plasmodium falciparum. Mol. Pharmacol. 50: 1559-1566, 1996.

Table 1. Antiproliferative Activity of Investigational Drugs

Compound NSC #	Antimalarial	Growth End-Points MTS IC50		SRB GI50	
		MCF-7	MDA-231	MCF-7	MDA-231
		uM		uM	
86372		.18	.14	.12	.16
4238		.35	.74	1.6	.85
4239		.66	1.1	2.3	5.9
146397		.9	2.3	1.1	2.6
157387	**Mefloquine**	3.0	0.3	nd	nd
10010		3.4	1.0	5.4	1.3
149765	**Primaquine**	3.4	26	16	44
85701		4.4	.63	4.2	nd
86371		5.7	1.1	nd	nd
85700		6.5	7.1	7.4	33
Amodiaquin	**Amodiaquin**	6.9	6.0	nd	nd
2039		7.7	7.5	1.7	3.0
305819		7.9	3.9	13	9.4
3852		11	2.0	1.8	6.4
305789	**Halofantrine**	11	21	10	2.5
86373		13	4.8	nd	nd
124637		13	14	14	17
69603		14	.85	.85	.57
Quinolinic Acid		28	1.4	nd	nd
14050	**Chloroquine**	33	11	19	16
5362	**Quinine**	40	173	60	100
OH-chloroquine		57	28	nd	nd
Quinoline		62	>500	nd	nd
Quinidine	**Quinidine**	113	104	nd	nd
249913		INACTIVE		nd	nd
15783		INACTIVE		4.3	16
339004		INACTIVE		45	70
TSA		.035	nd	nd	nd

Figure 1

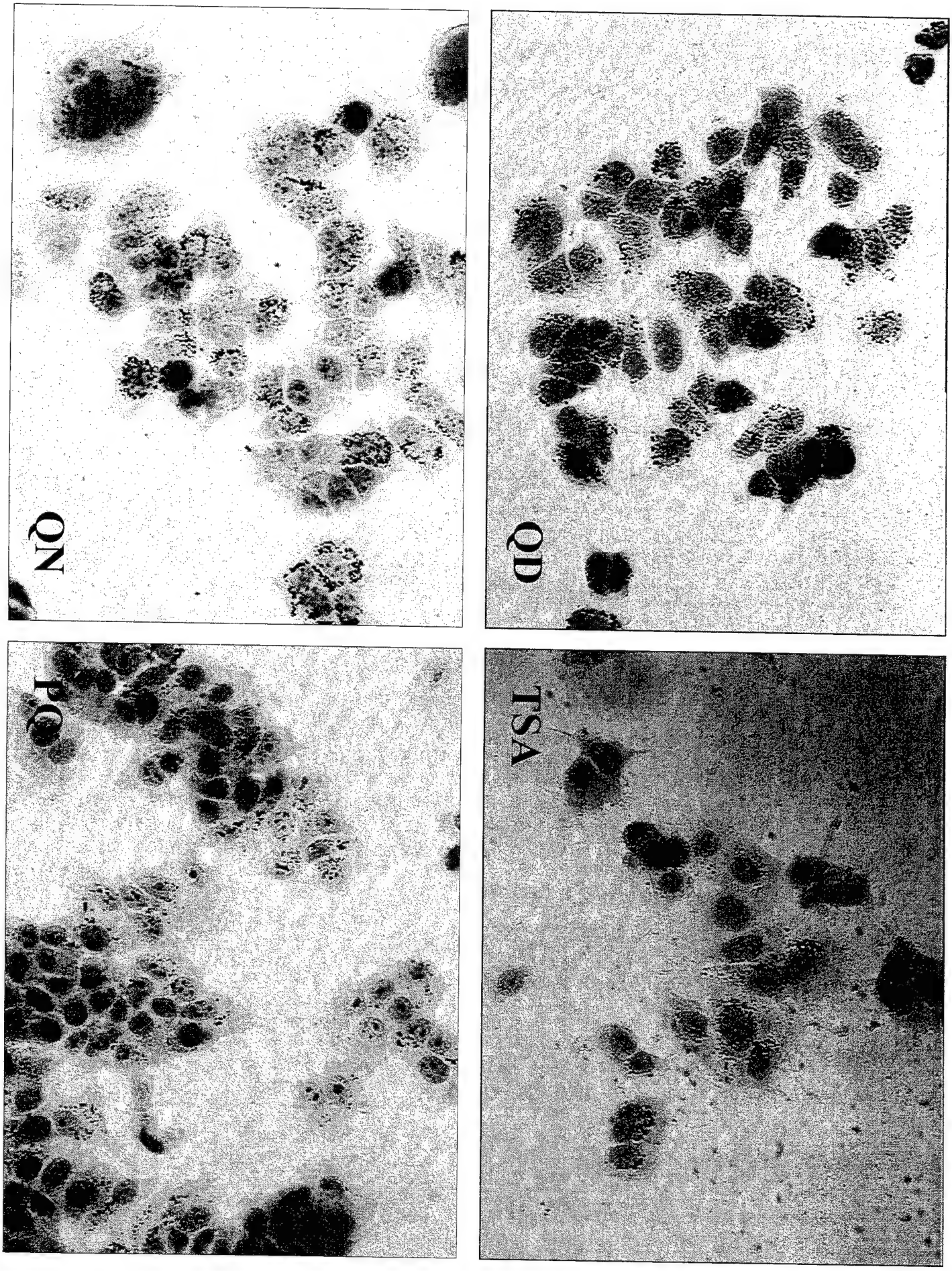

Figure 2

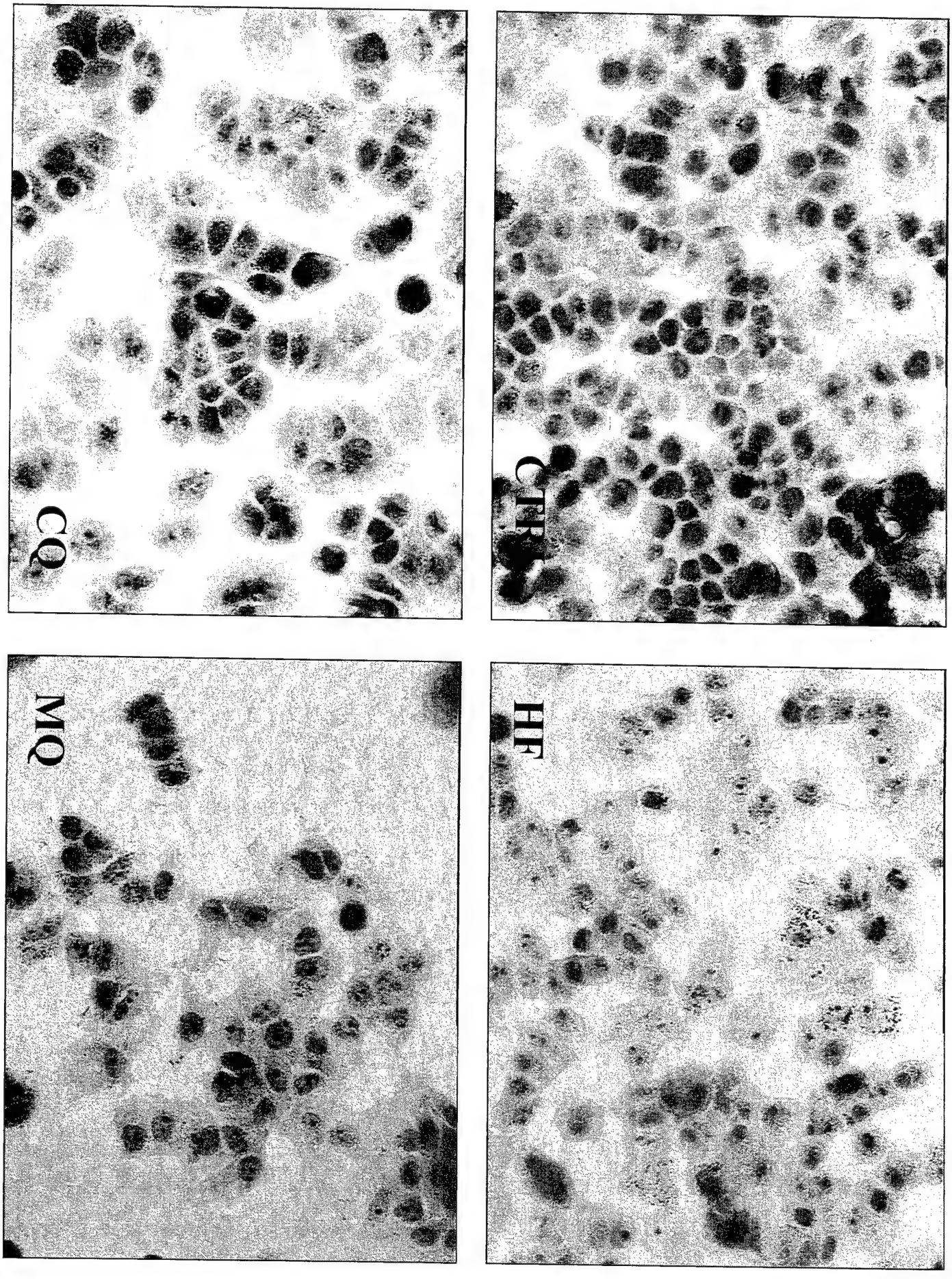

Figure 3

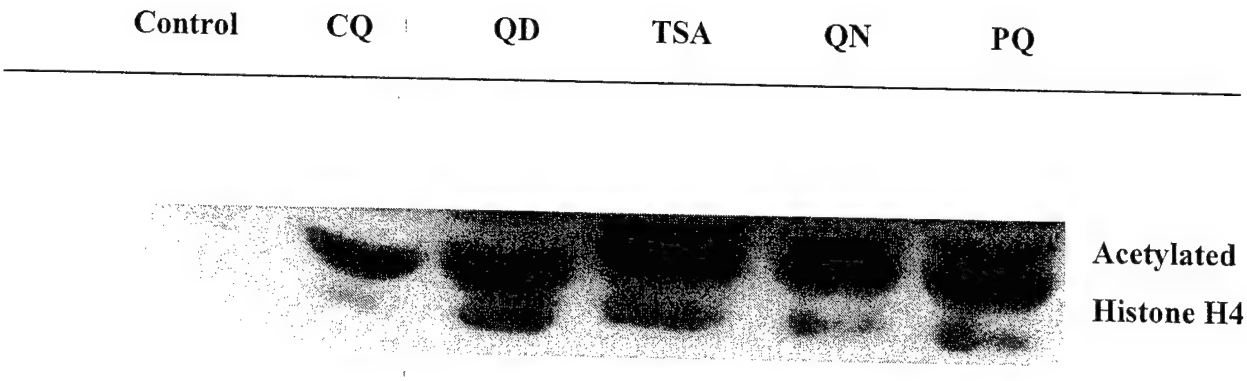

Figure 4

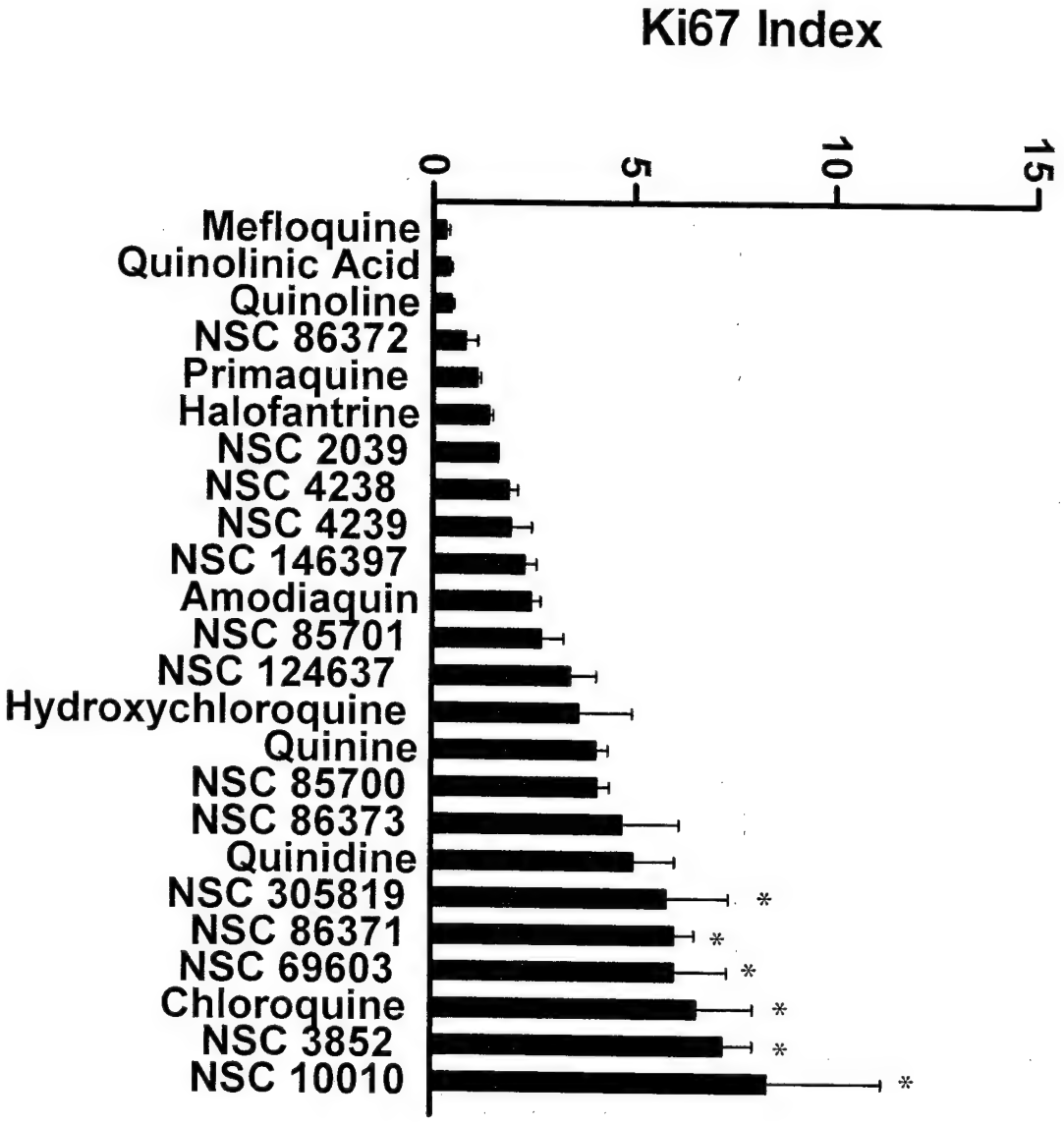
Ki67 Index
0
5
10
15
Mefloquine
Quinolinic Acid
Quinoline
NSC 86372
Primaquine
Halofantrine
NSC 2039
NSC 4238
NSC 4239
NSC 146397
Amodiaquin
NSC 85701
NSC 124637
Hydroxychloroquine
Quinine
NSC 85700
NSC 86373
Quinidine
NSC 305819
NSC 86371
NSC 69603
Chloroquine
NSC 3852
NSC 10010
*
*
*
*
*
*

Figure 5

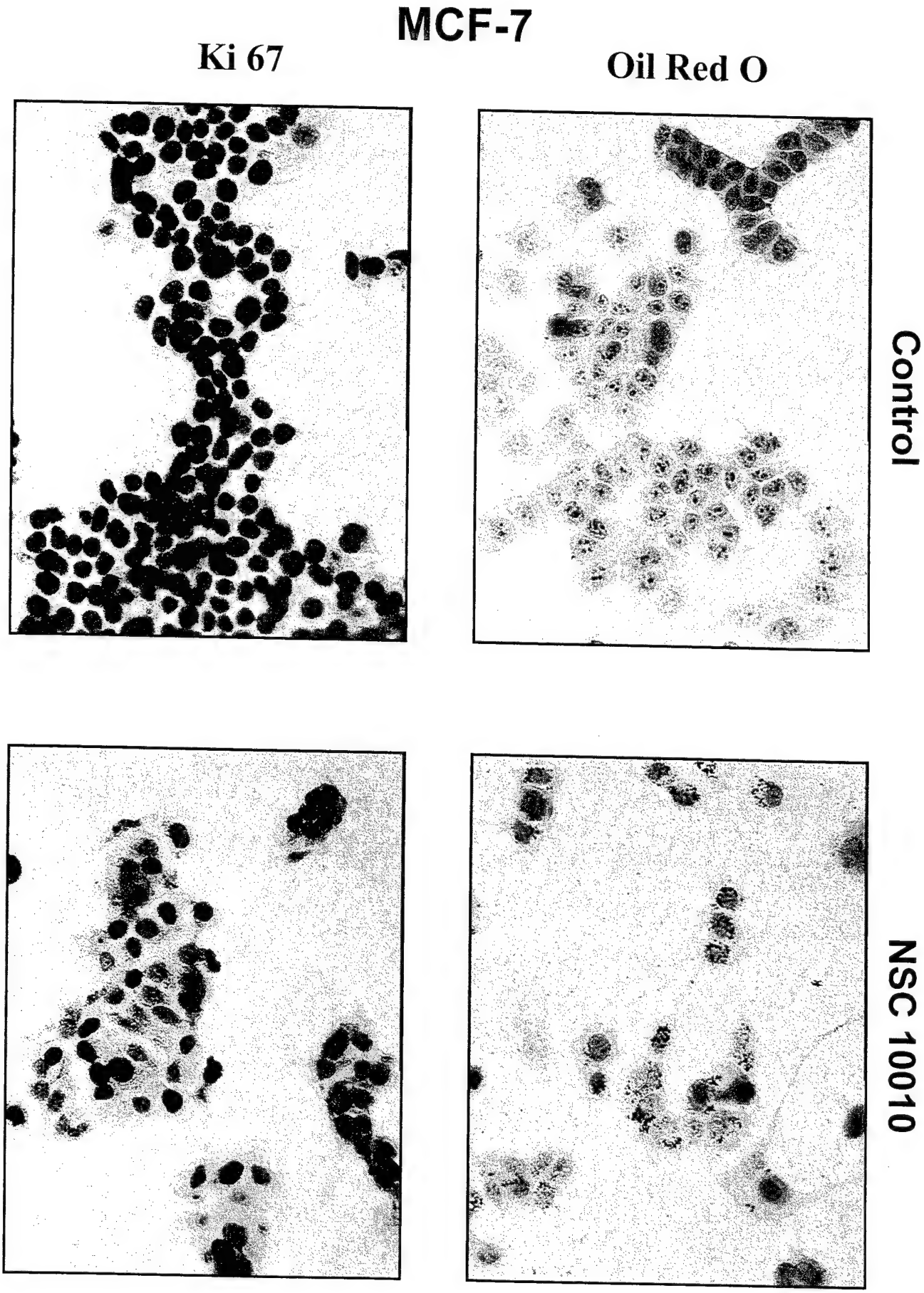

Figure 6

A. Reference Compounds: quinoline antimalarials

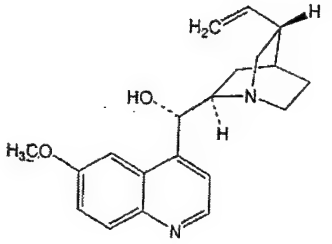

QUINIDINE

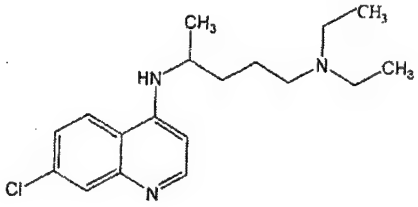

CHLOROQUINE

B. NCI Compounds: novel acting

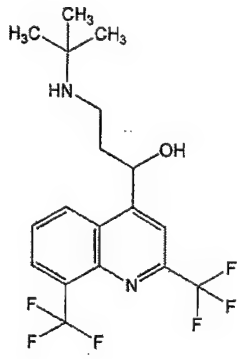

NSC 305819

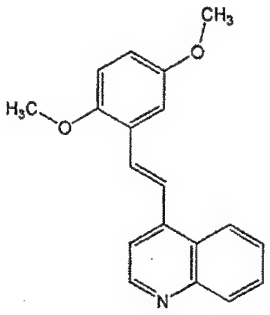

NSC 69603

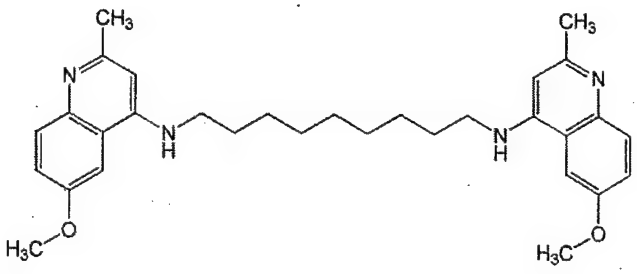

NSC 10010

C. NCI Compounds: HDAC inhibitors

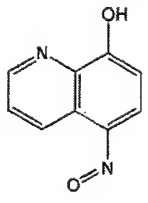

NSC 3852

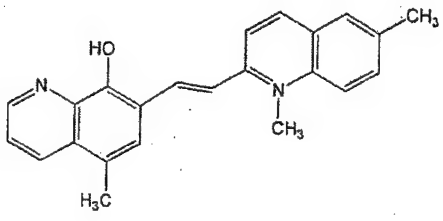

NSC 86371

Figure 7

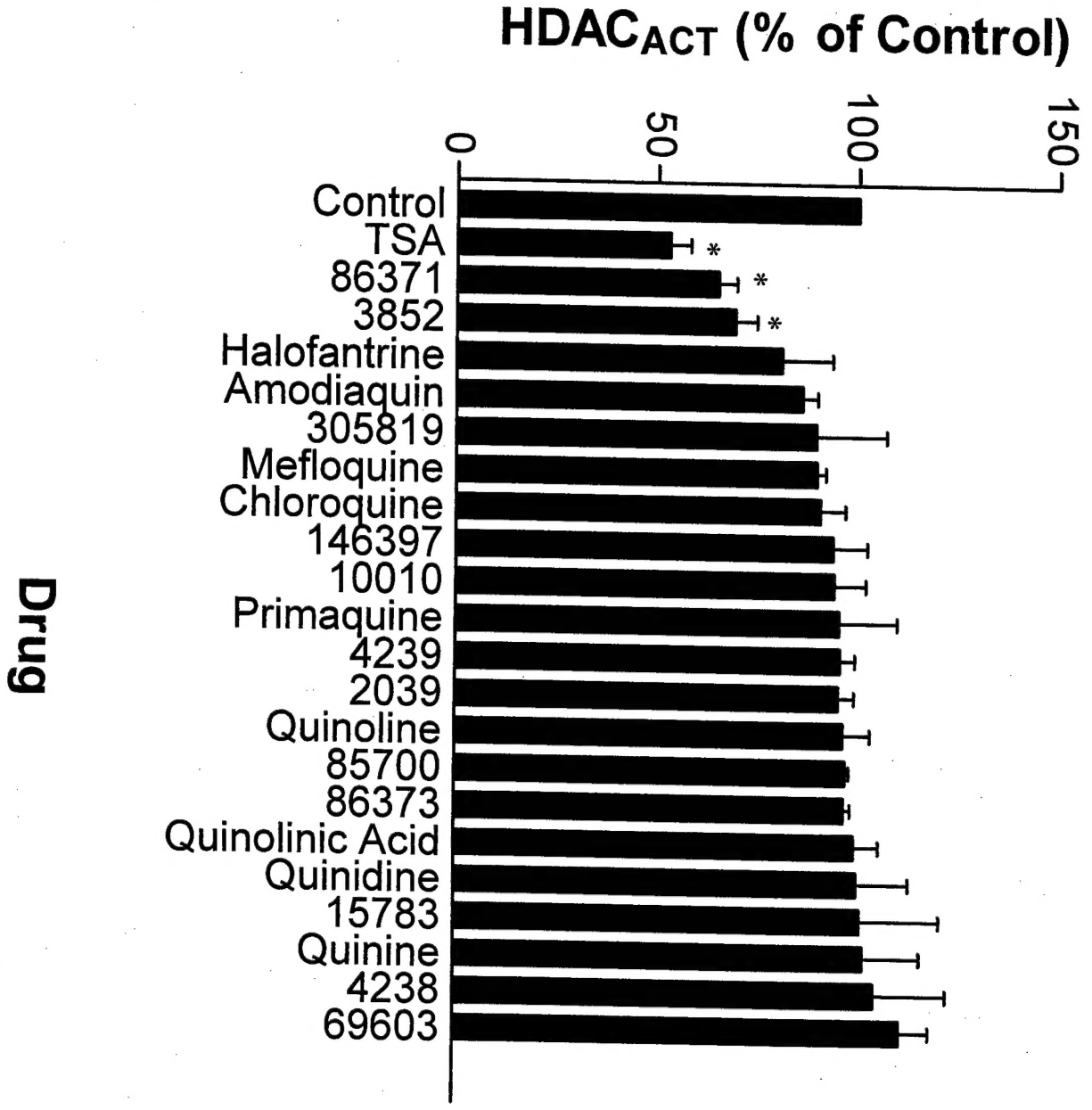
HDAC$_{ACT}$ (% of Control)
0
50
100
150
Drug
Control
TSA
86371
3852
Halofantrine
Amodiaquin
305819
Mefloquine
Chloroquine
146397
10010
Primaquine
4239
2039
Quinoline
85700
86373
Quinolinic Acid
Quinidine
15783
Quinine
4238
69603
*
*
*

Figure 8

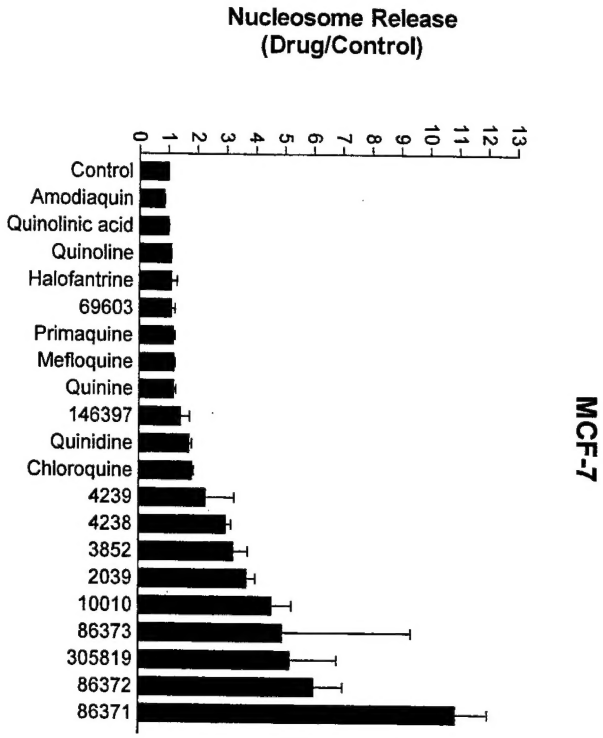
Nucleosome Release
(Drug/Control)
0
1
2
3
4
5
6
7
8
9
10
11
12
13
Control
Amodiaquin
Quinolinic acid
Quinoline
Halofantrine
69603
Primaquine
Mefloquine
Quinine
146397
Quinidine
Chloroquine
4239
4238
3852
2039
10010
86373
305819
86372
86371
MCF-7

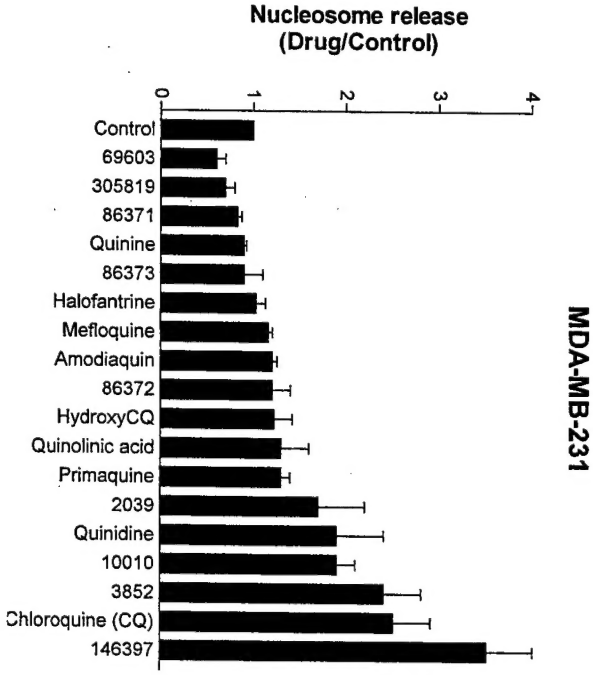
Nucleosome release
(Drug/Control)
0
1
2
3
4
Control
69603
305819
86371
Quinine
86373
Halofantrine
Mefloquine
Amodiaquin
86372
HydroxyCQ
Quinolinic acid
Primaquine
2039
Quinidine
10010
3852
Chloroquine (CQ)
146397
MDA-MB-231

NOVEL BREAST TUMOR DIFFERENTIATION AGENTS

Strobl J.S., Zhou Q., and Martirosyan A.

West Virginia University

jstrobl@hsc.wvu.edu

The use of breast tumor differentiating agents to complement existing therapies has the potential to improve breast cancer treatment. We are investigating the use of antimalarials as breast tumor differentiation agents on the basis of previous work showing that quinidine induces differentiation and apoptosis in human breast tumor cells in vitro. To test whether antitumor activity was a general property of antimalarial agents, we screened a panel of quinidine analogs. We found that MCF-7 cell exit from the cell cycle into G0, marked by a loss of Ki67 antigen expression, was a typical response to antimalarial drugs. The rank order of potency for MCF-7 cell growth inhibition (MTS, IC50) in a series of antimalarials showed quinidine was the least potent among common antimalarial agents: primaquine (3 μM)<amodiaquin (7 μM)< halofantrine (10 μM)< chloroquine (35 μM)< quinine (40 μM) < quinidine (110 μM). These antimalarial agents also increased acetylated histone H4 levels in MCF-7 cells a response that is associated with differentiation in human breast tumor cells. We suggest that antimalarials raise histone H4 acetylation levels by a novel mechanism, because none of the antimalarials were direct inhibitors of HDAC 1/ 2 activity. Although all the antimalarials tested elicited two novel and significant antitumor responses in MCF-7 human breast tumor cells, histone H4 hyperacetylation and cell cycle exit into a non-proliferative (G0) state, only quinidine and chloroquine stimulated apoptosis in MCF-7 cells. To search for more potent structural analogs of chloroquine with similar antitumor responses in MCF-7 cells, approximately twenty amino alkyl substituted quinoline ring compounds from the NCI Compound Library were screened for growth inhibition (MTS IC50) and cell cycle exit (Ki67 index). NCI 4238 and NCI 10010 inhibited cell survival at sub-micromolar concentrations, stimulated exit from the cell cycle (Ki67 index), and promoted morphological changes typical of differentiating breast tumor cells. In summary, antimalarial agents and structural analogs exhibit antitumor properties in human breast cancer cells in vitro that are consistent with a novel mechanism of action as breast tumor cell differentiating agents.

The U.S. Army Medical Research and Materiel Command under DAMD17-00-1-0500 supported this work.

NSC 3852, a new histone deacetylase inhibitor with breast tumor cell differentiation activity.

R. Martirosyan, J. S. Strobl. Dept. of Biochemistry and Molecular Pharmacology

We identified the quinoline, NSC 3852, as a differentiating agent in MCF-7 (10-20 uM) and MDA-231 (7-12 uM) cells in a screen using Oil Red O to monitor drug-induced lipid droplet accumulation. NSC 3852 (20 uM) inhibited histone deacetylase (HDAC) activity in HeLa cell extracts by 30%. NSC 3852 inhibited cell growth, using the MTS metabolism end-point, in MCF-7 (IC50, 14 uM) and MDA-231 (IC50, 2.0uM) cells over this concentration range. The apoptotic potential of this compound was demonstrated using a nucleosome release ELISA. By 24 h, levels of Myc protein and E2F1 protein in MCF-7 cells exposed to 10uM NSC 3852 were decreased by 70% and 90%, respectively. After 48h, ~50% of MCF-7 cells had accumulated in G0 phase of the cell cycle as marked by the loss of immunoreactive Ki67 antigen and the prominence of hypophosphorylated pRb. Total E2F transcription activity measured using E2F-driven luciferase reporter gene decreased by ~36 %. In conclusion, the quinoline, NSC 3852, promotes differentiation in human breast tumor cell lines in vitro. The biochemical actions of NSC 3852 include inhibition of HDAC activity and cell cycle arrest in G0 characterized by marked reductions in the levels of Myc and E2F1 protein. Support: DAMD 17-00-1-500.